Transdifferentiation and mesenchymal-to-epithelial transition during regeneration in Demospongiae (Porifera)

Alexander Ereskovsky, Daria B. Tokina, Stephen Baghdiguian, Emilie Le Goff, Andrey Lavrov

JEZ-B MOLECULAR AND DEVELOPMENTAL EVOLUTION

Transdifferentiation and mesenchymal-to-epithelial transition during regeneration in Demospongiae (Porifera)

Journal:	*JEZ Part B: Molecular and Developmental Evolution*
Manuscript ID	JEZ-B-2019-06-0045.R1
Wiley - Manuscript type:	Research Article
Date Submitted by the Author:	n/a
Complete List of Authors:	Ereskovsky, Alexander; CNRS, Aix-Marseille University, Institut Méditerranéen de Biodiversité et d'Ecologie marine et continentale (IMBE); Saint-Petersburg State University, Biological Faculty, depertment of Embryology; Koltzov Institute of Developmental Biology of Russian Academy of Sciences Tokina, Daria; CNRS, Aix-Marseille University, Institut Méditerranéen de Biodiversité et d'Ecologie marine et continentale (IMBE) Saidov , Danial; Dept. of Invertebrate Zoology, Biological Faculty, Lomonosov Moscow State University, 119234, Leninskie gory 1-12, Moscow Baghdiguian, Stephen ; ISEM, Univ Montpellier, CNRS, EPHE, IRD Le Goff , Emilie; ISEM, Univ Montpellier, CNRS, EPHE, IRD Lavrov, Andrey; Lomonosov Moscow State University, Faculty of Biology, Invertebrate Zoology
Keywords:	regeneration, demosponges, mesenchymal-to-epithelial transformation, blastema, apoptosis, transdifferentiation

Title[1] Transdifferentiation and mesenchymal-to-epithelial transition during regeneration in Demospongiae (Porifera)

Alexander V. Ereskovsky[1,2,3]*, Daria B. Tokina[1], Danial M. Saidov[4], Stephen Baghdiguian[5], Emilie Le Goff[5], Andrey I. Lavrov[2,6]

[1] Institut Méditerranéen de Biodiversité et d'Ecologie marine et continentale (IMBE), Aix Marseille University, CNRS, IRD, Avignon University, Station Marine d'Endoume, Rue de la Batterie des Lions, 13007, Marseille, France

[2] Dept. Embryology, Faculty of Biology, Saint-Petersburg State University, Universitetskaya emb. 7/9, 199034, Saint-Petersburg, Russia

[3] Koltzov Institute of Developmental Biology of Russian Academy of Sciences, Russia, Moscow

[4] Dept. of Invertebrate Zoology, Biological Faculty, Lomonosov Moscow State University, 119234, Leninskie gory 1-12, Moscow, Russia

[5] ISEM, Univ Montpellier, CNRS, EPHE, IRD, Montpellier, France.

[6] Pertsov White Sea Biological Station, Biological Faculty, Lomonosov Moscow State University, 119234, Leninskie gory 1-12, Moscow, Russia

Text figures – 16

Abbreviated title: Demosponges regeneration

***Correspondence to**: Alexander V. Ereskovsky, Institut Méditerranéen de Biodiversité et d'Ecologie marine et continentale (IMBE), Aix Marseille University, CNRS, IRD, Avignon University, Station Marine d'Endoume, Rue de la Batterie des Lions, 13007, Marseille, France, Tel. +33 04 91 04 16 21 ; Fax : e-mail alexander.ereskovsky@imbe.fr,

This work was supported by grants of Russian Foundation for Basic Research n° 16-04-00084, and the Russian Science Foundation n° 17-14-01089 (histological and ultrastructural studies).

[1] **Funding information**. This work was supported by grants of Russian Foundation for Basic Research n° 16-04-00084, the Russian Science Foundation n° 17-14-01089 (histological and ultrastructural studies). This work also is a contribution to Labex OT-Med (n° ANR-11-LABX-0061) and has received funding from Excellence Initiative of Aix-Marseille University_A*MIDEX, a French "Investissements d'Avenir" program for travel expenses.

Abstract

Origin and early evolution of regeneration mechanisms remain among the most pressing questions in animal regeneration biology. Porifera have exceptional regenerative capacities and, as early Metazoan lineage, are a promising model for studing evolutionary aspects of regeneration. Here, we focus on reparative regeneration of the body wall in the Mediterranean demosponge *Aplysina cavernicola*. The epithelialization of the wound surface is completed within two days, and the wound is completely healed within two weeks. The regeneration is accompanied with the formation of a mass of undifferentiated cells (blastema), which consists of archaeocytes, dedifferentiated choanocytes, anucleated amoebocytes, and differentiated spherulous cells. The main mechanisms of *A. cavernicola* regeneration are cell dedifferentiation with active migration and subsequent redifferentiation or transdifferentiation of polypotent cells through the mesenchymal-to-epithelial transformation. The main cell sources of the regeneration are archaeocytes and choanocytes. At early stages of the regeneration, the blastema almost devoid of cell proliferation, but after 24 hpo and up to 72 hpo numerous DNA-synthesizing cells appear there. In contrast to intact tissues, where vast majority of DNA-synthesizing cells are choanocytes, all EdU-labeled cells in the blastema are mesohyl cells. Intact tissues, distant from the wound, retains intact level of cell proliferation during whole regeneration process. For the first time, the apoptosis was studied during the regeneration of sponges. Two waves of apoptosis were detected during *A. cavernicola* regeneration: the first wave at 6-12 hpo and the second wave at 48-72 hpo.

Keywords: demosponges, regeneration, mesenchymal-to-epithelial transformation, blastema, apoptosis, transdifferentiation.

Highlights

1) Regeneration in the demosponge *Aplysina cavernicola* is accompanied with the formation of a mass of undifferentiated cells (blastema).

2) The main mechanisms of *A. cavernicola* regeneration are cell dedifferentiation with active migration and subsequent redifferentiation or transdifferentiation of polypotent cells - archaeocytes and choanocytes - through the mesenchymal-to-epithelial transformation.

3) Apoptosis during regeneration of *A. cavernicola* participate in damaged cells elimination and associated with the extensive ejection of spherulous cells from wound area.

Introduction

In spite of big interest in various problems concerning origin and early steps of evolution in animal regeneration, morphogenesis, cell turnover etc., up to now there are surprisingly small number of the studies, dealing with ultrastructural, morphogenetic, cell and genetic aspects of sponge reparative regeneration.

Phylum Porifera consists of four classes: syncytial Hexactinellida, and cellular Calcarea, Homoscleromorpha and Demospongiae. The last class is the largest and includes about 80% of living sponges. Studies of regeneration in sponges have begun on demosponges (Cavolini, 1785; Vaillant, 1869; Weltner, 1893). However, there are only few papers, concerning ultrastructural description of the morphogenesis and cell behavior in reparative regeneration of sponges. Moreover, three of them dealing with the regeneration of specific "organs" after amputation (oscular diaphragm in *Hippospongia communis* (Thiney, 1972), oscular tube in *Ephydatia fluviatilis* (Sukhodolskaya, 1973), and papillae in *Polymastia* (Boury-Esnault, 1976)). Reparative regeneration of the body wall is described only in seven species. Regeneration in *Spongilla lacustris* (Brondsted, 1953), *Halichondria panicea* (Korotkova & Nikitin, 1969), *Geodia barretti* (Hofmann et al., 2003) and *Halisarca caerulea* (Alexander et al., 2015) was studied only with light microscopy. In the case of *H. caerulea*, the light microscopy studies were supplemented with the investigations of the cell proliferation during the regenerative processes (Alexander et al., 2015). Reparative regeneration in *Chondrosia reniformis* was investigated with light and scanning electron microscopy (SEM) (Pozzolini et al., 2019). Finally, SEM studies supplemented with time-laps recordings were done for regeneration in *Hymeniacidon heliophila* (Coutinho et al., 2017).

At the same time, our complex detailed investigations of reparative regeneration, done with TEM, SEM, epifluorescent and light microscopy, immunocytochemistry and time-laps recordings, in homoscleromorphs (Ereskovsky et al., 2015), calcareous sponges (Ereskovsky et al., 2017; Lavrov et al., 2018) and demosponges (Borisenko et al., 2015) show a high diversity of morphogenesis, cell mechanisms, and cell turnover, accompanying these processes.

Thus, having comprehensive data about mechanisms of the regeneration for only one species from the huge and very diverse class Demospongiae, we cannot make any generalizations regarding the mechanisms of regeneration of this class of Porifera.

Representatives of the genus *Aplysina* are widely distributed in subtropical and tropical coastal waters (Bergquist & Cook, 2002). They are considered proper models in chemical ecology and microbiology (Azevedo et al., 2008; Betancourt-Lozano et al., 1998; Thoms et

al., 2004, 2006). *Aplysina cavernicola* is a popular and promising model for various researches, dealing with the sponge cell composition (Vacelet, 1966, 1967, 1970, 1971, 1975; Vacelet & Gallissian, 1978), bacterial symbionts (Vacelet, 1975; Fiedrich et al., 1999; Hentschel et al., 2001; Thoms et al., 2003), three-dimensional skeletal scaffolds (Vacelet, 1971a,b; Garrobe et al. 1973; Ehrlich et al. 2010a, b), biochemistry and secondary metabolites (D'Ambrosio et al., 1982, 1983; Ciminiello et al., 1997; Reverter et al., 2016), and temporal variability of secondary metabolism (Reverter et al., 2016). Life cycle researches showed that *A. cavernicola* is an oviparous sponge whose reproductive period lasts barely one month (Gallissian & Vacelet, 1976; Reverter et al., 2016).

The present study was aimed at investigation of the reparative regeneration in Mediterranean demosponge *Aplysina cavernicola* (Vacelet, 1959). The wide range of methods allow us to make a comprehensive analysis of mechanisms, which contribute to the regeneration in this species, including cell behavior and migrations, morphogenetic process, cell proliferation and apoptosis.

Materials and methods

Sampling

Aplysina cavernicola (Vacelet, 1959) (Demospongiae, Verongida) is a perennial sciaphilous species inhabiting coralligenous formations or the entrance of submarine caves generally between 8 to 60 m in the Mediterranean Sea (Figure 1). It presents a typical yellowish color. For regeneration experiments *A. cavernicola* specimens were collected by SCUBA diving in September-November 2017, July-August and October 2018 and March 2019 near Maire Island, Marseille (43.2096° N; 5.3353° E) at a depth of 12 - 15 m. Collected sponges were maintained in a 100 l laboratory aquarium with running natural seawater at a temperature of 15-16°C for 36 hours for sponge adaptation.

Surgical operations

Two type of surgical operations have been conducted: i) *in situ*, and ii) in laboratory. For *in situ* operations six individuals were used. The experiment was performed in June 2018 at the site of sponge sampling. In each sponge wounds were made in a wall of a cylindrical outgrowth using a sharp stainless dissecting scalpel. The wounds had a uniform size of 3 cm^2 in area and 1 cm deep. Each wound was measured and photographed at t = 0, 2, 7, 12, and 32 days post operation, using digital camera Nikon D300 equipped with waterproof camera

housing SUBAL ND300 and flash INON Z-240.

Surgical operations in laboratory were performed as an excision of a small part (approximately 0.3-0.5x0.3-0.5 cm) of the body wall at the base of a cylindrical outgrowth (Figure 2). A total of 24 individuals were used in the body wall regeneration experiments (Supporting Table 1).

The surgical operations were done manually under a stereomicroscope using scalpel. After the operations the sponges with excised body wall were maintained in a 100 l laboratory aquarium with running natural seawater at a temperature of 15-16°C. The sponges were inspected and photographed using a stereomicroscope Leica M165FC (Leica) equipped with a digital camera Leica DFC 320 (Leica) and LAS Store and Recall v.4.1 software (Leica). The observations were done at 3, 6, 12, 18, 24, 36, 48, 72, 96, and 120 hours post operation (hpo).

Light and electron microscopy

Specimens were fixed overnight at 4°C by 2.5% glutaraldehyde (Ted Pella) on 0.2M cacodylate buffer (pH 7.4) and post-fixed for 2 h with 1% OsO_4 (Spi Supplies) on the same buffer at room temperature (RT). Between fixation and post-fixation specimens were twice rinsed with cacodylate buffer for 30 min. Finally, specimens were dehydrated in an ethanol series at RT and stored in 70% ethanol at 4°C.

For semi-thin sections and transmission electron microscopy (TEM) specimens were embedded in Araldite (Sigma-Aldrich) epoxy embedding media according to the manufacturer instructions. Semi-thin sections (1 µm) were cut on a Reichert Jung ultramicrotome (Reichert) and Ultramicrotome PowerTome XL (RMC Boeckeler) and then stained with 1% toluidine blue – 0.2% methylene blue mixture. The semi-thin sections were studied under a WILD M20 microscope (Wild). Digital photos were taken with a Leica DMLB microscope (Leica) using Evolution LC color photo capture system (MediaCybernetics).

Ultrathin sections (60–80 nm) were cut with a Leica UCT6 and an Ultramicrotome PowerTome XL, equipped with a Drukkert 45° diamond knife, and contrasted with 4% aqueous uranyl acetate. Ultrathin sections were studied under Zeiss-1000 (Carl Zeiss) transmission electron microscope.

For scanning electron microscopy (SEM), fixed specimens were critical-point-dried, sputter-coated with gold-palladium, and observed under Hitachi S 570 (Hitachi) microscope.

Spherulous cell counting

Spherulous cells were counted on images of semi-thin sections of intact sponge tissues and regenerating specimens at 6, 12, 24, 48, and 96 hpo. The images were obtained with a Leica DMLB microscope (Leica) at 40x magnification using Evolution LC color photo capture system (MediaCybernetics). At each stage three images, arising from three independent individuals, were used for counting. Spherulous cells were counted in the approximate 50-µm thick lane beneath the exopinacoderm in intact sponges or beneath wound surface in regenerating individuals. The area of the studied lanes was measured for each image, and number of spherulous cells were extrapolated for an area of 1 mm^2. Cell counting and area measuring were done with ImageJ v.1.48 software (National Institute of Health). For each stage mean value and standard deviation were calculated (Supporting Table 4).

Statistical analysis was performed in R (R Core Team, 2019) with basic package "stats" ver. 3.6.0 (R Core Team, 2019) and additional packages "agricolae" ver. 4.2-0 (de Mendiburu, 2019), "car" 3.0-3 (Fox & Weisberg, 2019) and graphic package "ggplot2" ver. 3.3.1 (Wickham, 2019). To analyze the results, analysis of variance (ANOVA) was performed to evaluate differences for spherulous cell count in intact tissues and at different stages of regeneration. For ANOVA we prerequisitely performed box-cox transformation with $\lambda=0$ to normalize our data, and Leven's test for homogeneity of variances ($p = 0.3744$). For pairwise comparisons, we performed Tukey's honestly significant test and Duncan's multiple range test from "agricolae" package with 0.95 confidence level (Supporting Table 4).

Cell proliferation investigations

A total of 27 individuals with the excised body wall were used in cell proliferation studies (Supporting Table 2). The 5-Ethynyl-2′-deoxyuridine (EdU) (Thermo Fisher Scientific), which incorporates in nuclear DNA during its synthesis in S-phase and marks DNA-synthesizing cells, was used as a label for cell proliferation. The EdU stock solution was prepared in DMSO (MP Biomedicals). The optimal EdU concentration and incubation time were elucidated during the preliminary studies with the intact tissues of *Aplysina cavernicola.*

Labeling of DNA-synthesizing cells in the regenerating sponges were conducted during the following time periods: 0-6, 6-12, 0-24, 24-48, 48-72, 120-144 hpo. The EdU concentration in the experiments with 6-hour incubation period was 600 µM and in the experiments with 24-hour incubation period – 200 µM. Three individuals were used at each time period. Three additional sponges were cultured in FSW without the EdU and served as negative technical controls (Supporting Table 2).

The cell proliferation was also studied in the intact tissues of *A. cavernicola.* Three individuals were incubated 6 hours in FSW with 600 μM EdU and three individual – 24 hours in FSW with 200 μM EdU. One individual was cultured in FSW without the EdU and served as a negative technical control (Supporting Table 2). The mode of EdU incubation did not significantly influence the pattern of the staining of DNA-synthesizing cells: after both types of incubation sponge tissues show essentially the same amount and localization of the DNA-synthesizing cells.

During the EdU incubation, intact and regenerating sponges were cultivated in glass vessels with 200 ml FSW supplemented with required amount EdU at 13°C.

After the incubation period, all individuals were rinsed twice with FSW and fixed with 4% PFA (Sigma-Aldrich) in PBS (Amresco, Inc.) for 12-15 hours at 4°C. Fixed specimens were rinsed with PBS and the Click-iT reaction were performed in the following mixture: 4 мM $CuSO_4$ (ChimMed), 20 mg/ml Sodium L-ascorbate (Sigma-Aldrich) and 10 μM Sulfo-Cyanine3 Azide (Lumiprobe) in PBS. Finally, the specimens were rinsed several times with PBS and stained with DAPI (Sigma-Aldrich).

Stained specimens were mounted in 90% glycerol-DABCO (Sigma-Aldrich) and studied with a CLSM Nikon A1 (Nikon) using lasers with 405 nm, 488 nm and 546 nm wavelength. The tissues beneath the wound surface and tissues no less than 1 cm away from the wound were studied in each regenerating specimen.

The obtained Z-stacks and images were processed with ImageJ v.1.48 software (National Institute of Health). Nuclei measuring were done on separate optical slices with NIS Elements Viewer v. 4.5 (Nikon) and JR Screen Ruler v. 1.5 (Spadix Software). For all measurements mean value and standard deviation were calculated.

Apoptosis investigation

Four individuals were used for studies of apoptosis during regeneration and in intact sponge tissues (Supporting Table 3). The studies were performed using the In Situ Cell Death Detection Kit (Roche) or Click-iT Plus TUNEL Kit (Thermo Fischer Scientific). Both kits detect apoptotic cells using the TUNEL assay, i.e. by attaching labeled nucleotides to double-stranded DNA breaks that occur at the later stages of apoptosis.

Intact tissue and wounded areas at 6, 12, 24 and 48 hpo were fixed at 4°C by 4% PFA (Sigma-Aldrich) on PBS (Amresco, Inc.). Fixed specimens were rinsed with PBS and treated according to the manufacturer instructions for apoptotic cell visualization. Finally, the specimens were rinsed several times with PBS and stained with DAPI (Sigma-Aldrich).

Samples, incubated with DNase I recombinant purified from bovine pancreas (Thermo Fisher Scientific) prior to the TUNEL reaction, were used as positive technical controls. Samples, incubated without the TdT enzyme during the TUNEL reaction, were used as negative technical controls.

Stained specimens were mounted in Mowiol (12%) or 90% glycerol-DABCO (Sigma-Aldrich) and studied with a confocal microscope TCS-SPE (Leica) or CLSM Nikon A1 (Nikon) using lasers with 405 nm, 488 nm and 546 nm wavelength. The tissues beneath the wound surface and tissues no less than 1 cm away from the wound were studied in each regenerating specimen.

Field Study Permissions

No specific permissions were required for these locations because the study was done outside national parks, private lands or protected areas. We declare that the field studies did not involve endangered or protected species.

Results

Intact sponge morphology and histology

The body of *Aplysina cavernicola* has a branchy shape, with each cylindrical branch having 1-2 cm in diameter (Figure 1). Sponge tissues are dense and elastic. The sponge has leuconoid organization of aquiferous system (numerous small choanocyte chambers, scattered in the mesohyl). The skeleton represented exclusively by organic (spongin) fibers, covered with chitin (Ehrlich et al., 2010a), thus the surgical operations are easily conducted.

The body is composed of the peripheral ectosome and the internal endosome, bearing numerous choanocyte chambers (Figure 3A). The ectosomal region is up to 30 μm thick and consists of three layers: (1) external parts of the T-shaped exopinacocytes, connected by non-specialized cell junctions (Figure 3B,C) and covered by an acellular cuticle; (2) layer containing collagen fibrils, cell bodies of exopinacocytes and scattered spherulous cells; and (3) the inner layer, consisting of condensed collagen fibrils and spherulous cells. The endosome (Figure 3A) composes the major part of the sponge body. It includes choanocyte chambers, consisted of flagellated choanocytes, aquiferous canals, lined by endopinacocytes, (Figure 3D,E) and the mesohyl with the skeleton, abundant symbiotic bacteria and scattered specialized sponge cells.

Populations of free cells in the mesohyl of *A. cavernicola* include: lophocytes, archaeocytes, pocket cells, contractile cells (myocytes) (Figure 3F,H), spherulous cells at different stages of their maturation with two principal morphotypes: larger cells with clear inclusions (Figures 3C, 4G) and smaller ones with dense inclusions (Figure 4D,H), bacteriocytes, microgranular cells, spongocytes (Figure 4A-F) (Vacelet, 1966, 1967, 1970, 1971, 1975; Vacelet & Gallissian, 1978).

Regeneration

In spite of minor individual differences wound healing in *Aplysina cavernicola*, which is expressed in the epithelialization of the wound surface, is completed within two – six days (Figure 1). During our observations we did not reveal any significant differences in the onset of the stages and course of the regeneration, as well as in the morphogenesis accompanying it, across studied individuals. The regeneration ends within two weeks, when the wound is completely healed: only a small depression on the surface remains in its place.

At the histological level the observed regeneration processes can be subdivided into three stages: 1) internal milieu isolation – formation of a clot (3 – 12 hpo), 2) wound healing – epithelization (12 – 24 hpo), and 3) restoration of ectosome and endosome (36 – 96 hpo).

For detailed description of morphogenesis and cell behavior, accompanying the regeneration, we propose to subdivide a wound and tissue around the wound on several areas (Figure 5):

- Wound – a break in the continuity of any bodily tissue due to injury.
- Wound area – tissues directly adjacent to an excised part of the sponge body; their structure is severely disrupted during the surgery.
- Edge of the wound – peripheral parts of the wound, which is in direct contact with intact tissues.
- Regeneration area – an area of the sponge body (tissue), which is not directly affected by surgery, but in which anatomical structures (choanocyte chambers, canals of aquiferous system and skeleton) are reorganized, and the normal composition and distribution of cells disrupted due to their participation (dedifferentiation, transdifferentiation and migration) in the regenerative processes. The dimension of this area could vary, depending on size and type of the injury and on individual characteristics of a sponge.
- Intact issues – ectosome and endosome areas that are not affected by surgery and are not directly involved in regeneration and retaining the normal organization.

Stage I – Internal milieu isolation

Immediately after the surgical excision of ectosome with the directly adjacent endosome, the wound surface retracts, leaving the surface of the intact ectosome protruding around the edges of the wound. The ectosome and the upper areas of endosome are destroyed in the wound area.

During the first 3 hours post operation (hpo), the wound surface is covered with exudate, cell debris and numerous symbiotic bacteria. The extracellular matrix (ECM) does not show any signs of a condensation (Supporting Figure 1A-C). All cells in the wound area undergo morphological modifications. The epithelial cells - endopinacocytes and choanocytes of choanocyte chambers, begin losing contacts with adjacent cells in their epithelial layers and change their shape from trapeziform (choanocytes) and flat (endopinacocytes) to spherical or amoeboid (Figure 6). These dedifferentiated cells mix with the mesohyl cell population. During transformation of the choanocytes, their collar of microvilli and flagellum are resorbed (Figure 6D). However, the elements of the flagellar apparatus (the basal body and accessory centriole located near the nucleus) persist in the transformed cells for approximately two days and serve as the natural marker of dedifferentiated choanocytes. The dedifferentiated endopinacocytes have no specific morphological characteristics and therefore these cells cannot be distinguished from other mesohyl cells. The non-secreting cells of the mesohyl (archaeocytes, lophocytes, dedifferentiated choanocytes and endopinacocytes) actively phagocyted cell debris, symbiotic and invasive microbes, including diatoms in the wound area (Figure 6). Thus, all cells in the wound area, except the spherulous cells, are filled with large phagosomes. The ectosome, surrounding the wound slightly contracts and bends inward. After 3 hpo an active migration of the mesohyl cells and dedifferentiated choanocytes towards the wound surface begins from wound area, as these cells assume an elongated shape with the long axis, perpendicular to the wound surface (Figure 6). There are no changes in the regeneration area in this period.

At 6 hpo, the wound surface is aligned and becomes flat and smooth. It is covered by a thick layer of ECM, containing fragments of cells, dispersed symbiotic bacteria and few spherulous cells (some of which are beginning their dedifferentiation) (Figure 7A; Supporting Figure 1D). The amount of the spherulous cells in the wound area at this stage of the regeneration significantly decreases and is approximately 2,8-fold lower than in the ectosome of intact sponges (Figure 8; Supporting Table 4). This structure can be referred as a regenerative clot, by analogy with other animals (Carlson, 2007). The thickness of the clot is from 12 to 20 μm.

The cells of wound area have numerous small or few large phagosomes, which contained fragments of the spherulous and granular cells (Figure 7B-F). Such cells could be found not only in the upper part of the wound, but also in the deeper zone up to 100 μm beneath the wound surface. There still no visible changes in the regeneration area at this stage.

At 12 hpo a regenerative clot at the wound surface is getting thinner, and wound surface become aligned, flat and smooth (Figure 9A). The peripheral parts of the wound are clearly limited by the flat outgrowths of intact exopinacocytes (Figure 9F).

In the wound area, cell distribution begins ordering, and ECM condensation occurs (Supporting Figure 1E). The number of dedifferentiated choanocytes and endopinacocytes, archaeocytes, and lophocytes increases in this area in comparison with the previous period of regeneration (Figure 9B-E). Majority of these cells migrated from regenerated area. In contrast, the number of the spherulous cells shows insignificant variations and remains approximately the same as at 6 hpo (Figure 8; Supporting Table 4). Some of these spherulous cells undergo the dedifferentiation, which is accompanied by the release of the spherules from the cells. The amount of free mesohyl and concentration of the symbiotic bacteria decrease in comparison with previous periods of regeneration (Figure 9C, D).

Simultaneously, the migration of the amoeboid cells (archaeocytes, dedifferentiated choanocytes) from the regeneration area to the wound area and wound surface proceeds (Figure 9C,E), and some of the migrating cells reach the wound surface, where they become oriented with the long axis parallel to the wound surface (Figure 9B). Also first elongated contractile cells (myocytes) appear in the regeneration area.

Stage II. Wound healing - epithelization (12 – 24 hpo)

At 24 hpo a cell mass, consisting of heterogenous dedifferentiated and undifferentiated (archaeocytes) cells, is formed under the upper part of the wound area. We considered it as a blastema, as structurally it resembles blastemas formed during regeneration of other animals. Blastema occupies the wound area and the upper part of the regeneration area.

Simultaneously, the upper part of the wound area becomes similar to intact sponge ectosome, showing structured ECM with collagen fibrils (Figure 10A,B; Supporting Figure 1F). The wound surface is mosaically covered with very thin superficial outgrowths of developing T-shaped exopinacocytes, arising from blastema cells of the heterogeneous origin (Figure 10B,C,E). New exopinacocytes do not yet form close contacts with each other. In some places submerged nucleated bodies of these cells are found. New exopinacocytes, in

contrast to the cells located deeper under the wound surface, have only few phagosomes. There is no directed movement (contraction or creeping) of the intact exopinacoderm surrounding the wound.

The number of spherulous cells in the wound area significantly increases in approximately 2,3-folds in comparison with the previous stage of regeneration (Figure 8; Supporting Table 4). These cells show typical appearance (Figure 10B). Their shape is oval, not amoeboid, as in the earlier stages of regeneration. In contrast, near the wound surface, the number of dedifferentiated choanocytes, archaeocytes and spherulous cells decreases (Figure 10C-F). The lophocytes, granular cells, and myocytes are absent from this zone. The choanocyte chambers or their fragments completely disappear from the regeneration area at this stage of regeneration. They occur at a depth of about 200 μm, as in intact sponge.

Stage III. Restoration of ectosome and endosome (36 – 96 h)

At 48 hpo the ectosome of the regenerate is completely restored, but superficial cuticle, characteristic for intact sponge, is still absent (Figure 11A,B; Supporting Figure 1G). The wound epithelization is finished by new exopinacocytes, arose from the heterogeneous dedifferentiated cells population and archaeocytes. Some of new exopinacocytes clearly show their origin from the dedifferentiated choanocytes, as they still bear flagellar basal apparatus (Figure 11C). According to the orientation of this flagellated complex, it can be assumed that the basal part of the former choanocyte is flattened. Archaeocytes, reaching the wound, flatten and assume position parallel to the surface (Figures 10E,F, 11D). New exopinacocytes have normal T-shape and cell contacts.

During formation of the exopinacoderm active elimination of small apoptotic spherulous cells with compact inclusions and cells, filled with big heterophagosomes, begins (Figure 11E, F). However, the number of the spherulous cells shows insignificant variations and remains approximately the same as at 24 hpo (Figure 8; Supporting Table 4).

During this stage, the choanocyte chambers and aquiferous canals of the endosome are restored by association of previously disaggregated choanocytes and endopinacocytes, respectively (Figure 12). Archaeocytes also participate in the development of new choanocyte chambers (Figure 12D). Cells that form new structure of aquiferous system contact each other and connect by interdigitations. Individual choanocytes form groups of cells, forming structures less compact than in the intact choanocyte chamber (Figure 12D-F). These cells gradually transform from mesenchymal morphology to epithelial.

At 96 hpo, the regeneration is almost complete: the ectosome obtains the cuticle, while the endosome of the regeneration area begins to recover: choanocyte chambers and aquiferous canals are gradually developing (Figure 13; Supporting Figure 1H). The number of spherulous cells in the regenerated ectosome significantly increases, reaching the intact level (Figure 8; Supporting Table 4). The free cells of the mesohyl, with the exception of specialized secretory cells, still contain phagosomes.

Cell proliferation

The DNA-synthesizing (EdU-labelled) cells are irregularly distributed in the intact tissues of *A. cavernicola* (Figure 14). Numerous DNA-synthesizing cells are located in the sponge endosome (Figure 14B). The majority of these cells are choanocytes with small (3.87±0.46 μm; n=45) round to oval nuclei (Figure 14D). Nevertheless, some mesohyl cells with large (4.84±0.44 μm; n=50) round nuclei are also labelled by EdU (Figure 14E). These mesohyl DNA-synthesizing cells occurs all over sponge mesohyl: in the ectosome, endosome and tissues, adjacent to the large exhalant canals of the aquiferous system, which are structurally similar to the ectosome. The ectosome and tissues, adjacent to the large exhalant canals contain only few such mesohyl DNA-synthesizing cells (Figure 14A, C).

During the regeneration, the pattern of the cell proliferation dramatically changes (Figure 15). Immediately after the surgical operation, the level of the cell proliferation in the tissues, adjacent to the wound, decreases sharply: at 0-6 hpo, DNA-synthesizing cells are completely absent in a 100-μm zone below the wound surface (Figure 15A); at 6–12 hpo and 0-24 hpo, rare DNA-synthesizing cells appear in the tissues, located 30–40 μm below the wound surface. The majority of the labelled cells are choanocytes from disintegrating choanocyte chambers, however some mesohyl cells are also labelled. Similarly, to the intact tissues, the labelled choanocytes have small (3.85±0.4 μm; n=13) round to oval nuclei, while labelled mesohyl cells are characterized by large (4.79±0.37 μm; n=16) round nuclei.

After 24 hpo, further changes in the cell proliferation pattern occurs in the regeneration area. The samples at 24-48 hpo and 48-72 hpo show a similar pattern (Figure 15B, D): in a 100-μm zone below the wound surface, numerous DNA-synthesizing cells occur. Some of these cells are located just beneath the wound surface. Virtually all labeled cells are located in the mesohyl, since the choanocyte chambers disappear in the tissues, adjacent to the wound, by this time. These DNA-synthesizing cells have large (4.99±0.39 μm; n=16) round nuclei, similar to EdU-labelled mesohyl cells from intact tissues. Occasionally, single DNA-

synthesizing choanocytes occur in the tissues, located 60-70 µm below the wound surface, where intact choanocyte chambers could be retained.

At 120-144 hpo, after the recovery of ectosome and endosome structure in the regeneration area, the cell proliferation returns to the normal state, showing the intact pattern with majority of DNA-synthesizing cells, occurring in choanocyte chambers. However, the level of cell proliferation is still lower than in intact tissues (Figure 15E).

In the tissues, distant from the wound, the intact cell proliferation pattern persists during the whole regeneration process (Figure 15F).

Apoptosis

We found no apoptotic cell in the intact tissue of *A. cavernicola*.

Two waves of apoptosis occur during the regeneration process. The level of apoptosis is low during both waves with few apoptotic cells, located only at the upper part of the wound. In the endosome under the wound and in tissues distant from the zone of regeneration apoptotic cells are completely absent.

The first wave is associated with the early stages of regeneration. Apoptotic cells appear at 6 hpo, and their number gradually decline during further regeneration (Figure 16A). At 12 hpo only single apoptotic cells occur at the upper parts of the wound area (Figure 16B), while at 24 hpo they are virtually absent. Apparently, this wave of apoptosis participates in the elimination of damaged cells from the wound area.

The second wave of apoptosis occurs at 48 hpo, when relatively numerous apoptotic cells appears at the upper parts of the wound area (Figure 16C). This wave is probably associated with the active elimination of cells through the emerging exopinacoderm during later stage of regeneration (Figure 11E,F).

Discussion

1 General

***In vivo* observations**

Sponges are well known for their capacity to regenerate not only small body parts, but also after substantial partial mortality and damage. *In situ* monitoring of naturally and experimentally generated wounds confirms high recovery capacity of sponges from different taxa and of different growth forms (Connes, 1966, 1968; Ayling, 1983; Hoppe, 1988; Duckworth, 2003; Henry & Hart, 2005; Wulff, 2010, 2013). These studies also discovered

that regeneration can be influenced both by characteristics of the wound and by inherent characteristics of particular species of sponges.

Our observations *in situ* showed that wound epithelialization under natural conditions occurs in *Aplysina cavernicola* during two days. Other investigations provided with different demosponges showed the same results (Maas, 1910; Brondsted, 1953; Connes, 1966, 1968; Korotkova & Nikitin, 1969; Korotkova et al., 1983; Diaz, 1979; Hoppe, 1988; Hofmann et al., 2003; Wulff, 2010, 2013; Alexander et al., 2014; Borisenko et al., 2015; Pozzolini et al., 2019).

Previous investigations of regeneration demonstrated that in many individuals of the same species the amount of damage, type of damage, size of the sponge, and location on the individual sponge can influence recovery, and even susceptibility to further damage by other agents (Henry & Hart, 2005; Wulff, 2010, 2013). However, we find small individual variability during regeneration of *A. cavernicola*, probably because the wounds were applied in the same areas of the sponges and had the same size.

Histological observations

In this work we showed that regeneration processes in *Aplysina cavernicola* in general follow the stages similar to those described in other massive sponges with leuconoid aquiferous system - Demospongiae and Homoscleromorpha (Brondsted, 1953; Korotkova & Nikitin, 1969; Diaz, 1979; Hofmann et al., 2003; Borisenko et al., 2015; Ereskovsky et al., 2015; Pozzolini et al., 2019), and in various eumetazoans (Korotkova, 1997; Carlson, 2003). Therefore, *A. cavernicola* regeneration includes three main stages: 1) internal milieu isolation - formation of "regenerative clot", 2) wound healing - epithelization, and 3) restoration of damaged structures - ectosome and endosome. The wound epithelization in *A. cavernicola* occurs without formation of the regenerative membrane, a structure, characteristic for regeneration of asconoid and syconoid calcareous sponges (Jones, 1957; Korotkova, 1961, 1962; Ereskovsky et al., 2017; Lavrov et al., 2018).

The main mechanisms of *Aplysina cavernicola* reparative regeneration of the body wall are (1) cell dedifferentiation with their subsequent redifferentiation, (2) transdifferentiation, and (3) active migration of polypotent cells (archaeocytes and choanocytes) to the wound. The same basic mechanisms are also characteristic for regeneration in other studied demosponges: *Halichondria panicea* (Korotkova & Nikitin, 1969), *Suberites massa* (Diaz, 1979), *Halisarca dujardinii* (Borisenko et al., 2015), and *Suberites domuncula* (our unpublished results). However, these mechanisms strongly differ from those, participating in

regeneration process in calcareous sponges and homoscleromorphs, which show clear epithelial organization with specialized cell junctions in the epithelia (Ereskovsky et al., 2015; Lavrov et al., 2018).

2. Morphogenetic mechanisms of *A. cavernicola* regeneration

Main morphogenesis during body wall regeneration in *A. cavernicola* is mesenchymal-to-epithelial transformation (MET). Indeed, at 12 hpo archaeocytes and dedifferentiated choanocytes as well as the spherulous cells begin to move toward wound area, where they form a blastema-like structure. Part of external blastema cells begins to flat and form cover sponge epithelium (exopinacoderm) through the MET.

However, experimentally induced (by surgical operation) epithelial-to-mesenchymal transition (EMT) proceeds MET in *A. cavernicola*. During this process choanocytes and endopinacocytes leave the choanocyte chambers and the canals of aquiferous system, correspondingly, and move into the mesohyl, dedifferentiating and assuming an amoeboid shape. This morphogenesis is one of central for the creation of numerous organs and complex tissues during embryonic development, asexual reproduction, and regeneration and has been well described in Eumetazoa (Keller et al., 2003; Lim & Thiery, 2012). EMT is also well known during the normal ontogeny of sponges and occurs in the course of embryonic development, and larval metamorphosis (reviewed in Ereskovsky et al. 2013). This morphogenesis was described during the first stages of regeneration of other investigated demosponges and homoscleromorphs (Korotkova & Nikitin, 1969; Borisenko et al., 2015; Ereskovsky et al., 2015).

After wound epithelization, the restoration of elements of the aquiferous system begins. Both choanocyte chambers and aquiferous system canals are formed through MET: separate amoeboid cells coalescence into groups and gradually transform from mesenchymal morphology to epithelial-like cells (choanocytes and endopinacocytes, respectively).

The same MET mechanism is characteristic for exopinacoderm and choanoderm formation during regeneration of other investigated demosponges: *Halichondria panicea* (Korotkova & Nikitin, 1969), *Halisarca dujardini* (Borisenko et al., 2015), and basopinacoderm formation in *Hymeniacidon heliophila* regeneration (Coutinho et al., 2017).

It is fundamentally different from the regeneration in Calcarea and Homoscleromorpha, in which epithelial morphogenesis, e.g. flattening and spreading of epithelial layers, plays a leading role in the restoration of main structures (exopinacoderm and elements of aquiferous system) (Ereskovsky et al., 2015; Lavrov et al., 2018).

3. Blastema

In regenerative biology blastema is a mass of undifferentiated cells, located beneath the wound and produced by the dedifferentiation of many cell types and/or migration of polypotent cells. In some cases, differentiation of blastema cells, and further reconstruction the lost part of the body could be accompanied with cell proliferation. In this case, the mitotic rate of the blastema slows down as the structure grows, and it ceases completely when the new structure reaches the original size (Santos-Ruiz et al., 2002; Carlson, 2007; Tsonis, 2008; Vervoort, 2011).

The formation of a concentration of cells under the wound in the middle stages of a body wall regeneration has been shown for several demosponges (Thiney, 1972; Boury-Esnault, 1976; Borisenko et al., 2015; Coutinho et al., 2017). This cellular concentration consists of archaeocytes and choanocytes, which are principal stem cells of demosponges (Funayama, 2018), dedifferentiated cells (e.g., pinacocytes) and specialized differentiated cells (e.g., gray cells) (Thiney, 1972; Boury-Esnault, 1976; Borisenko et al., 2015; Coutinho et al., 2017). This structure could be referred as a blastema, characteristic for a regeneration in many animals.

Similarly, in the current study, we refer to the undifferentiated cell mass beneath a wound during the end of second and beginning of third stages of regeneration in *A. cavernicola* as a blastema. In *A. cavernicola,* it consists of archaeocytes, dedifferentiated choanocytes, mixed population of anucleated amoebocytes (dedifferentiated pinacocytes, myocytes, lophocytes), and differentiated spherulous cells.

At early stages of regeneration, the blastema almost devoid of DNA-synthesizing cell, but after 24 hpo and up to 72 hpo numerous DNA-synthesizing cells appears there. However, even during this period the level of cell proliferation in the blastema is much lower in comparison with intact sponge tissues. In contrast, intact tissues distant form the wound retains intact level of cell proliferation during whole regeneration process. The similar pattern of cell proliferation has been described during body wall regeneration of *Halisarca caerulea* (Alexander et al., 2014) and *Halisarca dujardinii* (Borisenko et al., 2015), for which decreased proliferation in the wound area is characteristic.

Moreover, in contrast to intact tissues of *A. cavernicola,* where vast majority of DNA-synthesizing cells are choanocytes, all EdU-labeled cells in the blastema are mesohyl cells, as blastema lacks choanocyte chambers. These EdU-labeled cells could arise directly in blastema through cell divisions or be EdU-labeled migrating descendants of proliferating cells in intact

tissues, distant from the wound. This issue requires further investigations, using additional markers, like antibodies against phospho-histone H3 for reveling cells in M-phase and cell tracers for the visualization of cell migrations.

Importantly, studied sponges from classes Calcarea (*Leucosolenia* cf. *variabilis*) (Lavrov et al., 2018) and Homoscleromorpha (*Oscarella lobularis*) (Ereskovsky et al., 2015) demonstrate a distinct mode of regeneration without blastema formation. In these sponges regeneration occurs due to the local remodeling of intact tissues, adjacent to the wound. Moreover, the cell proliferation is neither affected nor contributes to the regeneration at any stage.

4. Dedifferentiation, transdifferentiation and cell sources in *A. cavernicola* regeneration

Transdifferentiation is the transformation of one type of already differentiated cell into another type of differentiated cell. In some cases, transdifferentiation is accompanied by cell division, while in other cases it is not (Shen et al., 2004).

Sponge cell transdifferentiation is likely a driving force accompanying their restoration processes (Korotkova, 1997; Lavrov & Kosevich, 2014; Adamska, 2018). However, transdifferentiating cell types and mechanisms of this process vary in different sponge species (Diaz, 1979; Gaino et al., 1995; Korotkova, 1997; Ereskovsky et al., 2015; Borisenko et al., 2015; Lavrov & Kosevich, 2016; Lavrov et al., 2018). For example, direct transdifferentiation of cells in intact epithelia (pinacocytes and choanocytes) has been demonstrated during the reparative regeneration of the homoscleromorph *Oscarella lobularis* (Ereskovsky et al., 2015), the calcareous sponges *Sycon lingua* (Korotkova, Efremova, & Kadantseva, 1965; Korotkova, 1972b), and *Leucosolenia* ssp. (Lavrov et al., 2018). In these cases, the layer of choanocytes transdifferentiates into layer of pinacocytes without loss of epithelial structure, without mesenchymal-to-epithelial transformation, and without contribution from cell proliferation.

Cell transdifferentiation have also been described during reparative regeneration in all investigated demosponges (for review see: Korotkova, 1997; Borisenko et al., 2015). While archaeocytes directly differentiate into new cells, choanocytes and pinacocytes undergo transdifferentiation to give rise for other cell types. It is characteristic, mainly, for choanocytes from disintegrated choanocyte chambers, which can transdifferentiate, for example, into exopinacocytes (Korotkova & Nikitin, 1969a,b; Borisenko et al., 2015). Endopinacocytes in a less extent could also transdifferentiate into exopinacocytes (Thiney,

1972; Borisenko et al., 2015). The principal difference of the transdifferentiation in demosponges in comparison with Homoscleromorpha + Calcarea lineage is an occurrence of the disruption of epithelial layers and cell dedifferentiation prior to this process in the demosponges.

The similar processes were observed during *A. cavernicola* regeneration. The archaeocytes and dedifferentiated cells participate in the restoration of the lost structures in this sponge. We identify two cells types, which undergo dedifferentiation during *A. cavernicola* regeneration: choanocytes, spherulous cells, and population of anucleated cells of mesohyl, including dedifferentiated pinacocytes, myocytes, and lophocytes. The choanocytes, despite their dedifferentiation and loss of the flagella and collars of microvilles, are well distinguished on ultrathin sections due to the persistence of two centrioles in their apical part. Anucleated amoebocytes differ from archaeocytes by a smaller nucleus without nucleolus and the presence of small phagosomes. The dedifferentiation of the spherulous cells through a complete or almost complete loss of specific inclusions (spherules) was completely unexpected process. However, the dedifferentiation of spherulous cells is not so rapid, as in other dedifferentiating cells, because of high specialization of these secretory cells.

We identified two main cellular sources for the restoration of the lost tissue and structures in *A. cavernicola*: archaeocytes and choanocytes. Both cell types contribute to the restoration of the exopinacoderm and choanocyte chambers. The restoration of the choanocyte chambers is carried out mainly due to the redifferentiation of the choanocytes, and to lesser extent due to the differentiation of archaeocytes.

However, the future of dedifferentiated anucleated amoebocytes and spherulous cells could not be traced. This issue requires the search and use of a special marker of these cells. It is possible that dedifferentiated pinacocytes and spherulous cells could also participate in the formation of the new exopinacoderm.

According to last investigations in Porifera there are not only two types of adult stem cells (ASC): archaeocytes and choanocytes (Funayama, 2018), but at least four, including pinacocytes and particular amoeboid vacuolar cells (Ereskovsky et al., 2015; Fierro-Constain et al., 2017; Lavrov et al., 2018).

There are the differences in these ASC distributions among different sponge classes. In Demospongiae the principal (pluripotent) ASC are archaeocytes and choanocytes, however the experiments with their regeneration (including present data on *A. cavernicola* regeneration) and dissociated cells aggregation demonstrated, that pinacocytes could also be ASC (Korotkova & Nikitin, 1969a,b; Borisenko et al., 2015; Lavrov & Kosevich, 2016;

Ereskovsky et al., 2016). In Calcarea archaeocytes absent and pluripotent ASC in these sponges are choanocytes and pinacocytes (Korotkova, 1961a, 1962b; Korotkova & Gelihovskaia, 1963; Lavrov et al., 2018). In Homoscleromorpha the pluripotent ASC are as in Calcarea the choanocytes and pinacocytes, but also mesohyl amoeboid vacuolar cells (Gaino et al., 1986; Ereskovsky, 2010; Ereskovsky et al., 2015; Fierro-Constain et al., 2017).

5. Spherulous cells and their role in regeneration

Similarly, to intact tissues of *A. cavernicola* (Vacelet, 1967), two principal morphotypes of spherulous cells occurs in the wound area of this sponge: larger cells with clear inclusions and smaller ones with dense inclusions. In fact, these morphotypes represent different stages of the ontogenesis of spherulous cells (Vacelet, 1967). According to Vacelet (1967) in intact sponge "dense" small spherulous cells concentrate mostly in the ectosome and around big exhalant canals, while "clear" larger ones are distributed in the mesohyl of endosome.

We have detected that in *A. cavernicola* the wound surface was free from invasive microbes from the first hours after injury up to the end of the regeneration. All microbes, that we detected at the wound surface and in the wound area during regeneration, shows ultrastructure identical to the microbes, located in the deeper sponge tissues and described as symbiotic in the previous papers (Vacelet, 1975; Fiedrich et al., 1999; Hentschel et al., 2001). Such defense against invasive microbes is probably provided by the particular chemical substances in the spherulous cells.

X-ray microanalysis revealed that these specialized cells of *Aplysina* produce and store brominated metabolites (Turon et al., 2000). Turon et al. (2000) demonstrated that the concentration of bromine peaks is slightly higher in the spherules from "dense" spherulous cells than in "clear" ones. Thompson et al. (1983) have detected bromine in the spherulous cells of Caribbean *Aplysina fistularis*. Spherulous cells have been shown to produce defense metabolites in other species (Thompson et al., 1983; Bretting et al., 1983; Uriz et al., 1996a).

In addition, it was showed that tissue damage in *Aplysina* induces a bioconversion of isoxazoline alkaloids into aeroplysinin-1 and secondary metabolite dienone (Thoms et al., 2006). This reaction is likely catalyzed by enzymes, and it may be ecologically important as the dienone has the strong antibacterial power and toxicity (Reverter et al., 2016). Moreover, this injury-induced reaction takes place within less than 1 min after wounding (Thoms et al., 2006).

6. Apoptosis during *A. cavernicola* regeneration

We have directly visualized and investigated apoptosis in the regeneration of sponges for the first time. The only previous data on the involvement of apoptosis in sponge regeneration emerge from the comparative transcriptomic analysis of the early stages of body wall regeneration in *Halisarca caerulea* (Kenny et al., 2017).

We have observed two waves of apoptosis during *Aplysina cavernicola* regeneration. The first wave, occurring around 6 hpo, is probably involved in the elimination of damaged cells and is characteristic for the early stages of regeneration of various animals, from cnidarians to vertebrates (Vlaskalin et al., 2004; Tseng et al., 2007; Chera et al., 2009; Pellettiere et al., 2010; DuBuc et al., 2014; Brandshaw et al., 2015; Kenny et al., 2017; Cebrià et al., 2018). For *Hydra* head regeneration after mid-gastric bisection (Chera et al., 2009) and tail regeneration in tadpole larva of *Xenopus laevis* (Tseng et al., 2007) it was shown that early wave of apoptosis not only clean a wound from damaged cells, but also generate signals, essential for initiation of subsequent regenerative processes. Inhibition of this apoptotic wave completely abolishes the regeneration. In particular, in both cases, apoptotic cells initiate a synchronous burst of proliferative activity in neighboring cells (Tseng et al., 2007; Chera et al., 2009), which is similar to the well-known apoptosis-induced compensatory proliferation in the imaginal disks of *Drosophila* (Fan & Bergmann, 2008; Bergmann & Steller, 2010). Apoptotic cells may be involved in the proliferation induction also during *A. cavernicola* body wall regeneration, as numerous DNA-synthesizing cells appears in the blastema only after the first apoptotic wave, at 24 hpo. These observations illustrate a novel active instructing role of apoptosis in morphogenetic processes, in contrast to its canonical passive role as a destructive agent (Duffy, 2012).

The second wave of apoptosis during *A. cavernicola* regeneration is likely associated with the extensive thrown out of spherulous cells though the forming exopinacoderm. Spherulous cells of *A. cavernicola* demonstrate the similar behavior in the intact sponges. Being one of the few terminally differentiated sponge cell lines, spherulous cells leave the mesohyl through aquiferous system canals or external surfaces (Vacelet, 1967). Their release outside from sponge is part of their normal physiology and possibly involved in the release of various chemicals (Uriz et al., 1996a; Ternon et al., 2016) and/or discharge processes (Maldonado, 2016) to the environment. The ultrastructure of spherulous cells eliminated through the exopinacoderm during the third phase of *A. cavernicola* regeneration is identical to that of the spherulous cells at the last stage of their evolution (Vacelet, 1967). Similarly, in the intact tissues of *H. caerulea*, many caspase-3 positive cells have a spherulous cell morphology (De Goeij et al., 2009), which indicates that apoptosis involved in the waste

control system in sponges in addition to maintaining tissue homeostasis (De Goeij et al., 2009).

Thus, the described increase in the level of apoptosis at the late stages of the *A. cavernicola* regeneration could be referred as a general tissue response, involved in the restoration of the normal sponge physiology in the area of injury, rather than in regeneration process itself. In planarians, the similar late general apoptotic response is also described, but it participates in the intensive remodeling of intact tissues, adjacent to a wound, to restore proper scale and proportions (Pellettiere et al., 2010; Cebrià et al., 2018).

Conclusion

Finally, we can made some principal conclusions:

1. In Porifera there are two principal mode of reparative regeneration: blastemal regeneration and tissue remodeling. From the literature data and results, obtained in this work we can conclude that first mode is characteristic for Demospongiae regeneration and the second – for Calcarea + Homoscleromorpha clade.

2. The results of our research also showed that sponges have more than two lines of adult stem cells, the potencies of which are clearly manifested during reparative regeneration. Our data support previous investigations, showed that archaeocytes and choanocytes are main players, or principal adult stem cells during demosponges regeneration (Korotkova & Nikitin, 1969; Thiney, 1972; Boury-Esnault, 1976; Diaz, 1979; Borisenko et al. 2015). However, the pinacocytes also could be considered as multipotent stem cells. Moreover, for the first time we showed, that spherulous cells of *Aplysina cavernicola* have a capacity to dedifferentiation during regeneration. It is first evidence that highly specialized cells of demosponges have capacity to dedifferentiation and possibly transdifferentiation.

3. Cell transdifferentiation plays an extremely significant role in sponge regeneration, as we have shown that regardless of the phylogenetic position, type of aquiferous system, and structure of epithelia, all studied sponges intensively utilize it for restoration of lost structures (Borisenko et al., 2015; Ereskovsky et al., 2015, 2017; Lavrov et al., 2018).

4. For the first time was investigated apoptosis during sponge regeneration. In *Aplysina cavernicola* regeneration this processes participate in damaged cells elimination and associated with the extensive ejection of spherulous cells from wound area.

Author contributions

A.V.E. and A.I.L. designed the study, conducted the experimental procedures with the living animals; A.I.L. performed the cell proliferation studies; A.V.E. and D.B.T. performed histological and ultrastructural studies. A.V.E.: Project administration and funding acquisition; S.B., E.L.G., and A.I.L.: performed the apoptosis studies; A.V.E. and A.I.L. prepared the manuscript with contributions from all authors. All authors reviewed and approved the final manuscript.

Acknowledgements

Authors gratefully thank Alexandre Altié of Plateforme C2VN de Microscopie Électronique TIMONE, Aix-Marseille Université, France, the Electron Microscopy Laboratory of the Shared Facilities Center of Lomonosov Moscow State University sponsored by the RF Ministry of Education and Science and Research Resource Center for Molecular and Cell Technologies at St. Petersburg State University, the staff of the Common Service of morphology in IMBE, and Dr. Jean Philippe Mévy (IMBE) - for help and assistance with electron and confocal microscopy studies. Data used in this study were partly produced using the Montpellier RIO imaging platform (confocal microscopy) (Montpellier, France). This work was supported by grants of Russian Foundation for Basic Research no. 16-04-00084, the Russian Science Foundation no. 17-14-01089 (histological and ultrastructural studies), and Metchnikov fellowship 2019 by French Embassy in Russia. This work also is a contribution to Labex OT-Med (n° ANR-11-LABX-0061) and has received funding from Excellence Initiative of Aix-Marseille University-A*MIDEX, a French ''Investissements d'Avenir'' program for travel expenses.

References

Adamska, M. (2018). Differentiation and Transdifferentiation of Sponge Cells. In M. Kloc, M., Kubiak, J. Z. (Eds.), *Marine Organisms as Model Systems in Biology and Medicine, Results and Problems in Cell Differentiation* 65 (pp. 229-253). Cham, Springer. https://doi.org/10.1007/978-3-319-92486-1_12.

Ayling, A.L. (1983). Growth and regeneration rates in thinly encrusting Demospongiae from temperate waters. *Biological Bulletin, 165*, 343-352.

Azevedo, L.G., Muccillo-Baisch, A.L., Filgueira, M., Boyle, R.T., Ramos, D.F., Soares, A.D., Lerner, C., Silva, P.A. & Trindade, G.S. (2008). Comparative cytotoxic and anti-tuberculosis activity of *Aplysina caissara* marine sponge crude extracts. *Comp Biochem Physiol C Toxicol Pharmacol, 147*, 36–42. DOI: 10.1016/j.cbpc.2007.07.007.

Bergquist, P. & Cook, S. (2002). Family Aplysinidae Carter, 1875. In Hooper, J.N.A., Van Soest, R.W.M. (Eds.), *Systema Porifera: A Guide to the Classification of Sponges*. (pp. 1082-1085). NY, Kluwer Academic/Plenum Publishers.

Bergmann, A., & Steller, H. (2010). Apoptosis, stem cells, and tissue regeneration. *Sci. Signal*, *3*, 1–8. https://doi.org/10.1126/scisignal.3145re8

Betancourt-Lozano, M., González-Farias, F.A., González-Acosta, B., & García-Gasca, A. (1998). Variation of antimicrobial activity of the sponge *Aplysina fistularis* (Pallas, 1766) and its relation to associated fauna. *J Exp Mar Biol Ecol, 223*, 1–18.

Borisenko, I.E., Adamska, M., Tokina, D.B., & Ereskovsky, A.V. (2015). Transdifferentiation is a driving force of regeneration in *Halisarca dujardini* (Demospongiae, Porifera). *PeerJ*, *3*, e1211. https://doi.org/10.7717/peerj.1211

Boury-Esnault, N. (1976). Morphogenese experimentale des papilles inhalantes de l'eponge *Polymastia mamillaris* (Muller). *Arch. Zool. Exp. Gén.*, *117*(2), 181–196.

Bradshaw, B., Thompson, K., & Frank, U. (2015). Distinct mechanisms underlie oral vs aboral regeneration in the cnidarian *Hydractinia echinata*. *Elife 2015*, 1–19. doi.org/10.7554/eLife.05506.

Brondsted, H.V. (1953). The ability to differentiate and the size of regenerated cells after repeated regeneration. *Quart Journal of Microscopy Sciences,* 94, 177-184.

Carlson, B.M. (2007). *Principles of regenerative biology*. New York: Academic Press.

Cavolini, F. (1785). Memorie per servire alia storia dei polipi marini. Napoli, 1785. (Cited by Cotte, 1908.)

Bretting H., Jacobs, G., Donadey, C., & Vacelet, J. (1983). Immunohistochemical

studies on the distribution and the function of the D. galactose-specific lectins in the sponge *Axinella polypoides* (Schmidt). *Cell and Tissue Research*, *229*, 551-571.

Cebrià, F., Adell, T., & Saló, E. (2018). Rebuilding a planarian: from early signaling to final shape. *International Journal of Developmental Biology, 62*, 537–550. https://doi.org/10.1387/ijdb.180042es

Chera, S., Ghila, L., Dobretz, K., Wenger, Y., Bauer, C., Buzgariu, W., Martinou, J.-C., & Galliot, B. (2009). Apoptotic Cells Provide an Unexpected Source of Wnt3 Signaling to Drive *Hydra* Head Regeneration. *Development & Cells, 17*, 279–289. doi.org/10.1016/j.devcel.2009.07.014.

Ciminiello, P., Fattorusso, E., Forino, M., Magno, S., & Pansini, M. (1997). Chemistry of Verongida sponges. 8. Bromocompounds from the Mediterranean sponges *Aplysina aerophoba* and *Aplysina cavernicola*. *Tetrahedron, 53,* 6565-6572.

Connes, R. (1966). Contribution a l'etude histologique des premiers stades d'embryogenese somatique chez *Tethya lyncurium* Lamarck. *Bull Soc Zool France, 91*, 639-645.

Connes, R. (1968). Etude histologique, cytologique et expérimentale de la régénération et de la reproduction asexuée chez *Tethya lyncurium* Lamarck (=*T. aurantium* Pallas (Démosponges). (PhD Thesis, Fac. Sci. Montpellier).

Coutinho, C.C., Rosa, I.A., Teixeira, J.D.O., Andrade, L.R., Costa, M.L., & Mermelstein, C. (2017). Cellular migration, transition and interaction during regeneration of the sponge *Hymeniacidon heliophila*. *PLoS One, 12, 5*. e0178350. DOI : 10.1371/journal.pone.0178350.

D'Ambrosio, M., Guerriero, A., Traldi, P., & Pietra, F. (1982). Cavernicolin-1 and cavernicolin-2, two epimeric dibromolactams from the Mediterranean sponge *Aplysina (Verongia) cavernicola*. *Tetrahedron Letters, 23,* 4403-4406.

D'Ambrosio, M., Guerriero, A., De-Clauser, R., De-Stanchina, G., & Pietra, F. (1983). Dichloroverongiaquinol, a new marine antibacterial compound from *Aplysina cavernicola*. Isolation and synthesis. *Experientia, 39,* 1091-1092.

De Goeij, J.M., De Kluijver, A., Van Duyl, F.C., Vacelet, J., Wijffels, R.H., De Goeij, A.F.P.M., Cleutjens, J.P.M., & Schutte, B. (2009). Cell kinetics of the marine sponge *Halisarca caerulea* reveal rapid cell turnover and shedding. *The Journal of Experimental Biology, 212*, 3892-3900. DOI: 10.1242/jeb.034561.

de Mendiburu, F. (2019). agricolae: Statistical Procedures for Agricultural Research. R package version 1.3-1. https://CRAN.R-project.org/package=agricolae

Diaz, J.P. (1979). Variations, differentiations et functions des categories cellulaires de la demosponge d'eaux saumatres, *Suberites massa*, Nardo, au cours du cycle biologique annuel et dans des conditions experimentales. These doct. Acad Montpellier

DuBuc, T.Q., Traylor-Knowles, N., & Martindale, M.Q. (2014). Initiating a regenerative response; cellular and molecular features of wound healing in the cnidarian *Nematostella vectensis*. *BMC Biology, 12*, 24. doi.org/10.1186/1741-7007-12-24.

Duffy, D.J. (2012). Instructive reconstruction: A new role for apoptosis in pattern formation. *BioEssays, 34*, 561–564. https://doi.org/10.1002/bies.201200018

Duckworth, A.R. (2003). Effect of wound size on the growth and regeneration of two temperate subtidal sponges. *Journal of Experimental Marine Biology and Ecology, 287*, 139–153. DOI: 10.1016/S0022-0981(02)00552-X.

Ehrlich, H., Ilan, M., Maldonado, M., Muricy, G., Bavestrello, G., Kljajic, Z., Carballo, J.L., Schiaparelli, S., Ereskovsky, A., Schupp, P., Bornk, R., Worch, H., Bazhenov, V.V., Kurek, D., Varlamov, V., Vyalikh, D., Kummer, K., Sivkov, V.V., Molodtsov, S.L., Meissner, H., Richter, G., Steck, E., Richter, W., Hunoldt, S., Kammer, M., Paasch, S., Krasokhin, V., Patzke, G., & Brunner, E. (2010a). Three-dimensional chitin-based scaffolds from Verongida sponges (Demospongiae: Porifera). Part I. Isolation and identification of chitin. *International Journal of Biological Macromolecules, 47,* 132-140. DOI: 10.1016/j.ijbiomac.2010.05.007.

Ehrlich, H., Steck, E., Ilan, M., Maldonado, M., Muricy, G., Bavestrello, G., Kljajic, Z., Carballo, J.L., Schiaparelli, S., Ereskovsky, A., Schupp, P., Bornk, R., Worch, H., Bazhenov, V.V., Kurek, D., Varlamov, V., Vyalikh, D., Kummer, K., Sivkov, V.V., Molodtsov, S.L., Meissner, H., Richter, G., Hunoldt, S., Kammer, M., Paasch, S., Krasokhin, V., Patzke, G., Brunner, E., & Richter, W. (2010 b). Three-dimensional chitin-based scaffolds from Verongida sponges (Demospongiae: Porifera). Part II: Biomimetic potential and applications. *International Journal of Biological Macromolecules, 47,* 141-145. DOI: 10.1016/j.ijbiomac.2010.05.009.

Ereskovsky, A.V., Renard, E., Borchiellini, C. (2013). Cellular and molecular processes leading to embryo formation in sponges: evidences for high conservation of processes throughout animal evolution. *Development, Genes & Evolution*, *223*, 5-22. DOI 10.1007/s00427-012-0399-3

Ereskovsky, A.V., Borisenko, I.E., Lapébie, P., Gazave, E., Tokina, D.B., & Borchiellini, C. (2015). *Oscarella lobularis* (Homoscleromorpha, Porifera) Regeneration:

Epithelial Morphogenesis and Metaplasia. *Plos One*, *10*(8), e0134566. https://doi.org/10.1371/journal.pone.0134566

Ereskovsky, A.V., Chernogor, L.I., & Belikov, S.I. (2016). Ultrastructural description of development and cell composition of primmorphs in the endemic Baikal sponge *Lubomirskia baicalensis*. *Zoomorphology*, *135*(1), 1–17. https://doi.org/10.1007/s00435-015-0289-0

Ereskovsky, A.V., Lavrov, A.I., Bolshakov, F.V., & Tokina, D.B. (2017). Regeneration in White Sea sponge *Leucosolenia complicata* (Porifera, Calcarea). *Invertebrate Zoology*, *14*(2), 108–113. https://doi.org/10.15298/invertzool.14.2.02

Fiedrich, A.B., Merkert, H., Fendert, T., Hacker, J., Proksch, P., & Hentschel, U. (1999). Microbial diversity in the marine sponge *Aplysina cavernicola* (formerly *Verongia cavernicola*) analyzed by fluorescence in situ hybridization. *Marine Biology, 134,* 461-470.

Fan, Y. & Bergmann, A. (2008). Apoptosis-induced compensatory proliferation. The Cell is dead. Long live the Cell! *Trends Cell Biology, 18*, 467–473. https://doi.org/10.1016/j.tcb.2008.08.001

Fox, J. & Weisberg, S. (2019). An {R} Companion to Applied Regression (3rd ed.). Thousand Oaks CA: Sage.

Funayama, N. (2018). The cellular and molecular bases of the sponge stem cell systems underlying reproduction, homeostasis and regeneration. *International Journal of Developmental Biology, 62*(6-8), 513–525. https://doi.org/10.1387/ijdb.180016nf

Gaino, E., Manconi, R., & Pronzato, R. (1995). Organizational plasticity as a successful conservative tactics in sponges. *Animal Biology, 4,* 31-43.

Gallissian, M.F., & Vacelet J. (1976). Ultrastructure de quelques stades de l'ovogenèse de spongiaires du genre *Verongia* (Dictyoceratida). *Annales des Sciences Naturelles, Biologie Animale, 18*, 381-404.

Garrone R., Vacelet, J., Pavans de Ceccatty, M., Junqua, S., & Robert, L. (1973). Une formation collagene particuliere: les filaments des Eponges cornées *Ircinia*. Etude ultrastructurale, physico-chimique et biochimique. *Journal de Microscopie, 17,* 241-260.

Henry, L-F., & Hart, M. (2005). Regeneration from Injury and Resource Allocation in Sponges and Corals – a Review. *International Review in Hydrobiology, 90,* 125–158.

Hentschel, U., Schmid, M., Wagner, M., Fieseler, L., Gernert, C., & Hacker, J. (2001). Isolation and phylogenetic analysis of bacteria with antimicrobial activities from the Mediterranean sponges *Aplysina aerophoba* and *Aplysina cavernicola*. *FEMS Microbiol Ecol, 35,* 305-312.

Hoffmann, F., Rapp, H.T., Zoller, T., & Reitner, J. (2003). Growth and regeneration in cultivated fragments of the boreal deep water sponge *Geodia barretti* Bowerbank, 1858 (Geodiidae, Tetractinellida, Demospongiae). *Journal of Biotechnology, 100,* 109-118.

Hoppe, W.F. (1988). Growth, regeneration and predation in three species of large coral reef sponges. *Marine Ecology Progress Series, 50*: 117-125. DOI: 10.1016/s0168-1656(02)00258-4.

Keller, R., Davidson, L.A., & Shook, D.S. (2003). How we are shaped: the biomechanics of gastrulation. *Differentiation, 71*, 171-205. DOI:10.1046/j.1432-0436.2003.710301.x.

Korotkova, G.P. (1961). Regeneration and somatic embryogenesis in the calcareous sponge *Leucosolenia complicata* Mont. *Acta Biologica Academiae Scientiarum Hungaricae, 11*(4), 315–334.

Korotkova, G.P. (1972a). Comparative morphological investigations of development of sponges from dissociated cells. *Transactions of Leningrad Society of Naturalists, 78*(4), 74–109.

Korotkova, G.P. (1972b). Regeneration of the calcareus sponge *Sycon lingua*. *Transactions of Leningrad Society of Naturalists, 78*(4), 155–169.

Korotkova, G.P. (1997). *Regeneration in animals*. Saint-Petersburg: Saint-Petersburg University Press.

Korotkova, G.P., Efremova, S.M., & Kadantseva, A.G. (1965). The pecularities of morphogenesis of the development of *Sycon lingua* from the small part of the body. *Vestnik of Leningrad University*, *4*(21), 14–30.

Korotkova, G.P., & Nikitin, N.S. (1969). The comparative morphological analysis of regeneration and somatic embryogenesis of the cornacusponge *Halichondria panicea*. In B. P. Tokin (Ed.), *Reconstructional processes and immunological reactions. Morphological investigations of different stages of development of the marine organisms* (pp. 9–16). Leninrad: Nauka.

Korotkova, G.P., Sukhodolskaya, A.N., & Krasukevitch, T.N. (1983). The pecularities of morphogenesis of the development of *Halisarca dujardini* from the small part of the body. *Vestnik Leningrad University*, *9*, 41–46.

Lavrov, A.I., & Kosevich, I.A. (2016). Sponge cell reaggregation: Cellular structure and morphogenetic potencies of multicellular aggregates. *Journal of Experimental Zoology Part A: Ecological Genetics and Physiology, 325*(2), 158–177. https://doi.org/10.1002/jez.2006

Lavrov, A.I., Bolshakov, F.V., Tokina, D.B., & Ereskovsky, A.V. (2018). Sewing wounds up: the epithelial morphogenesis as a central mechanism of calcaronean sponge regeneration. *Journal of Experimental Zoology Part B: Molecular and Developmental Evolution. 330*(6-7): 351-371. https://doi.org/10.1002/jezb.22830

Lim, J., & Thiery, J.P. (2012). Epithelial-mesenchymal transitions: insights from development. *Development, 139*, 3471-3486. doi:10.1242/dev.071209.

Maas, O. (1910). Über Nichtregeneration bei Spongien. *Zeitschrift fur R. Hertwig, 3,* 93-130.

Maldonado, M. (2016). Sponge waste that fuels marine oligotrophic food webs: a re-assessment of its origin and nature. *Marine Ecology, 37,* 477-491. DOI : 10.1111/maec.12256.

Pellettieri, J., Fitzgerald, P., Watanabe, S., Mancuso, J., Green, D.R., & Sánchez Alvarado, A.S. (2010). Cell death and tissue remodeling in planarian regeneration. *Developmental Biology, 338,* 76–78. doi.org/10.1016/j.ydbio.2009.09.015

Pozzolini, M., Gallus, L., Ghignone, S., Ferrando, S., Candiani, S., Bozzo, M., Bertolino, M., Costa, G., Bavestrello, G., & Scarfì, S. (2019). Insights into the evolution of metazoan regenerative mechanisms: roles of TGF superfamily members in tissue regeneration of the marine sponge *Chondrosia reniformis*. *Journal of Experimental Biology,* 222, jeb207894. doi:10.1242/jeb.207894.

R Core Team (2019). R: A language and environment for statistical computing. R Foundation for Statistical Computing, Vienna, Austria. https://www.R-project.org/

Reverter, M., Perez, T., Ereskovsky, A., & Banaigs, B. (2016). Secondary Metabolome Variability and Inducible Chemical Defenses in the Mediterranean Sponge *Aplysina cavernicola. Journal of Chemical Ecology*, *42*, 60-70. doi: 10.1007/s10886-015-0664-9

Sukhodolskaya, A.N. (1973). The mechanism of oscular tube restoration in *Ephydatia fluviatilis* (L). In Tokin, B.P. (Ed.), *Morphogenetic Processes during Asexual Reproduction, Somatic Embryogenesis and Regeneration*. (pp. 127-145), Leningrad State University. Leningrad.

Ternon, E., Zarate, L., Chenesseau, S., Croue, J., Dumollard, R., Suzuki, M.T., & Thomas, O.P. (2016). Spherulization as a process for the exudation of chemical cues by the encrusting sponge *C. crambe*. *Sci Rep, 6,* 29474. DOI : 10.1038/srep29474

Thiney, Y. (1972). Morphologie et cytochimie ultrastructurale de l'oscule *d'Hippospongia communis* LMK et de sa régénération (Ph.D. thesis, University Claude Bernard, Lyon).

Thompson, J.A., Barrow, K.D. & Faulkner, D.J. (1983). Localization of Two Brominated Metabolites, Aerothionin and Homoaerothionin, in Spherulous Cells of the Marine Sponge *Aplysina fistularis* (= *Verongia thiona*). *Acta Zoologica, 64,* 199-210.

Thoms, C., Horn, M., Wagner, M., Hentschel, U., & Proksch P. (2003). Monitoring microbial diversity and natural product profiles of the sponge *Aplysina cavernicola* following transplantation. *Marine Biology. 142,* 685–692. DOI https://doi.org/10.1007/s00227-002-1000-9

Thoms, C., Wolff, M., Padmakumar, K., Ebel, R., & Proksch, P. (2004). Chemical defense of Mediterranean sponges *Aplysina ca*vernicola and *Aplysina aerophoba*. Zeitschrift fur *Naturforschung C J Bioscience, 59*, 113–122. DOI: 10.1515/znc-2004-1-222.

Thoms, C., Ebel, R., & Proksch, P. (2006). Activated chemical defense in *Aplysina* sponges revisited. *Journal of Chemical Ecology, 32*, 97–123.

Tseng, A.-S., Adams, D.S., Qiu, D., Koustubhan, P., & Levin, M. (2007). Apoptosis is required during early stages of tail regeneration in *Xenopus laevis*. *Developmental Biology, 301*, 62–69. https://doi.org/10.1016/j.ydbio.2006.10.048

Turon, X., Becerro, M.A., & Uriz, M.J. (2000). Distribution of brominated compounds within the sponge *Aplysina aerophoba*: coupling of X-ray microanalysis with cryofixation techniques. *Cell and Tissue Research. 301,* 311-322.

Uriz, M.J., Becerro, M.A., Tur, J.M., & Turon, X. (1996). Location of toxicity within the Mediterranean sponge *Crambe crambe* (Demospongiae: Poecilosclerida). *Marine Biology, 124*, 583–590.

Vaillant, L. (1869). Note sur la vitalité d'une Sponge de la famille des Corticatae, la *Tethya lyncurium*. *Comptes rendus de 1'Académie des Sciences*, t. Lxviii.

Vacelet, J. (1959). Répartition générale des éponges et systématique des éponges cornées de la région de Marseille et de quelques stations méditerranéennes. *Recueil des travaux de la Station Marine d'Endoume, 16*, 39-101.

Vacelet, J. (1966). Les cellules contractiles de l'éponge cornée *Verongia cavernicola* Vacelet. *Comptes-Rendus de l'Académie des Sciences de Paris, 263,* 1330-1332.

Vacelet, J. (1967). Les cellules à inclusions de l'éponge cornée *Verongia cavernicola* Vacelet. *Journal de Microscopie (Paris), 6,* 237-240.

Vacelet, J. 1970. Description de cellules a bactéries intranucléaires chez des éponges *Verongia*. *Journal de Microscopie (Paris), 9,* 333-346.

Vacelet J. (1971a). Ultrastructure et formation des fibres collagénes de spongine d'Eponges Cornées *Verongia*. *Journal de Microscopie (Paris), 10,* 13-32.

Vacelet, J. (1971b). L'ultrastructure de la cuticule d'Eponges Cornées *Verongia*. *Journal de Microscopie (Paris), 10,* 113-116.

Vacelet, J. (1975). Etude en microscopie électronique de l'association entre bactéries et spongiaires du genre *Verongia* (Dictyoceratida). *Journal de Microscopie et de Biologie cellulaire, 23*, 271-288.

Vacelet, J., & Gallissian, M.F. (1978). Virus-like particles in cells of the sponge *Verongia cavernicola* (Demospongiae, Dictyoceratida) and accompanying tissue changes. *Journal of Invertebrate Pathology, 31,* 246-254.

Vlaskalin, T., Wong, C.J., & Tsilfidis, C. (2004). Growth and apoptosis during larval forelimb development and adult forelimb regeneration in the newt (*Notophthalmus viridescens*). *Development, Genes Evolution, 214*, 423–431. https://doi.org/10.1007/s00427-004-0417-1

Weltner, V. (1893). Spongillidcnstudicn. *U Arch Naturgesch, 59,* 245- 282.

Wickham, H. (2016). ggplot2: Elegant Graphics for Data Analysis. Springer-Verlag: New York

Wulff, J. (2010). Regeneration of sponges in ecological context: Is regeneration an integral part of life history and morphological strategies? *Integrative and Comparative Biology, 50*, 494–505. doi:10.1093/icb/icq100.

Wulff, J. (2013). Recovery of sponges after extreme mortality events: morphological and taxonomic patterns in regeneration versus recruitment. *Integrative and Comparative Biology, 53*, 512-523. DOI : 10.1093/icb/ict059.

Figure legends for *Aplysina cavernicola* regeneration

Figure 1. Time series photographs *in situ* of wounds to *Aplysina cavernicola.*

Time series photographs of wounds to *Aplysina cavernicola*, Corrals Cave, Marseille, France June-July 2018. Two examples were chosen to illustrate individual variety of regeneration after experimental wounding. W – wound. Scale bar – 1.2 cm.

Figure 2. *Aplysina cavernicola in vivo*

A – intact sponge before operation; B – sponge just after operation; C – sponge after 48 hours after operation.

o – osculum, w – wound.

Figure 3. Intact *Aplysina cavernicola*

A – semi-fin section of upper part of sponge; B – TEM image of ectosome; C – exopinacocyte and spherulous cells (inset: detail of cell junctions between exopinacocytes); D – endopinacocyte; E – choanocyte chamber (inset: choanocyte); F – pocket cell with symbiotic bacteria; G – archaeocyte; H – myocytes (inset: detail of myocytes with myofibrils).

ar – archaeocyte, cb – cell body of exopinacocyte, cc – choanocyte chamber, ch – choanocyte, ect – ectosome, en – endopinacocyte, end – endosome, ex- exopinacocytes, f – flagellum, fp – flat part of exopinacocyte, in – inclusions in spherulous cells, my – myocyte, pc - pocket cell, n – nucleus, sb – symbiotic bacteria, sc – spherulous cell.

Figure 4. Cells of the mesohyl in intact *Aplysina cavernicola*

A – bacteriocyte; B – spongocyte; C – lophocytes; D - spherulous cell at the late stage of evolution expelled into exhalant canal; E – microgranular cell; F – granular cell; G, H – spherulous cells in two stages of their development.

ar – archaeocyte, ba – bacteriocyte, ex- exopinacocytes, exc – exhalant canal, in – inclusions in spherulous cells, lo – lophocyte, mc – microgranular cell, n – nucleus, sb – symbiotic bacteria, sc – spherulous cell, sf – skeleton fiber, sp - spongocyte.

Figure 5. Scheme of wound and their parts in *Aplysina cavernicola.*

ect – ectosome, end – endosome, it - intact tissues, ra – regenerated area, w – wound, wa – wound area, we – wound edge.

Figure 6. 3h of regeneration in *Aplysina cavernicola*

A – wound and a marginal zone; B – zone under the wound; C – internal part of the wound with encapsulated invasive diatoms; D – dedifferentiated choanocyte (flash show the basal flagellum apparatus)

ar – archaeocyte, ba – bacteriocyte, dch – dedifferentiated choanocyte, di – encapsulated diatom, en – endopinacocyte, in – inclusions in spherulous cells, lo – lophocyte, n – nucleus, ph – phagosome, sb – symbiotic bacteria, sc – spherulous cell, scf – spherulous cells fragments, w - wound.

Figure 7. 6h of regeneration in *Aplysina cavernicola*

A – semi thin section of the wound and upper part of endosome; B, C – TEM of the upper part of the wound: it is a choanocyte chamber during their destruction, fragments of spherulous cells, phagocyted spherulous cell; D, E – wound zone with the fragments of cells and phagocytosis of spherulous cells; F – inner part of the wound, degraded choanocyte chamber.

ar – archaeocyte, cc – choanocyte chamber, dcc - destructed choanocyte chamber, dch – dedifferentiated choanocyte, end – endosome, in – inclusions in spherulous cells, n – nucleus, ph – phagosome, sb – symbiotic bacteria, sc – spherulous cell, scf – spherulous cells fragments, w – wound, ws – wound surface.

Figure 8. Boxplot diagram of the number of spherulous cells per mm^2 in intact tissues and during regeneration in *A. cavernicola*. The differences between some of the means are statistically significant (ANOVA p-value = 2.36E-07(<0.01)). Tukey's multiple comparisons showed no significant differences only in 3 pairs: Intact tissues–96 hpo; 6 hpo–12 hpo; 24 hpo–48 hpo. Duncan's new multiple range test (MRT) approve this, grouping these pairs into three clusters (A, B, C). The differences between Duncan's clusters are statistically significant (Supporting Table 4).

Figure 9. 12h of regeneration in *Aplysina cavernicola*

A – semi thin section of the wound and upper part of endosome; B, C – TEM of the upper part of the wound, there are some non-secret cells at the wound surface (arrowheads), dedifferentiated choanocytes and spherulous cells; D – detail of the upper part of the wound;

E – wound zone with dedifferentiated choanocytes; F – marginal zone of the wound with the part of intact exopinacocyte.

ar – archaeocyte, cf – cells fragments, dch – dedifferentiated choanocyte, dsc - dedifferentiated spherulous cell, end – endosome, in – inclusions in spherulous cells, n – nucleus, ph – phagosome, sb – symbiotic bacteria, sc – spherulous cell, scf – spherulous cells fragments, w – wound, ws – wound surface.

Figure 10. 24h of regeneration in *Aplysina cavernicola*

A – semi thin section of the wound and upper part of endosome; B, C – TEM of the upper part of the wound, with flat parts of new exopinacocytes, spherulous and non-secret cells with the phagosomes (arrowhead - basal body of choanocyte flagellum); D – wound zone with dedifferentiated choanocytes; E - upper part of the wound zone with archaeocyte and dedifferentiated choanocyte in the beginning of differentiation into new exopinacocyte, arrow show the basal apparatus of dedifferentiated choanocyte; F - archaeocyte differentiated into exopinacocyte at the upper part of the wound.

ar – archaeocyte, cf – cells fragments, dch – dedifferentiated choanocyte, dsc - dedifferentiated spherulous cell, end – endosome, in – inclusions in spherulous cells, n – nucleus, nu – nucleolus, ph – phagosome, sb – symbiotic bacteria, sc – spherulous cell, scf – spherulous cells fragments, w - wound.

Figure 11. 48h of regeneration in *Aplysina cavernicola*

A – semi thin section of the wound and upper part of endosome; B – TEM of the upper part of the wound, with restored ectosome; C – TEM of the upper part of the wound, showed transdifferentiation of a choanocyte into exopinacocyte; inset – basal apparatus of dedifferentiated choanocyte (arrowhead); D – TEM of the upper part of the wound, showing transdifferentiation of an archaeocyte into exopinacocyte; E, F - TEM of the small apoptotic spherulous cells elimination of apoptotic spherulous cells through forming exopinacoderm.

ac – apoptic cell, asc – apoptic spherulous cell, ar – archaeocyte, cc – choanocyte chamber, ch – choanocyte, cf – cells fragments, dch – dedifferentiated choanocyte, end – endosome, ex-exopinacocytes, fp – flat part of exopinacocyte, in – inclusions in spherulous cells, lo – lophocyte, mc – microgranular cell, my – myocyte, n – nucleus, ph – phagosome, sb – symbiotic bacteria, sc – spherulous cell, scf – spherulous cells fragments, w – wound zone.

Figure 12. 48h of endosome regeneration in *Aplysina cavernicola*

A-C – TEM of the endosome under the wound, showing different stages of restoration of exhalant canals of the aquiferous system; D-F - TEM of the endosome under the wound, showing different stages of restoration of choanocyte chambers.
cc – choanocyte chamber, ch – choanocyte, en – endopinacocyte, exc – exhalant canal, sb – symbiotic bacteria.

Figure 13. 96h of regeneration in *Aplysina cavernicola*
A – semi thin section of the completely restored ectosome and upper part of endosome; B – TEM of the upper part of the restored ectosome; C - the endosome with new choanocyte chamber; D – the endosome with normal cell composition.
ar – archaeocyte, cc – choanocyte chamber, ch – choanocyte, ect – ectosome, end – endosome, exc- exhalant canal, lo – lophocyte, n – nucleus, sb – symbiotic bacteria, sc – spherulous cell.

Figure 14. Cell proliferation in intact tissues of *Aplysina cavernicola*. A – ectosome; B – endosome; C – endosome near the exhalant canal of the aquiferous system; D – DNA-synthesizing choanocytes with small round to oval nuclei; E – mesohyl DNA-synthesizing cells with large round nuclei. Cyan – DAPI, green – α-tubulin, magenta – EdU. cc – choanocyte chamber, end – endosome, ect – ectosome, exc – exhalant canal of the aquiferous system. White arrowheads marks EdU-positive nuclei of DNA-synthesizing cells. Each image is a maximum projection, obtained from 55 μm Z stack.

Figure 15. Cell proliferation during *Aplysina cavernicola* body wall regeneration. A-E – cell proliferation in the wound area at different stages of regeneration: A – 0-6 hpo; B – 0-24 hpo; C – 24-48 hpo; D – 48-72 hpo; E – 120-144 hpo; F – cell proliferation in intact tissues, distant from the wound, during regeneration. Cyan – DAPI, magenta – EdU. Dcc – disintegrating choanocyte chamber, cc – choanocyte chamber. White arrowheads marks EdU-positive nuclei of DNA-synthesizing cells. Each image is a maximum projection, obtained from 15 μm Z stack.

Figure 16. Apoptosis during *Aplysina cavernicola* body wall regeneration. A – 6 hpo; B – 12 hpo; C – 48 hpo. Blue – DAPI, red – TUNEL. White dashed line marks the wound edge, white arrows – TUNEL-positive nuclei of apoptotic cells. Each image is an optical slice through the wound area.

Supporting Figure 1. TEM images of ECM dynamic at the wound surface.

A – intact ; B – 0 hpo ; C - 3 hpo ; D – 6 hpo ; E – 12 hpo ; F – 24 hpo ; G – 48 hpo ; H – 96 hpo.

Title[1] Transdifferentiation and mesenchymal-to-epithelial transition during regeneration in Demospongiae (Porifera)

Alexander V. Ereskovsky[1,2,3]*, Daria B. Tokina[1], Danial M. Saidov[4], Stephen Baghdiguian[5], Emilie Le Goff[5], Andrey I. Lavrov[2,6]

[1] Institut Méditerranéen de Biodiversité et d'Ecologie marine et continentale (IMBE), Aix Marseille University, CNRS, IRD, Avignon University, Station Marine d'Endoume, Rue de la Batterie des Lions, 13007, Marseille, France

[2] Dept. Embryology, Faculty of Biology, Saint-Petersburg State University, Universitetskaya emb. 7/9, 199034, Saint-Petersburg, Russia

[3] Koltzov Institute of Developmental Biology of Russian Academy of Sciences, Russia, Moscow

[4] Dept. of Invertebrate Zoology, Biological Faculty, Lomonosov Moscow State University, 119234, Leninskie gory 1-12, Moscow, Russia

[5] ISEM, Univ Montpellier, CNRS, EPHE, IRD, Montpellier, France.

[6] Pertsov White Sea Biological Station, Biological Faculty, Lomonosov Moscow State University, 119234, Leninskie gory 1-12, Moscow, Russia

Text figures – 16

Abbreviated title: Demosponges regeneration

***Correspondence to**: Alexander V. Ereskovsky, Institut Méditerranéen de Biodiversité et d'Ecologie marine et continentale (IMBE), Aix Marseille University, CNRS, IRD, Avignon University, Station Marine d'Endoume, Rue de la Batterie des Lions, 13007, Marseille, France, Tel. +33 04 91 04 16 21 ; Fax : e-mail alexander.ereskovsky@imbe.fr,

This work was supported by grants of Russian Foundation for Basic Research n° 16-04-00084, and the Russian Science Foundation n° 17-14-01089 (histological and ultrastructural studies).

[1] **Funding information**. This work was supported by grants of Russian Foundation for Basic Research n° 16-04-00084, the Russian Science Foundation n° 17-14-01089 (histological and ultrastructural studies). This work also is a contribution to Labex OT-Med (n° ANR-11-LABX-0061) and has received funding from Excellence Initiative of Aix-Marseille University_A*MIDEX, a French "Investissements d'Avenir" program for travel expenses.

Abstract

Origin and early evolution of regeneration mechanisms remain among the most pressing questions in animal regeneration biology. Porifera have exceptional regenerative capacities and, as early Metazoan lineage, are a promising model for studing evolutionary aspects of regeneration. Here, we focus on reparative regeneration of the body wall in the Mediterranean demosponge *Aplysina cavernicola*. The epithelialization of the wound surface is completed within two days, and the wound is completely healed within two weeks. The regeneration is accompanied with the formation of a mass of undifferentiated cells (blastema), which consists of archaeocytes, dedifferentiated choanocytes, anucleated amoebocytes, and differentiated spherulous cells. The main mechanisms of *A. cavernicola* regeneration are cell dedifferentiation with active migration and subsequent redifferentiation or transdifferentiation of polypotent cells through the mesenchymal-to-epithelial transformation. The main cell sources of the regeneration are archaeocytes and choanocytes. At early stages of the regeneration, the blastema almost devoid of cell proliferation, but after 24 hpo and up to 72 hpo numerous DNA-synthesizing cells appear there. In contrast to intact tissues, where vast majority of DNA-synthesizing cells are choanocytes, all EdU-labeled cells in the blastema are mesohyl cells. Intact tissues, distant from the wound, retains intact level of cell proliferation during whole regeneration process. For the first time, the apoptosis was studied during the regeneration of sponges. Two waves of apoptosis were detected during *A. cavernicola* regeneration: the first wave at 6-12 hpo and the second wave at 48-72 hpo.

Keywords: demosponges, regeneration, mesenchymal-to-epithelial transformation, blastema, apoptosis, transdifferentiation.

Highlights

1) Regeneration in the demosponge *Aplysina cavernicola* is accompanied with the formation of a mass of undifferentiated cells (blastema).

2) The main mechanisms of *A. cavernicola* regeneration are cell dedifferentiation with active migration and subsequent redifferentiation or transdifferentiation of polypotent cells - archaeocytes and choanocytes - through the mesenchymal-to-epithelial transformation.

3) Apoptosis during regeneration of *A. cavernicola* participate in damaged cells elimination and associated with the extensive ejection of spherulous cells from wound area.

Introduction

In spite of big interest in various problems concerning origin and early steps of evolution in animal regeneration, morphogenesis, cell turnover etc., up to now there are surprisingly small number of the studies, dealing with ultrastructural, morphogenetic, cell and genetic aspects of sponge reparative regeneration.

Phylum Porifera consists of four classes: syncytial Hexactinellida, and cellular Calcarea, Homoscleromorpha and Demospongiae. The last class is the largest and includes about 80% of living sponges. Studies of regeneration in sponges have begun on demosponges (Cavolini, 1785; Vaillant, 1869; Weltner, 1893). However, there are only few papers, concerning ultrastructural description of the morphogenesis and cell behavior in reparative regeneration of sponges. Moreover, three of them dealing with the regeneration of specific "organs" after amputation (oscular diaphragm in *Hippospongia communis* (Thiney, 1972), oscular tube in *Ephydatia fluviatilis* (Sukhodolskaya, 1973), and papillae in *Polymastia* (Boury-Esnault, 1976)). Reparative regeneration of the body wall is described only in seven species. Regeneration in *Spongilla lacustris* (Brondsted, 1953), *Halichondria panicea* (Korotkova & Nikitin, 1969), *Geodia barretti* (Hofmann et al., 2003) and *Halisarca caerulea* (Alexander et al., 2015) was studied only with light microscopy. In the case of *H. caerulea*, the light microscopy studies were supplemented with the investigations of the cell proliferation during the regenerative processes (Alexander et al., 2015). Reparative regeneration in *Chondrosia reniformis* was investigated with light and scanning electron microscopy (SEM) (Pozzolini et al., 2019). Finally, SEM studies supplemented with time-laps recordings were done for regeneration in *Hymeniacidon heliophila* (Coutinho et al., 2017).

At the same time, our complex detailed investigations of reparative regeneration, done with TEM, SEM, epifluorescent and light microscopy, immunocytochemistry and time-laps recordings, in homoscleromorphs (Ereskovsky et al., 2015), calcareous sponges (Ereskovsky et al., 2017; Lavrov et al., 2018) and demosponges (Borisenko et al., 2015) show a high diversity of morphogenesis, cell mechanisms, and cell turnover, accompanying these processes.

Thus, having comprehensive data about mechanisms of the regeneration for only one species from the huge and very diverse class Demospongiae, we cannot make any generalizations regarding the mechanisms of regeneration of this class of Porifera.

Representatives of the genus *Aplysina* are widely distributed in subtropical and tropical coastal waters (Bergquist & Cook, 2002). They are considered proper models in chemical ecology and microbiology (Azevedo et al., 2008; Betancourt-Lozano et al., 1998; Thoms et

al., 2004, 2006). *Aplysina cavernicola* is a popular and promising model for various researches, dealing with the sponge cell composition (Vacelet, 1966, 1967, 1970, 1971, 1975; Vacelet & Gallissian, 1978), bacterial symbionts (Vacelet, 1975; Fiedrich et al., 1999; Hentschel et al., 2001; Thoms et al., 2003), three-dimensional skeletal scaffolds (Vacelet, 1971a,b; Garrobe et al. 1973; Ehrlich et al. 2010a, b), biochemistry and secondary metabolites (D'Ambrosio et al., 1982, 1983; Ciminiello et al., 1997; Reverter et al., 2016), and temporal variability of secondary metabolism (Reverter et al., 2016). Life cycle researches showed that *A. cavernicola* is an oviparous sponge whose reproductive period lasts barely one month (Gallissian & Vacelet, 1976; Reverter et al., 2016).

The present study was aimed at investigation of the reparative regeneration in Mediterranean demosponge *Aplysina cavernicola* (Vacelet, 1959). The wide range of methods allow us to make a comprehensive analysis of mechanisms, which contribute to the regeneration in this species, including cell behavior and migrations, morphogenetic process, cell proliferation and apoptosis.

Materials and methods

Sampling

Aplysina cavernicola (Vacelet, 1959) (Demospongiae, Verongida) is a perennial sciaphilous species inhabiting coralligenous formations or the entrance of submarine caves generally between 8 to 60 m in the Mediterranean Sea (Figure 1). It presents a typical yellowish color. For regeneration experiments *A. cavernicola* specimens were collected by SCUBA diving in September-November 2017, July-August and October 2018 and March 2019 near Maire Island, Marseille (43.2096° N; 5.3353° E) at a depth of 12 - 15 m. Collected sponges were maintained in a 100 l laboratory aquarium with running natural seawater at a temperature of 15-16°C for 36 hours for sponge adaptation.

Surgical operations

Two type of surgical operations have been conducted: i) *in situ*, and ii) in laboratory. For *in situ* operations six individuals were used. The experiment was performed in June 2018 at the site of sponge sampling. In each sponge wounds were made in a wall of a cylindrical outgrowth using a sharp stainless dissecting scalpel. The wounds had a uniform size of 3 cm^2 in area and 1 cm deep. Each wound was measured and photographed at t = 0, 2, 7, 12, and 32 days post operation, using digital camera Nikon D300 equipped with waterproof camera

housing SUBAL ND300 and flash INON Z-240.

Surgical operations in laboratory were performed as an excision of a small part (approximately 0.3-0.5x0.3-0.5 cm) of the body wall at the base of a cylindrical outgrowth (Figure 2). A total of 24 individuals were used in the body wall regeneration experiments (Supporting Table 1).

The surgical operations were done manually under a stereomicroscope using scalpel. After the operations the sponges with excised body wall were maintained in a 100 l laboratory aquarium with running natural seawater at a temperature of 15-16°C. The sponges were inspected and photographed using a stereomicroscope Leica M165FC (Leica) equipped with a digital camera Leica DFC 320 (Leica) and LAS Store and Recall v.4.1 software (Leica). The observations were done at 3, 6, 12, 18, 24, 36, 48, 72, 96, and 120 hours post operation (hpo).

Light and electron microscopy

Specimens were fixed overnight at 4°C by 2.5% glutaraldehyde (Ted Pella) on 0.2M cacodylate buffer (pH 7.4) and post-fixed for 2 h with 1% OsO_4 (Spi Supplies) on the same buffer at room temperature (RT). Between fixation and post-fixation specimens were twice rinsed with cacodylate buffer for 30 min. Finally, specimens were dehydrated in an ethanol series at RT and stored in 70% ethanol at 4°C.

For semi-thin sections and transmission electron microscopy (TEM) specimens were embedded in Araldite (Sigma-Aldrich) epoxy embedding media according to the manufacturer instructions. Semi-thin sections (1 µm) were cut on a Reichert Jung ultramicrotome (Reichert) and Ultramicrotome PowerTome XL (RMC Boeckeler) and then stained with 1% toluidine blue – 0.2% methylene blue mixture. The semi-thin sections were studied under a WILD M20 microscope (Wild). Digital photos were taken with a Leica DMLB microscope (Leica) using Evolution LC color photo capture system (MediaCybernetics).

Ultrathin sections (60–80 nm) were cut with a Leica UCT6 and an Ultramicrotome PowerTome XL, equipped with a Drukkert 45° diamond knife, and contrasted with 4% aqueous uranyl acetate. Ultrathin sections were studied under Zeiss-1000 (Carl Zeiss) transmission electron microscope.

For scanning electron microscopy (SEM), fixed specimens were critical-point-dried, sputter-coated with gold-palladium, and observed under Hitachi S 570 (Hitachi) microscope.

Spherulous cell counting

Spherulous cells were counted on images of semi-thin sections of intact sponge tissues and regenerating specimens at 6, 12, 24, 48, and 96 hpo. The images were obtained with a Leica DMLB microscope (Leica) at 40x magnification using Evolution LC color photo capture system (MediaCybernetics). At each stage three images, arising from three independent individuals, were used for counting. Spherulous cells were counted in the approximate 50-µm thick lane beneath the exopinacoderm in intact sponges or beneath wound surface in regenerating individuals. The area of the studied lanes was measured for each image, and number of spherulous cells were extrapolated for an area of 1 mm^2. Cell counting and area measuring were done with ImageJ v.1.48 software (National Institute of Health). For each stage mean value and standard deviation were calculated (Supporting Table 4).

Statistical analysis was performed in R (R Core Team, 2019) with basic package "stats" ver. 3.6.0 (R Core Team, 2019) and additional packages "agricolae" ver. 4.2-0 (de Mendiburu, 2019), "car" 3.0-3 (Fox & Weisberg, 2019) and graphic package "ggplot2" ver. 3.3.1 (Wickham, 2019). To analyze the results, analysis of variance (ANOVA) was performed to evaluate differences for spherulous cell count in intact tissues and at different stages of regeneration. For ANOVA we prerequisitely performed box-cox transformation with $\lambda=0$ to normalize our data, and Leven's test for homogeneity of variances ($p = 0.3744$). For pairwise comparisons, we performed Tukey's honestly significant test and Duncan's multiple range test from "agricolae" package with 0.95 confidence level (Supporting Table 4).

Cell proliferation investigations

A total of 27 individuals with the excised body wall were used in cell proliferation studies (Supporting Table 2). The 5-Ethynyl-2′-deoxyuridine (EdU) (Thermo Fisher Scientific), which incorporates in nuclear DNA during its synthesis in S-phase and marks DNA-synthesizing cells, was used as a label for cell proliferation. The EdU stock solution was prepared in DMSO (MP Biomedicals). The optimal EdU concentration and incubation time were elucidated during the preliminary studies with the intact tissues of *Aplysina cavernicola.*

Labeling of DNA-synthesizing cells in the regenerating sponges were conducted during the following time periods: 0-6, 6-12, 0-24, 24-48, 48-72, 120-144 hpo. The EdU concentration in the experiments with 6-hour incubation period was 600 µM and in the experiments with 24-hour incubation period – 200 µM. Three individuals were used at each time period. Three additional sponges were cultured in FSW without the EdU and served as negative technical controls (Supporting Table 2).

The cell proliferation was also studied in the intact tissues of *A. cavernicola*. Three individuals were incubated 6 hours in FSW with 600 µM EdU and three individual – 24 hours in FSW with 200 µM EdU. One individual was cultured in FSW without the EdU and served as a negative technical control (Supporting Table 2). The mode of EdU incubation did not significantly influence the pattern of the staining of DNA-synthesizing cells: after both types of incubation sponge tissues show essentially the same amount and localization of the DNA-synthesizing cells.

During the EdU incubation, intact and regenerating sponges were cultivated in glass vessels with 200 ml FSW supplemented with required amount EdU at 13°C.

After the incubation period, all individuals were rinsed twice with FSW and fixed with 4% PFA (Sigma-Aldrich) in PBS (Amresco, Inc.) for 12-15 hours at 4°C. Fixed specimens were rinsed with PBS and the Click-iT reaction were performed in the following mixture: 4 мM $CuSO_4$ (ChimMed), 20 mg/ml Sodium L-ascorbate (Sigma-Aldrich) and 10 µM Sulfo-Cyanine3 Azide (Lumiprobe) in PBS. Finally, the specimens were rinsed several times with PBS and stained with DAPI (Sigma-Aldrich).

Stained specimens were mounted in 90% glycerol-DABCO (Sigma-Aldrich) and studied with a CLSM Nikon A1 (Nikon) using lasers with 405 nm, 488 nm and 546 nm wavelength. The tissues beneath the wound surface and tissues no less than 1 cm away from the wound were studied in each regenerating specimen.

The obtained Z-stacks and images were processed with ImageJ v.1.48 software (National Institute of Health). Nuclei measuring were done on separate optical slices with NIS Elements Viewer v. 4.5 (Nikon) and JR Screen Ruler v. 1.5 (Spadix Software). For all measurements mean value and standard deviation were calculated.

Apoptosis investigation

Four individuals were used for studies of apoptosis during regeneration and in intact sponge tissues (Supporting Table 3). The studies were performed using the In Situ Cell Death Detection Kit (Roche) or Click-iT Plus TUNEL Kit (Thermo Fischer Scientific). Both kits detect apoptotic cells using the TUNEL assay, i.e. by attaching labeled nucleotides to double-stranded DNA breaks that occur at the later stages of apoptosis.

Intact tissue and wounded areas at 6, 12, 24 and 48 hpo were fixed at 4°C by 4% PFA (Sigma-Aldrich) on PBS (Amresco, Inc.). Fixed specimens were rinsed with PBS and treated according to the manufacturer instructions for apoptotic cell visualization. Finally, the specimens were rinsed several times with PBS and stained with DAPI (Sigma-Aldrich).

Samples, incubated with DNase I recombinant purified from bovine pancreas (Thermo Fisher Scientific) prior to the TUNEL reaction, were used as positive technical controls. Samples, incubated without the TdT enzyme during the TUNEL reaction, were used as negative technical controls.

Stained specimens were mounted in Mowiol (12%) or 90% glycerol-DABCO (Sigma-Aldrich) and studied with a confocal microscope TCS-SPE (Leica) or CLSM Nikon A1 (Nikon) using lasers with 405 nm, 488 nm and 546 nm wavelength. The tissues beneath the wound surface and tissues no less than 1 cm away from the wound were studied in each regenerating specimen.

Field Study Permissions

No specific permissions were required for these locations because the study was done outside national parks, private lands or protected areas. We declare that the field studies did not involve endangered or protected species.

Results

Intact sponge morphology and histology

The body of *Aplysina cavernicola* has a branchy shape, with each cylindrical branch having 1-2 cm in diameter (Figure 1). Sponge tissues are dense and elastic. The sponge has leuconoid organization of aquiferous system (numerous small choanocyte chambers, scattered in the mesohyl). The skeleton represented exclusively by organic (spongin) fibers, covered with chitin (Ehrlich et al., 2010a), thus the surgical operations are easily conducted.

The body is composed of the peripheral ectosome and the internal endosome, bearing numerous choanocyte chambers (Figure 3A). The ectosomal region is up to 30 μm thick and consists of three layers: (1) external parts of the T-shaped exopinacocytes, connected by non-specialized cell junctions (Figure 3B,C) and covered by an acellular cuticle; (2) layer containing collagen fibrils, cell bodies of exopinacocytes and scattered spherulous cells; and (3) the inner layer, consisting of condensed collagen fibrils and spherulous cells. The endosome (Figure 3A) composes the major part of the sponge body. It includes choanocyte chambers, consisted of flagellated choanocytes, aquiferous canals, lined by endopinacocytes, (Figure 3D,E) and the mesohyl with the skeleton, abundant symbiotic bacteria and scattered specialized sponge cells.

Populations of free cells in the mesohyl of *A. cavernicola* include: lophocytes, archaeocytes, pocket cells, contractile cells (myocytes) (Figure 3F,H), spherulous cells at different stages of their maturation with two principal morphotypes: larger cells with clear inclusions (Figures 3C, 4G) and smaller ones with dense inclusions (Figure 4D,H), bacteriocytes, microgranular cells, spongocytes (Figure 4A-F) (Vacelet, 1966, 1967, 1970, 1971, 1975; Vacelet & Gallissian, 1978).

Regeneration

In spite of minor individual differences wound healing in *Aplysina cavernicola*, which is expressed in the epithelialization of the wound surface, is completed within two – six days (Figure 1). During our observations we did not reveal any significant differences in the onset of the stages and course of the regeneration, as well as in the morphogenesis accompanying it, across studied individuals. The regeneration ends within two weeks, when the wound is completely healed: only a small depression on the surface remains in its place.

At the histological level the observed regeneration processes can be subdivided into three stages: 1) internal milieu isolation – formation of a clot (3 – 12 hpo), 2) wound healing – epithelization (12 – 24 hpo), and 3) restoration of ectosome and endosome (36 – 96 hpo).

For detailed description of morphogenesis and cell behavior, accompanying the regeneration, we propose to subdivide a wound and tissue around the wound on several areas (Figure 5):

- Wound – a break in the continuity of any bodily tissue due to injury.
- Wound area – tissues directly adjacent to an excised part of the sponge body; their structure is severely disrupted during the surgery.
- Edge of the wound – peripheral parts of the wound, which is in direct contact with intact tissues.
- Regeneration area – an area of the sponge body (tissue), which is not directly affected by surgery, but in which anatomical structures (choanocyte chambers, canals of aquiferous system and skeleton) are reorganized, and the normal composition and distribution of cells disrupted due to their participation (dedifferentiation, transdifferentiation and migration) in the regenerative processes. The dimension of this area could vary, depending on size and type of the injury and on individual characteristics of a sponge.
- Intact issues – ectosome and endosome areas that are not affected by surgery and are not directly involved in regeneration and retaining the normal organization.

Stage I – Internal milieu isolation

Immediately after the surgical excision of ectosome with the directly adjacent endosome, the wound surface retracts, leaving the surface of the intact ectosome protruding around the edges of the wound. The ectosome and the upper areas of endosome are destroyed in the wound area.

During the first 3 hours post operation (hpo), the wound surface is covered with exudate, cell debris and numerous symbiotic bacteria. The extracellular matrix (ECM) does not show any signs of a condensation (Supporting Figure 1A-C). All cells in the wound area undergo morphological modifications. The epithelial cells - endopinacocytes and choanocytes of choanocyte chambers, begin losing contacts with adjacent cells in their epithelial layers and change their shape from trapeziform (choanocytes) and flat (endopinacocytes) to spherical or amoeboid (Figure 6). These dedifferentiated cells mix with the mesohyl cell population. During transformation of the choanocytes, their collar of microvilli and flagellum are resorbed (Figure 6D). However, the elements of the flagellar apparatus (the basal body and accessory centriole located near the nucleus) persist in the transformed cells for approximately two days and serve as the natural marker of dedifferentiated choanocytes. The dedifferentiated endopinacocytes have no specific morphological characteristics and therefore these cells cannot be distinguished from other mesohyl cells. The non-secreting cells of the mesohyl (archaeocytes, lophocytes, dedifferentiated choanocytes and endopinacocytes) actively phagocyted cell debris, symbiotic and invasive microbes, including diatoms in the wound area (Figure 6). Thus, all cells in the wound area, except the spherulous cells, are filled with large phagosomes. The ectosome, surrounding the wound slightly contracts and bends inward. After 3 hpo an active migration of the mesohyl cells and dedifferentiated choanocytes towards the wound surface begins from wound area, as these cells assume an elongated shape with the long axis, perpendicular to the wound surface (Figure 6). There are no changes in the regeneration area in this period.

At 6 hpo, the wound surface is aligned and becomes flat and smooth. It is covered by a thick layer of ECM, containing fragments of cells, dispersed symbiotic bacteria and few spherulous cells (some of which are beginning their dedifferentiation) (Figure 7A; Supporting Figure 1D). The amount of the spherulous cells in the wound area at this stage of the regeneration significantly decreases and is approximately 2,8-fold lower than in the ectosome of intact sponges (Figure 8; Supporting Table 4). This structure can be referred as a regenerative clot, by analogy with other animals (Carlson, 2007). The thickness of the clot is from 12 to 20 μm.

The cells of wound area have numerous small or few large phagosomes, which contained fragments of the spherulous and granular cells (Figure 7B-F). Such cells could be found not only in the upper part of the wound, but also in the deeper zone up to 100 μm beneath the wound surface. There still no visible changes in the regeneration area at this stage.

At 12 hpo a regenerative clot at the wound surface is getting thinner, and wound surface become aligned, flat and smooth (Figure 9A). The peripheral parts of the wound are clearly limited by the flat outgrowths of intact exopinacocytes (Figure 9F).

In the wound area, cell distribution begins ordering, and ECM condensation occurs (Supporting Figure 1E). The number of dedifferentiated choanocytes and endopinacocytes, archaeocytes, and lophocytes increases in this area in comparison with the previous period of regeneration (Figure 9B-E). Majority of these cells migrated from regenerated area. In contrast, the number of the spherulous cells shows insignificant variations and remains approximately the same as at 6 hpo (Figure 8; Supporting Table 4). Some of these spherulous cells undergo the dedifferentiation, which is accompanied by the release of the spherules from the cells. The amount of free mesohyl and concentration of the symbiotic bacteria decrease in comparison with previous periods of regeneration (Figure 9C, D).

Simultaneously, the migration of the amoeboid cells (archaeocytes, dedifferentiated choanocytes) from the regeneration area to the wound area and wound surface proceeds (Figure 9C,E), and some of the migrating cells reach the wound surface, where they become oriented with the long axis parallel to the wound surface (Figure 9B). Also first elongated contractile cells (myocytes) appear in the regeneration area.

Stage II. Wound healing - epithelization (12 – 24 hpo)

At 24 hpo a cell mass, consisting of heterogenous dedifferentiated and undifferentiated (archaeocytes) cells, is formed under the upper part of the wound area. We considered it as a blastema, as structurally it resembles blastemas formed during regeneration of other animals. Blastema occupies the wound area and the upper part of the regeneration area.

Simultaneously, the upper part of the wound area becomes similar to intact sponge ectosome, showing structured ECM with collagen fibrils (Figure 10A,B; Supporting Figure 1F). The wound surface is mosaically covered with very thin superficial outgrowths of developing T-shaped exopinacocytes, arising from blastema cells of the heterogeneous origin (Figure 10B,C,E). New exopinacocytes do not yet form close contacts with each other. In some places submerged nucleated bodies of these cells are found. New exopinacocytes, in

contrast to the cells located deeper under the wound surface, have only few phagosomes. There is no directed movement (contraction or creeping) of the intact exopinacoderm surrounding the wound.

The number of spherulous cells in the wound area significantly increases in approximately 2,3-folds in comparison with the previous stage of regeneration (Figure 8; Supporting Table 4). These cells show typical appearance (Figure 10B). Their shape is oval, not amoeboid, as in the earlier stages of regeneration. In contrast, near the wound surface, the number of dedifferentiated choanocytes, archaeocytes and spherulous cells decreases (Figure 10C-F). The lophocytes, granular cells, and myocytes are absent from this zone. The choanocyte chambers or their fragments completely disappear from the regeneration area at this stage of regeneration. They occur at a depth of about 200 µm, as in intact sponge.

Stage III. Restoration of ectosome and endosome (36 – 96 h)

At 48 hpo the ectosome of the regenerate is completely restored, but superficial cuticle, characteristic for intact sponge, is still absent (Figure 11A,B; Supporting Figure 1G). The wound epithelization is finished by new exopinacocytes, arose from the heterogeneous dedifferentiated cells population and archaeocytes. Some of new exopinacocytes clearly show their origin from the dedifferentiated choanocytes, as they still bear flagellar basal apparatus (Figure 11C). According to the orientation of this flagellated complex, it can be assumed that the basal part of the former choanocyte is flattened. Archaeocytes, reaching the wound, flatten and assume position parallel to the surface (Figures 10E,F, 11D). New exopinacocytes have normal T-shape and cell contacts.

During formation of the exopinacoderm active elimination of small apoptotic spherulous cells with compact inclusions and cells, filled with big heterophagosomes, begins (Figure 11E, F). However, the number of the spherulous cells shows insignificant variations and remains approximately the same as at 24 hpo (Figure 8; Supporting Table 4).

During this stage, the choanocyte chambers and aquiferous canals of the endosome are restored by association of previously disaggregated choanocytes and endopinacocytes, respectively (Figure 12). Archaeocytes also participate in the development of new choanocyte chambers (Figure 12D). Cells that form new structure of aquiferous system contact each other and connect by interdigitations. Individual choanocytes form groups of cells, forming structures less compact than in the intact choanocyte chamber (Figure 12D-F). These cells gradually transform from mesenchymal morphology to epithelial.

At 96 hpo, the regeneration is almost complete: the ectosome obtains the cuticle, while the endosome of the regeneration area begins to recover: choanocyte chambers and aquiferous canals are gradually developing (Figure 13; Supporting Figure 1H). The number of spherulous cells in the regenerated ectosome significantly increases, reaching the intact level (Figure 8; Supporting Table 4). The free cells of the mesohyl, with the exception of specialized secretory cells, still contain phagosomes.

Cell proliferation

The DNA-synthesizing (EdU-labelled) cells are irregularly distributed in the intact tissues of *A. cavernicola* (Figure 14). Numerous DNA-synthesizing cells are located in the sponge endosome (Figure 14B). The majority of these cells are choanocytes with small (3.87±0.46 µm; n=45) round to oval nuclei (Figure 14D). Nevertheless, some mesohyl cells with large (4.84±0.44 µm; n=50) round nuclei are also labelled by EdU (Figure 14E). These mesohyl DNA-synthesizing cells occurs all over sponge mesohyl: in the ectosome, endosome and tissues, adjacent to the large exhalant canals of the aquiferous system, which are structurally similar to the ectosome. The ectosome and tissues, adjacent to the large exhalant canals contain only few such mesohyl DNA-synthesizing cells (Figure 14A, C).

During the regeneration, the pattern of the cell proliferation dramatically changes (Figure 15). Immediately after the surgical operation, the level of the cell proliferation in the tissues, adjacent to the wound, decreases sharply: at 0-6 hpo, DNA-synthesizing cells are completely absent in a 100-µm zone below the wound surface (Figure 15A); at 6–12 hpo and 0-24 hpo, rare DNA-synthesizing cells appear in the tissues, located 30–40 µm below the wound surface. The majority of the labelled cells are choanocytes from disintegrating choanocyte chambers, however some mesohyl cells are also labelled. Similarly, to the intact tissues, the labelled choanocytes have small (3.85±0.4 µm; n=13) round to oval nuclei, while labelled mesohyl cells are characterized by large (4.79±0.37 µm; n=16) round nuclei.

After 24 hpo, further changes in the cell proliferation pattern occurs in the regeneration area. The samples at 24-48 hpo and 48-72 hpo show a similar pattern (Figure 15B, D): in a 100-µm zone below the wound surface, numerous DNA-synthesizing cells occur. Some of these cells are located just beneath the wound surface. Virtually all labeled cells are located in the mesohyl, since the choanocyte chambers disappear in the tissues, adjacent to the wound, by this time. These DNA-synthesizing cells have large (4.99±0.39 µm; n=16) round nuclei, similar to EdU-labelled mesohyl cells from intact tissues. Occasionally, single DNA-

synthesizing choanocytes occur in the tissues, located 60-70 µm below the wound surface, where intact choanocyte chambers could be retained.

At 120-144 hpo, after the recovery of ectosome and endosome structure in the regeneration area, the cell proliferation returns to the normal state, showing the intact pattern with majority of DNA-synthesizing cells, occurring in choanocyte chambers. However, the level of cell proliferation is still lower than in intact tissues (Figure 15E).

In the tissues, distant from the wound, the intact cell proliferation pattern persists during the whole regeneration process (Figure 15F).

Apoptosis

We found no apoptotic cell in the intact tissue of *A. cavernicola*.

Two waves of apoptosis occur during the regeneration process. The level of apoptosis is low during both waves with few apoptotic cells, located only at the upper part of the wound. In the endosome under the wound and in tissues distant from the zone of regeneration apoptotic cells are completely absent.

The first wave is associated with the early stages of regeneration. Apoptotic cells appear at 6 hpo, and their number gradually decline during further regeneration (Figure 16A). At 12 hpo only single apoptotic cells occur at the upper parts of the wound area (Figure 16B), while at 24 hpo they are virtually absent. Apparently, this wave of apoptosis participates in the elimination of damaged cells from the wound area.

The second wave of apoptosis occurs at 48 hpo, when relatively numerous apoptotic cells appears at the upper parts of the wound area (Figure 16C). This wave is probably associated with the active elimination of cells through the emerging exopinacoderm during later stage of regeneration (Figure 11E,F).

Discussion

1 General

***In vivo* observations**

Sponges are well known for their capacity to regenerate not only small body parts, but also after substantial partial mortality and damage. *In situ* monitoring of naturally and experimentally generated wounds confirms high recovery capacity of sponges from different taxa and of different growth forms (Connes, 1966, 1968; Ayling, 1983; Hoppe, 1988; Duckworth, 2003; Henry & Hart, 2005; Wulff, 2010, 2013). These studies also discovered

that regeneration can be influenced both by characteristics of the wound and by inherent characteristics of particular species of sponges.

Our observations *in situ* showed that wound epithelialization under natural conditions occurs in *Aplysina cavernicola* during two days. Other investigations provided with different demosponges showed the same results (Maas, 1910; Brondsted, 1953; Connes, 1966, 1968; Korotkova & Nikitin, 1969; Korotkova et al., 1983; Diaz, 1979; Hoppe, 1988; Hofmann et al., 2003; Wulff, 2010, 2013; Alexander et al., 2014; Borisenko et al., 2015; Pozzolini et al., 2019).

Previous investigations of regeneration demonstrated that in many individuals of the same species the amount of damage, type of damage, size of the sponge, and location on the individual sponge can influence recovery, and even susceptibility to further damage by other agents (Henry & Hart, 2005; Wulff, 2010, 2013). However, we find small individual variability during regeneration of *A. cavernicola*, probably because the wounds were applied in the same areas of the sponges and had the same size.

Histological observations

In this work we showed that regeneration processes in *Aplysina cavernicola* in general follow the stages similar to those described in other massive sponges with leuconoid aquiferous system - Demospongiae and Homoscleromorpha (Brondsted, 1953; Korotkova & Nikitin, 1969; Diaz, 1979; Hofmann et al., 2003; Borisenko et al., 2015; Ereskovsky et al., 2015; Pozzolini et al., 2019), and in various eumetazoans (Korotkova, 1997; Carlson, 2003). Therefore, *A. cavernicola* regeneration includes three main stages: 1) internal milieu isolation - formation of "regenerative clot", 2) wound healing - epithelization, and 3) restoration of damaged structures - ectosome and endosome. The wound epithelization in *A. cavernicola* occurs without formation of the regenerative membrane, a structure, characteristic for regeneration of asconoid and syconoid calcareous sponges (Jones, 1957; Korotkova, 1961, 1962; Ereskovsky et al., 2017; Lavrov et al., 2018).

The main mechanisms of *Aplysina cavernicola* reparative regeneration of the body wall are (1) cell dedifferentiation with their subsequent redifferentiation, (2) transdifferentiation, and (3) active migration of polypotent cells (archaeocytes and choanocytes) to the wound. The same basic mechanisms are also characteristic for regeneration in other studied demosponges: *Halichondria panicea* (Korotkova & Nikitin, 1969), *Suberites massa* (Diaz, 1979), *Halisarca dujardinii* (Borisenko et al., 2015), and *Suberites domuncula* (our unpublished results). However, these mechanisms strongly differ from those, participating in

regeneration process in calcareous sponges and homoscleromorphs, which show clear epithelial organization with specialized cell junctions in the epithelia (Ereskovsky et al., 2015; Lavrov et al., 2018).

2. Morphogenetic mechanisms of *A. cavernicola* regeneration

Main morphogenesis during body wall regeneration in *A. cavernicola* is mesenchymal-to-epithelial transformation (MET). Indeed, at 12 hpo archaeocytes and dedifferentiated choanocytes as well as the spherulous cells begin to move toward wound area, where they form a blastema-like structure. Part of external blastema cells begins to flat and form cover sponge epithelium (exopinacoderm) through the MET.

However, experimentally induced (by surgical operation) epithelial-to-mesenchymal transition (EMT) proceeds MET in *A. cavernicola*. During this process choanocytes and endopinacocytes leave the choanocyte chambers and the canals of aquiferous system, correspondingly, and move into the mesohyl, dedifferentiating and assuming an amoeboid shape. This morphogenesis is one of central for the creation of numerous organs and complex tissues during embryonic development, asexual reproduction, and regeneration and has been well described in Eumetazoa (Keller et al., 2003; Lim & Thiery, 2012). EMT is also well known during the normal ontogeny of sponges and occurs in the course of embryonic development, and larval metamorphosis (reviewed in Ereskovsky et al. 2013). This morphogenesis was described during the first stages of regeneration of other investigated demosponges and homoscleromorphs (Korotkova & Nikitin, 1969; Borisenko et al., 2015; Ereskovsky et al., 2015).

After wound epithelization, the restoration of elements of the aquiferous system begins. Both choanocyte chambers and aquiferous system canals are formed through MET: separate amoeboid cells coalescence into groups and gradually transform from mesenchymal morphology to epithelial-like cells (choanocytes and endopinacocytes, respectively).

The same MET mechanism is characteristic for exopinacoderm and choanoderm formation during regeneration of other investigated demosponges: *Halichondria panicea* (Korotkova & Nikitin, 1969), *Halisarca dujardini* (Borisenko et al., 2015), and basopinacoderm formation in *Hymeniacidon heliophila* regeneration (Coutinho et al., 2017).

It is fundamentally different from the regeneration in Calcarea and Homoscleromorpha, in which epithelial morphogenesis, e.g. flattening and spreading of epithelial layers, plays a leading role in the restoration of main structures (exopinacoderm and elements of aquiferous system) (Ereskovsky et al., 2015; Lavrov et al., 2018).

3. Blastema

In regenerative biology blastema is a mass of undifferentiated cells, located beneath the wound and produced by the dedifferentiation of many cell types and/or migration of polypotent cells. In some cases, differentiation of blastema cells, and further reconstruction the lost part of the body could be accompanied with cell proliferation. In this case, the mitotic rate of the blastema slows down as the structure grows, and it ceases completely when the new structure reaches the original size (Santos-Ruiz et al., 2002; Carlson, 2007; Tsonis, 2008; Vervoort, 2011).

The formation of a concentration of cells under the wound in the middle stages of a body wall regeneration has been shown for several demosponges (Thiney, 1972; Boury-Esnault, 1976; Borisenko et al., 2015; Coutinho et al., 2017). This cellular concentration consists of archaeocytes and choanocytes, which are principal stem cells of demosponges (Funayama, 2018), dedifferentiated cells (e.g., pinacocytes) and specialized differentiated cells (e.g., gray cells) (Thiney, 1972; Boury-Esnault, 1976; Borisenko et al., 2015; Coutinho et al., 2017). This structure could be referred as a blastema, characteristic for a regeneration in many animals.

Similarly, in the current study, we refer to the undifferentiated cell mass beneath a wound during the end of second and beginning of third stages of regeneration in *A. cavernicola* as a blastema. In *A. cavernicola,* it consists of archaeocytes, dedifferentiated choanocytes, mixed population of anucleated amoebocytes (dedifferentiated pinacocytes, myocytes, lophocytes), and differentiated spherulous cells.

At early stages of regeneration, the blastema almost devoid of DNA-synthesizing cell, but after 24 hpo and up to 72 hpo numerous DNA-synthesizing cells appears there. However, even during this period the level of cell proliferation in the blastema is much lower in comparison with intact sponge tissues. In contrast, intact tissues distant form the wound retains intact level of cell proliferation during whole regeneration process. The similar pattern of cell proliferation has been described during body wall regeneration of *Halisarca caerulea* (Alexander et al., 2014) and *Halisarca dujardinii* (Borisenko et al., 2015), for which decreased proliferation in the wound area is characteristic.

Moreover, in contrast to intact tissues of *A. cavernicola,* where vast majority of DNA-synthesizing cells are choanocytes, all EdU-labeled cells in the blastema are mesohyl cells, as blastema lacks choanocyte chambers. These EdU-labeled cells could arise directly in blastema through cell divisions or be EdU-labeled migrating descendants of proliferating cells in intact

tissues, distant from the wound. This issue requires further investigations, using additional markers, like antibodies against phospho-histone H3 for reveling cells in M-phase and cell tracers for the visualization of cell migrations.

Importantly, studied sponges from classes Calcarea (*Leucosolenia* cf. *variabilis*) (Lavrov et al., 2018) and Homoscleromorpha (*Oscarella lobularis*) (Ereskovsky et al., 2015) demonstrate a distinct mode of regeneration without blastema formation. In these sponges regeneration occurs due to the local remodeling of intact tissues, adjacent to the wound. Moreover, the cell proliferation is neither affected nor contributes to the regeneration at any stage.

4. Dedifferentiation, transdifferentiation and cell sources in *A. cavernicola* regeneration

Transdifferentiation is the transformation of one type of already differentiated cell into another type of differentiated cell. In some cases, transdifferentiation is accompanied by cell division, while in other cases it is not (Shen et al., 2004).

Sponge cell transdifferentiation is likely a driving force accompanying their restoration processes (Korotkova, 1997; Lavrov & Kosevich, 2014; Adamska, 2018). However, transdifferentiating cell types and mechanisms of this process vary in different sponge species (Diaz, 1979; Gaino et al., 1995; Korotkova, 1997; Ereskovsky et al., 2015; Borisenko et al., 2015; Lavrov & Kosevich, 2016; Lavrov et al., 2018). For example, direct transdifferentiation of cells in intact epithelia (pinacocytes and choanocytes) has been demonstrated during the reparative regeneration of the homoscleromorph *Oscarella lobularis* (Ereskovsky et al., 2015), the calcareous sponges *Sycon lingua* (Korotkova, Efremova, & Kadantseva, 1965; Korotkova, 1972b), and *Leucosolenia* ssp. (Lavrov et al., 2018). In these cases, the layer of choanocytes transdifferentiates into layer of pinacocytes without loss of epithelial structure, without mesenchymal-to-epithelial transformation, and without contribution from cell proliferation.

Cell transdifferentiation have also been described during reparative regeneration in all investigated demosponges (for review see: Korotkova, 1997; Borisenko et al., 2015). While archaeocytes directly differentiate into new cells, choanocytes and pinacocytes undergo transdifferentiation to give rise for other cell types. It is characteristic, mainly, for choanocytes from disintegrated choanocyte chambers, which can transdifferentiate, for example, into exopinacocytes (Korotkova & Nikitin, 1969a,b; Borisenko et al., 2015). Endopinacocytes in a less extent could also transdifferentiate into exopinacocytes (Thiney,

1972; Borisenko et al., 2015). The principal difference of the transdifferentiation in demosponges in comparison with Homoscleromorpha + Calcarea lineage is an occurrence of the disruption of epithelial layers and cell dedifferentiation prior to this process in the demosponges.

The similar processes were observed during *A. cavernicola* regeneration. The archaeocytes and dedifferentiated cells participate in the restoration of the lost structures in this sponge. We identify two cells types, which undergo dedifferentiation during *A. cavernicola* regeneration: choanocytes, spherulous cells, and population of anucleated cells of mesohyl, including dedifferentiated pinacocytes, myocytes, and lophocytes. The choanocytes, despite their dedifferentiation and loss of the flagella and collars of microvilles, are well distinguished on ultrathin sections due to the persistence of two centrioles in their apical part. Anucleated amoebocytes differ from archaeocytes by a smaller nucleus without nucleolus and the presence of small phagosomes. The dedifferentiation of the spherulous cells through a complete or almost complete loss of specific inclusions (spherules) was completely unexpected process. However, the dedifferentiation of spherulous cells is not so rapid, as in other dedifferentiating cells, because of high specialization of these secretory cells.

We identified two main cellular sources for the restoration of the lost tissue and structures in *A. cavernicola*: archaeocytes and choanocytes. Both cell types contribute to the restoration of the exopinacoderm and choanocyte chambers. The restoration of the choanocyte chambers is carried out mainly due to the redifferentiation of the choanocytes, and to lesser extent due to the differentiation of archaeocytes.

However, the future of dedifferentiated anucleated amoebocytes and spherulous cells could not be traced. This issue requires the search and use of a special marker of these cells. It is possible that dedifferentiated pinacocytes and spherulous cells could also participate in the formation of the new exopinacoderm.

According to last investigations in Porifera there are not only two types of adult stem cells (ASC): archaeocytes and choanocytes (Funayama, 2018), but at least four, including pinacocytes and particular amoeboid vacuolar cells (Ereskovsky et al., 2015; Fierro-Constain et al., 2017; Lavrov et al., 2018).

There are the differences in these ASC distributions among different sponge classes. In Demospongiae the principal (pluripotent) ASC are archaeocytes and choanocytes, however the experiments with their regeneration (including present data on *A. cavernicola* regeneration) and dissociated cells aggregation demonstrated, that pinacocytes could also be ASC (Korotkova & Nikitin, 1969a,b; Borisenko et al., 2015; Lavrov & Kosevich, 2016;

Ereskovsky et al., 2016). In Calcarea archaeocytes absent and pluripotent ASC in these sponges are choanocytes and pinacocytes (Korotkova, 1961a, 1962b; Korotkova & Gelihovskaia, 1963; Lavrov et al., 2018). In Homoscleromorpha the pluripotent ASC are as in Calcarea the choanocytes and pinacocytes, but also mesohyl amoeboid vacuolar cells (Gaino et al., 1986; Ereskovsky, 2010; Ereskovsky et al., 2015; Fierro-Constain et al., 2017).

5. Spherulous cells and their role in regeneration

Similarly, to intact tissues of *A. cavernicola* (Vacelet, 1967), two principal morphotypes of spherulous cells occurs in the wound area of this sponge: larger cells with clear inclusions and smaller ones with dense inclusions. In fact, these morphotypes represent different stages of the ontogenesis of spherulous cells (Vacelet, 1967). According to Vacelet (1967) in intact sponge "dense" small spherulous cells concentrate mostly in the ectosome and around big exhalant canals, while "clear" larger ones are distributed in the mesohyl of endosome.

We have detected that in *A. cavernicola* the wound surface was free from invasive microbes from the first hours after injury up to the end of the regeneration. All microbes, that we detected at the wound surface and in the wound area during regeneration, shows ultrastructure identical to the microbes, located in the deeper sponge tissues and described as symbiotic in the previous papers (Vacelet, 1975; Fiedrich et al., 1999; Hentschel et al., 2001). Such defense against invasive microbes is probably provided by the particular chemical substances in the spherulous cells.

X-ray microanalysis revealed that these specialized cells of *Aplysina* produce and store brominated metabolites (Turon et al., 2000). Turon et al. (2000) demonstrated that the concentration of bromine peaks is slightly higher in the spherules from "dense" spherulous cells than in "clear" ones. Thompson et al. (1983) have detected bromine in the spherulous cells of Caribbean *Aplysina fistularis*. Spherulous cells have been shown to produce defense metabolites in other species (Thompson et al., 1983; Bretting et al., 1983; Uriz et al., 1996a).

In addition, it was showed that tissue damage in *Aplysina* induces a bioconversion of isoxazoline alkaloids into aeroplysinin-1 and secondary metabolite dienone (Thoms et al., 2006). This reaction is likely catalyzed by enzymes, and it may be ecologically important as the dienone has the strong antibacterial power and toxicity (Reverter et al., 2016). Moreover, this injury-induced reaction takes place within less than 1 min after wounding (Thoms et al., 2006).

6. Apoptosis during *A. cavernicola* regeneration

We have directly visualized and investigated apoptosis in the regeneration of sponges for the first time. The only previous data on the involvement of apoptosis in sponge regeneration emerge from the comparative transcriptomic analysis of the early stages of body wall regeneration in *Halisarca caerulea* (Kenny et al., 2017).

We have observed two waves of apoptosis during *Aplysina cavernicola* regeneration. The first wave, occurring around 6 hpo, is probably involved in the elimination of damaged cells and is characteristic for the early stages of regeneration of various animals, from cnidarians to vertebrates (Vlaskalin et al., 2004; Tseng et al., 2007; Chera et al., 2009; Pellettiere et al., 2010; DuBuc et al., 2014; Brandshaw et al., 2015; Kenny et al., 2017; Cebrià et al., 2018). For *Hydra* head regeneration after mid-gastric bisection (Chera et al., 2009) and tail regeneration in tadpole larva of *Xenopus laevis* (Tseng et al., 2007) it was shown that early wave of apoptosis not only clean a wound from damaged cells, but also generate signals, essential for initiation of subsequent regenerative processes. Inhibition of this apoptotic wave completely abolishes the regeneration. In particular, in both cases, apoptotic cells initiate a synchronous burst of proliferative activity in neighboring cells (Tseng et al., 2007; Chera et al., 2009), which is similar to the well-known apoptosis-induced compensatory proliferation in the imaginal disks of *Drosophila* (Fan & Bergmann, 2008; Bergmann & Steller, 2010). Apoptotic cells may be involved in the proliferation induction also during *A. cavernicola* body wall regeneration, as numerous DNA-synthesizing cells appears in the blastema only after the first apoptotic wave, at 24 hpo. These observations illustrate a novel active instructing role of apoptosis in morphogenetic processes, in contrast to its canonical passive role as a destructive agent (Duffy, 2012).

The second wave of apoptosis during *A. cavernicola* regeneration is likely associated with the extensive thrown out of spherulous cells though the forming exopinacoderm. Spherulous cells of *A. cavernicola* demonstrate the similar behavior in the intact sponges. Being one of the few terminally differentiated sponge cell lines, spherulous cells leave the mesohyl through aquiferous system canals or external surfaces (Vacelet, 1967). Their release outside from sponge is part of their normal physiology and possibly involved in the release of various chemicals (Uriz et al., 1996a; Ternon et al., 2016) and/or discharge processes (Maldonado, 2016) to the environment. The ultrastructure of spherulous cells eliminated through the exopinacoderm during the third phase of *A. cavernicola* regeneration is identical to that of the spherulous cells at the last stage of their evolution (Vacelet, 1967). Similarly, in the intact tissues of *H. caerulea*, many caspase-3 positive cells have a spherulous cell morphology (De Goeij et al., 2009), which indicates that apoptosis involved in the waste

control system in sponges in addition to maintaining tissue homeostasis (De Goeij et al., 2009).

Thus, the described increase in the level of apoptosis at the late stages of the *A. cavernicola* regeneration could be referred as a general tissue response, involved in the restoration of the normal sponge physiology in the area of injury, rather than in regeneration process itself. In planarians, the similar late general apoptotic response is also described, but it participates in the intensive remodeling of intact tissues, adjacent to a wound, to restore proper scale and proportions (Pellettiere et al., 2010; Cebrià et al., 2018).

Conclusion

Finally, we can made some principal conclusions:

1. In Porifera there are two principal mode of reparative regeneration: blastemal regeneration and tissue remodeling. From the literature data and results, obtained in this work we can conclude that first mode is characteristic for Demospongiae regeneration and the second – for Calcarea + Homoscleromorpha clade.

2. The results of our research also showed that sponges have more than two lines of adult stem cells, the potencies of which are clearly manifested during reparative regeneration. Our data support previous investigations, showed that archaeocytes and choanocytes are main players, or principal adult stem cells during demosponges regeneration (Korotkova & Nikitin, 1969; Thiney, 1972; Boury-Esnault, 1976; Diaz, 1979; Borisenko et al. 2015). However, the pinacocytes also could be considered as multipotent stem cells. Moreover, for the first time we showed, that spherulous cells of *Aplysina cavernicola* have a capacity to dedifferentiation during regeneration. It is first evidence that highly specialized cells of demosponges have capacity to dedifferentiation and possibly transdifferentiation.

3. Cell transdifferentiation plays an extremely significant role in sponge regeneration, as we have shown that regardless of the phylogenetic position, type of aquiferous system, and structure of epithelia, all studied sponges intensively utilize it for restoration of lost structures (Borisenko et al., 2015; Ereskovsky et al., 2015, 2017; Lavrov et al., 2018).

4. For the first time was investigated apoptosis during sponge regeneration. In *Aplysina cavernicola* regeneration this processes participate in damaged cells elimination and associated with the extensive ejection of spherulous cells from wound area.

Author contributions

A.V.E. and A.I.L. designed the study, conducted the experimental procedures with the living animals; A.I.L. performed the cell proliferation studies; A.V.E. and D.B.T. performed histological and ultrastructural studies. A.V.E.: Project administration and funding acquisition; S.B., E.L.G., and A.I.L.: performed the apoptosis studies; A.V.E. and A.I.L. prepared the manuscript with contributions from all authors. All authors reviewed and approved the final manuscript.

Acknowledgements

Authors gratefully thank Alexandre Altié of Plateforme C2VN de Microscopie Électronique TIMONE, Aix-Marseille Université, France, the Electron Microscopy Laboratory of the Shared Facilities Center of Lomonosov Moscow State University sponsored by the RF Ministry of Education and Science and Research Resource Center for Molecular and Cell Technologies at St. Petersburg State University, the staff of the Common Service of morphology in IMBE, and Dr. Jean Philippe Mévy (IMBE) - for help and assistance with electron and confocal microscopy studies. Data used in this study were partly produced using the Montpellier RIO imaging platform (confocal microscopy) (Montpellier, France). This work was supported by grants of Russian Foundation for Basic Research no. 16-04-00084, the Russian Science Foundation no. 17-14-01089 (histological and ultrastructural studies), and Metchnikov fellowship 2019 by French Embassy in Russia. This work also is a contribution to Labex OT-Med (n° ANR-11-LABX-0061) and has received funding from Excellence Initiative of Aix-Marseille University-A*MIDEX, a French ''Investissements d'Avenir'' program for travel expenses.

References

Adamska, M. (2018). Differentiation and Transdifferentiation of Sponge Cells. In M. Kloc, M., Kubiak, J. Z. (Eds.), *Marine Organisms as Model Systems in Biology and Medicine, Results and Problems in Cell Differentiation* 65 (pp. 229-253). Cham, Springer. https://doi.org/10.1007/978-3-319-92486-1_12.

Ayling, A.L. (1983). Growth and regeneration rates in thinly encrusting Demospongiae from temperate waters. *Biological Bulletin, 165*, 343-352.

Azevedo, L.G., Muccillo-Baisch, A.L., Filgueira, M., Boyle, R.T., Ramos, D.F., Soares, A.D., Lerner, C., Silva, P.A. & Trindade, G.S. (2008). Comparative cytotoxic and anti-tuberculosis activity of *Aplysina caissara* marine sponge crude extracts. *Comp Biochem Physiol C Toxicol Pharmacol, 147*, 36–42. DOI: 10.1016/j.cbpc.2007.07.007.

Bergquist, P. & Cook, S. (2002). Family Aplysinidae Carter, 1875. In Hooper, J.N.A., Van Soest, R.W.M. (Eds.), *Systema Porifera: A Guide to the Classification of Sponges*. (pp. 1082-1085). NY, Kluwer Academic/Plenum Publishers.

Bergmann, A., & Steller, H. (2010). Apoptosis, stem cells, and tissue regeneration. *Sci. Signal*, *3*, 1–8. https://doi.org/10.1126/scisignal.3145re8

Betancourt-Lozano, M., González-Farias, F.A., González-Acosta, B., & García-Gasca, A. (1998). Variation of antimicrobial activity of the sponge *Aplysina fistularis* (Pallas, 1766) and its relation to associated fauna. *J Exp Mar Biol Ecol, 223*, 1–18.

Borisenko, I.E., Adamska, M., Tokina, D.B., & Ereskovsky, A.V. (2015). Transdifferentiation is a driving force of regeneration in *Halisarca dujardini* (Demospongiae, Porifera). *PeerJ*, *3*, e1211. https://doi.org/10.7717/peerj.1211

Boury-Esnault, N. (1976). Morphogenese experimentale des papilles inhalantes de l'eponge *Polymastia mamillaris* (Muller). *Arch. Zool. Exp. Gén.*, *117*(2), 181–196.

Bradshaw, B., Thompson, K., & Frank, U. (2015). Distinct mechanisms underlie oral vs aboral regeneration in the cnidarian *Hydractinia echinata*. *Elife 2015*, 1–19. doi.org/10.7554/eLife.05506.

Brondsted, H.V. (1953). The ability to differentiate and the size of regenerated cells after repeated regeneration. *Quart Journal of Microscopy Sciences,* 94, 177-184.

Carlson, B.M. (2007). *Principles of regenerative biology*. New York: Academic Press.

Cavolini, F. (1785). Memorie per servire alia storia dei polipi marini. Napoli, 1785. (Cited by Cotte, 1908.)

Bretting H., Jacobs, G., Donadey, C., & Vacelet, J. (1983). Immunohistochemical

studies on the distribution and the function of the D. galactose-specific lectins in the sponge *Axinella polypoides* (Schmidt). *Cell and Tissue Research*, *229*, 551-571.

Cebrià, F., Adell, T., & Saló, E. (2018). Rebuilding a planarian: from early signaling to final shape. *International Journal of Developmental Biology, 62*, 537–550. https://doi.org/10.1387/ijdb.180042es

Chera, S., Ghila, L., Dobretz, K., Wenger, Y., Bauer, C., Buzgariu, W., Martinou, J.-C., & Galliot, B. (2009). Apoptotic Cells Provide an Unexpected Source of Wnt3 Signaling to Drive *Hydra* Head Regeneration. *Development & Cells, 17*, 279–289. doi.org/10.1016/j.devcel.2009.07.014.

Ciminiello, P., Fattorusso, E., Forino, M., Magno, S., & Pansini, M. (1997). Chemistry of Verongida sponges. 8. Bromocompounds from the Mediterranean sponges *Aplysina aerophoba* and *Aplysina cavernicola*. *Tetrahedron, 53,* 6565-6572.

Connes, R. (1966). Contribution a l'etude histologique des premiers stades d'embryogenese somatique chez *Tethya lyncurium* Lamarck. *Bull Soc Zool France, 91*, 639-645.

Connes, R. (1968). Etude histologique, cytologique et expérimentale de la régénération et de la reproduction asexuée chez *Tethya lyncurium* Lamarck (=*T. aurantium* Pallas (Démosponges). (PhD Thesis, Fac. Sci. Montpellier).

Coutinho, C.C., Rosa, I.A., Teixeira, J.D.O., Andrade, L.R., Costa, M.L., & Mermelstein, C. (2017). Cellular migration, transition and interaction during regeneration of the sponge *Hymeniacidon heliophila*. *PLoS One, 12, 5*. e0178350. DOI : 10.1371/journal.pone.0178350.

D'Ambrosio, M., Guerriero, A., Traldi, P., & Pietra, F. (1982). Cavernicolin-1 and cavernicolin-2, two epimeric dibromolactams from the Mediterranean sponge *Aplysina (Verongia) cavernicola*. *Tetrahedron Letters, 23,* 4403-4406.

D'Ambrosio, M., Guerriero, A., De-Clauser, R., De-Stanchina, G., & Pietra, F. (1983). Dichloroverongiaquinol, a new marine antibacterial compound from *Aplysina cavernicola*. Isolation and synthesis. *Experientia, 39,* 1091-1092.

De Goeij, J.M., De Kluijver, A., Van Duyl, F.C., Vacelet, J., Wijffels, R.H., De Goeij, A.F.P.M., Cleutjens, J.P.M., & Schutte, B. (2009). Cell kinetics of the marine sponge *Halisarca caerulea* reveal rapid cell turnover and shedding. *The Journal of Experimental Biology, 212*, 3892-3900. DOI: 10.1242/jeb.034561.

de Mendiburu, F. (2019). agricolae: Statistical Procedures for Agricultural Research. R package version 1.3-1. https://CRAN.R-project.org/package=agricolae

Diaz, J.P. (1979). Variations, differentiations et functions des categories cellulaires de la demosponge d'eaux saumatres, *Suberites massa*, Nardo, au cours du cycle biologique annuel et dans des conditions experimentales. These doct. Acad Montpellier

DuBuc, T.Q., Traylor-Knowles, N., & Martindale, M.Q. (2014). Initiating a regenerative response; cellular and molecular features of wound healing in the cnidarian *Nematostella vectensis*. *BMC Biology, 12*, 24. doi.org/10.1186/1741-7007-12-24.

Duffy, D.J. (2012). Instructive reconstruction: A new role for apoptosis in pattern formation. *BioEssays, 34*, 561–564. https://doi.org/10.1002/bies.201200018

Duckworth, A.R. (2003). Effect of wound size on the growth and regeneration of two temperate subtidal sponges. *Journal of Experimental Marine Biology and Ecology, 287*, 139–153. DOI: 10.1016/S0022-0981(02)00552-X.

Ehrlich, H., Ilan, M., Maldonado, M., Muricy, G., Bavestrello, G., Kljajic, Z., Carballo, J.L., Schiaparelli, S., Ereskovsky, A., Schupp, P., Bornk, R., Worch, H., Bazhenov, V.V., Kurek, D., Varlamov, V., Vyalikh, D., Kummer, K., Sivkov, V.V., Molodtsov, S.L., Meissner, H., Richter, G., Steck, E., Richter, W., Hunoldt, S., Kammer, M., Paasch, S., Krasokhin, V., Patzke, G., & Brunner, E. (2010a). Three-dimensional chitin-based scaffolds from Verongida sponges (Demospongiae: Porifera). Part I. Isolation and identification of chitin. *International Journal of Biological Macromolecules, 47,* 132-140. DOI: 10.1016/j.ijbiomac.2010.05.007.

Ehrlich, H., Steck, E., Ilan, M., Maldonado, M., Muricy, G., Bavestrello, G., Kljajic, Z., Carballo, J.L., Schiaparelli, S., Ereskovsky, A., Schupp, P., Bornk, R., Worch, H., Bazhenov, V.V., Kurek, D., Varlamov, V., Vyalikh, D., Kummer, K., Sivkov, V.V., Molodtsov, S.L., Meissner, H., Richter, G., Hunoldt, S., Kammer, M., Paasch, S., Krasokhin, V., Patzke, G., Brunner, E., & Richter, W. (2010 b). Three-dimensional chitin-based scaffolds from Verongida sponges (Demospongiae: Porifera). Part II: Biomimetic potential and applications. *International Journal of Biological Macromolecules, 47,* 141-145. DOI: 10.1016/j.ijbiomac.2010.05.009.

Ereskovsky, A.V., Renard, E., Borchiellini, C. (2013). Cellular and molecular processes leading to embryo formation in sponges: evidences for high conservation of processes throughout animal evolution. *Development, Genes & Evolution*, *223*, 5-22. DOI 10.1007/s00427-012-0399-3

Ereskovsky, A.V., Borisenko, I.E., Lapébie, P., Gazave, E., Tokina, D.B., & Borchiellini, C. (2015). *Oscarella lobularis* (Homoscleromorpha, Porifera) Regeneration:

Epithelial Morphogenesis and Metaplasia. *Plos One*, *10*(8), e0134566. https://doi.org/10.1371/journal.pone.0134566

Ereskovsky, A.V., Chernogor, L.I., & Belikov, S.I. (2016). Ultrastructural description of development and cell composition of primmorphs in the endemic Baikal sponge *Lubomirskia baicalensis*. *Zoomorphology*, *135*(1), 1–17. https://doi.org/10.1007/s00435-015-0289-0

Ereskovsky, A.V., Lavrov, A.I., Bolshakov, F.V., & Tokina, D.B. (2017). Regeneration in White Sea sponge *Leucosolenia complicata* (Porifera, Calcarea). *Invertebrate Zoology*, *14*(2), 108–113. https://doi.org/10.15298/invertzool.14.2.02

Fiedrich, A.B., Merkert, H., Fendert, T., Hacker, J., Proksch, P., & Hentschel, U. (1999). Microbial diversity in the marine sponge *Aplysina cavernicola* (formerly *Verongia cavernicola*) analyzed by fluorescence in situ hybridization. *Marine Biology, 134,* 461-470.

Fan, Y. & Bergmann, A. (2008). Apoptosis-induced compensatory proliferation. The Cell is dead. Long live the Cell! *Trends Cell Biology, 18*, 467–473. https://doi.org/10.1016/j.tcb.2008.08.001

Fox, J. & Weisberg, S. (2019). An {R} Companion to Applied Regression (3rd ed.). Thousand Oaks CA: Sage.

Funayama, N. (2018). The cellular and molecular bases of the sponge stem cell systems underlying reproduction, homeostasis and regeneration. *International Journal of Developmental Biology, 62*(6-8), 513–525. https://doi.org/10.1387/ijdb.180016nf

Gaino, E., Manconi, R., & Pronzato, R. (1995). Organizational plasticity as a successful conservative tactics in sponges. *Animal Biology, 4,* 31-43.

Gallissian, M.F., & Vacelet J. (1976). Ultrastructure de quelques stades de l'ovogenèse de spongiaires du genre *Verongia* (Dictyoceratida). *Annales des Sciences Naturelles, Biologie Animale, 18*, 381-404.

Garrone R., Vacelet, J., Pavans de Ceccatty, M., Junqua, S., & Robert, L. (1973). Une formation collagene particuliere: les filaments des Eponges cornées *Ircinia*. Etude ultrastructurale, physico-chimique et biochimique. *Journal de Microscopie, 17,* 241-260.

Henry, L-F., & Hart, M. (2005). Regeneration from Injury and Resource Allocation in Sponges and Corals – a Review. *International Review in Hydrobiology, 90,* 125–158.

Hentschel, U., Schmid, M., Wagner, M., Fieseler, L., Gernert, C., & Hacker, J. (2001). Isolation and phylogenetic analysis of bacteria with antimicrobial activities from the Mediterranean sponges *Aplysina aerophoba* and *Aplysina cavernicola*. *FEMS Microbiol Ecol, 35,* 305-312.

Hoffmann, F., Rapp, H.T., Zoller, T., & Reitner, J. (2003). Growth and regeneration in cultivated fragments of the boreal deep water sponge *Geodia barretti* Bowerbank, 1858 (Geodiidae, Tetractinellida, Demospongiae). *Journal of Biotechnology, 100,* 109-118.

Hoppe, W.F. (1988). Growth, regeneration and predation in three species of large coral reef sponges. *Marine Ecology Progress Series, 50*: 117-125. DOI: 10.1016/s0168-1656(02)00258-4.

Keller, R., Davidson, L.A., & Shook, D.S. (2003). How we are shaped: the biomechanics of gastrulation. *Differentiation, 71*, 171-205. DOI:10.1046/j.1432-0436.2003.710301.x.

Korotkova, G.P. (1961). Regeneration and somatic embryogenesis in the calcareous sponge *Leucosolenia complicata* Mont. *Acta Biologica Academiae Scientiarum Hungaricae, 11*(4), 315–334.

Korotkova, G.P. (1972a). Comparative morphological investigations of development of sponges from dissociated cells. *Transactions of Leningrad Society of Naturalists, 78*(4), 74–109.

Korotkova, G.P. (1972b). Regeneration of the calcareus sponge *Sycon lingua*. *Transactions of Leningrad Society of Naturalists, 78*(4), 155–169.

Korotkova, G.P. (1997). *Regeneration in animals*. Saint-Petersburg: Saint-Petersburg University Press.

Korotkova, G.P., Efremova, S.M., & Kadantseva, A.G. (1965). The pecularities of morphogenesis of the development of *Sycon lingua* from the small part of the body. *Vestnik of Leningrad University*, *4*(21), 14–30.

Korotkova, G.P., & Nikitin, N.S. (1969). The comparative morphological analysis of regeneration and somatic embryogenesis of the cornacusponge *Halichondria panicea*. In B. P. Tokin (Ed.), *Reconstructional processes and immunological reactions. Morphological investigations of different stages of development of the marine organisms* (pp. 9–16). Leninrad: Nauka.

Korotkova, G.P., Sukhodolskaya, A.N., & Krasukevitch, T.N. (1983). The pecularities of morphogenesis of the development of *Halisarca dujardini* from the small part of the body. *Vestnik Leningrad University*, *9*, 41–46.

Lavrov, A.I., & Kosevich, I.A. (2016). Sponge cell reaggregation: Cellular structure and morphogenetic potencies of multicellular aggregates. *Journal of Experimental Zoology Part A: Ecological Genetics and Physiology, 325*(2), 158–177. https://doi.org/10.1002/jez.2006

Lavrov, A.I., Bolshakov, F.V., Tokina, D.B., & Ereskovsky, A.V. (2018). Sewing wounds up: the epithelial morphogenesis as a central mechanism of calcaronean sponge regeneration. *Journal of Experimental Zoology Part B: Molecular and Developmental Evolution. 330*(6-7): 351-371. https://doi.org/10.1002/jezb.22830

Lim, J., & Thiery, J.P. (2012). Epithelial-mesenchymal transitions: insights from development. *Development, 139*, 3471-3486. doi:10.1242/dev.071209.

Maas, O. (1910). Über Nichtregeneration bei Spongien. *Zeitschrift fur R. Hertwig, 3,* 93-130.

Maldonado, M. (2016). Sponge waste that fuels marine oligotrophic food webs: a re-assessment of its origin and nature. *Marine Ecology, 37,* 477-491. DOI : 10.1111/maec.12256.

Pellettieri, J., Fitzgerald, P., Watanabe, S., Mancuso, J., Green, D.R., & Sánchez Alvarado, A.S. (2010). Cell death and tissue remodeling in planarian regeneration. *Developmental Biology, 338,* 76–78. doi.org/10.1016/j.ydbio.2009.09.015

Pozzolini, M., Gallus, L., Ghignone, S., Ferrando, S., Candiani, S., Bozzo, M., Bertolino, M., Costa, G., Bavestrello, G., & Scarfì, S. (2019). Insights into the evolution of metazoan regenerative mechanisms: roles of TGF superfamily members in tissue regeneration of the marine sponge *Chondrosia reniformis*. *Journal of Experimental Biology,* 222, jeb207894. doi:10.1242/jeb.207894.

R Core Team (2019). R: A language and environment for statistical computing. R Foundation for Statistical Computing, Vienna, Austria. https://www.R-project.org/

Reverter, M., Perez, T., Ereskovsky, A., & Banaigs, B. (2016). Secondary Metabolome Variability and Inducible Chemical Defenses in the Mediterranean Sponge *Aplysina cavernicola*. *Journal of Chemical Ecology*, *42*, 60-70. doi: 10.1007/s10886-015-0664-9

Sukhodolskaya, A.N. (1973). The mechanism of oscular tube restoration in *Ephydatia fluviatilis* (L). In Tokin, B.P. (Ed.), *Morphogenetic Processes during Asexual Reproduction, Somatic Embryogenesis and Regeneration*. (pp. 127-145), Leningrad State University. Leningrad.

Ternon, E., Zarate, L., Chenesseau, S., Croue, J., Dumollard, R., Suzuki, M.T., & Thomas, O.P. (2016). Spherulization as a process for the exudation of chemical cues by the encrusting sponge *C. crambe*. *Sci Rep, 6,* 29474. DOI : 10.1038/srep29474

Thiney, Y. (1972). Morphologie et cytochimie ultrastructurale de l'oscule *d'Hippospongia communis* LMK et de sa régénération (Ph.D. thesis, University Claude Bernard, Lyon).

Thompson, J.A., Barrow, K.D. & Faulkner, D.J. (1983). Localization of Two Brominated Metabolites, Aerothionin and Homoaerothionin, in Spherulous Cells of the Marine Sponge *Aplysina fistularis* (= *Verongia thiona*). *Acta Zoologica, 64,* 199-210.

Thoms, C., Horn, M., Wagner, M., Hentschel, U., & Proksch P. (2003). Monitoring microbial diversity and natural product profiles of the sponge *Aplysina cavernicola* following transplantation. *Marine Biology. 142,* 685–692. DOI https://doi.org/10.1007/s00227-002-1000-9

Thoms, C., Wolff, M., Padmakumar, K., Ebel, R., & Proksch, P. (2004). Chemical defense of Mediterranean sponges *Aplysina ca*vernicola and *Aplysina aerophoba*. Zeitschrift fur *Naturforschung C J Bioscience, 59*, 113–122. DOI: 10.1515/znc-2004-1-222.

Thoms, C., Ebel, R., & Proksch, P. (2006). Activated chemical defense in *Aplysina* sponges revisited. *Journal of Chemical Ecology, 32*, 97–123.

Tseng, A.-S., Adams, D.S., Qiu, D., Koustubhan, P., & Levin, M. (2007). Apoptosis is required during early stages of tail regeneration in *Xenopus laevis*. *Developmental Biology, 301*, 62–69. https://doi.org/10.1016/j.ydbio.2006.10.048

Turon, X., Becerro, M.A., & Uriz, M.J. (2000). Distribution of brominated compounds within the sponge *Aplysina aerophoba*: coupling of X-ray microanalysis with cryofixation techniques. *Cell and Tissue Research. 301,* 311-322.

Uriz, M.J., Becerro, M.A., Tur, J.M., & Turon, X. (1996). Location of toxicity within the Mediterranean sponge *Crambe crambe* (Demospongiae: Poecilosclerida). *Marine Biology, 124*, 583–590.

Vaillant, L. (1869). Note sur la vitalité d'une Sponge de la famille des Corticatae, la *Tethya lyncurium*. *Comptes rendus de 1'Académie des Sciences*, t. Lxviii.

Vacelet, J. (1959). Répartition générale des éponges et systématique des éponges cornées de la région de Marseille et de quelques stations méditerranéennes. *Recueil des travaux de la Station Marine d'Endoume, 16*, 39-101.

Vacelet, J. (1966). Les cellules contractiles de l'éponge cornée *Verongia cavernicola* Vacelet. *Comptes-Rendus de l'Académie des Sciences de Paris, 263,* 1330-1332.

Vacelet, J. (1967). Les cellules à inclusions de l'éponge cornée *Verongia cavernicola* Vacelet. *Journal de Microscopie (Paris), 6,* 237-240.

Vacelet, J. 1970. Description de cellules a bactéries intranucléaires chez des éponges *Verongia*. *Journal de Microscopie (Paris), 9,* 333-346.

Vacelet J. (1971a). Ultrastructure et formation des fibres collagénes de spongine d'Eponges Cornées *Verongia*. *Journal de Microscopie (Paris), 10,* 13-32.

Vacelet, J. (1971b). L'ultrastructure de la cuticule d'Eponges Cornées *Verongia*. *Journal de Microscopie (Paris), 10,* 113-116.

Vacelet, J. (1975). Etude en microscopie électronique de l'association entre bactéries et spongiaires du genre *Verongia* (Dictyoceratida). *Journal de Microscopie et de Biologie cellulaire, 23*, 271-288.

Vacelet, J., & Gallissian, M.F. (1978). Virus-like particles in cells of the sponge *Verongia cavernicola* (Demospongiae, Dictyoceratida) and accompanying tissue changes. *Journal of Invertebrate Pathology, 31,* 246-254.

Vlaskalin, T., Wong, C.J., & Tsilfidis, C. (2004). Growth and apoptosis during larval forelimb development and adult forelimb regeneration in the newt (*Notophthalmus viridescens*). *Development, Genes Evolution, 214*, 423–431. https://doi.org/10.1007/s00427-004-0417-1

Weltner, V. (1893). Spongillidcnstudicn. *U Arch Naturgesch, 59,* 245- 282.

Wickham, H. (2016). ggplot2: Elegant Graphics for Data Analysis. Springer-Verlag: New York

Wulff, J. (2010). Regeneration of sponges in ecological context: Is regeneration an integral part of life history and morphological strategies? *Integrative and Comparative Biology, 50*, 494–505. doi:10.1093/icb/icq100.

Wulff, J. (2013). Recovery of sponges after extreme mortality events: morphological and taxonomic patterns in regeneration versus recruitment. *Integrative and Comparative Biology, 53*, 512-523. DOI : 10.1093/icb/ict059.

Figure legends for *Aplysina cavernicola* regeneration

Figure 1. Time series photographs *in situ* of wounds to *Aplysina cavernicola.*

Time series photographs of wounds to *Aplysina cavernicola*, Corrals Cave, Marseille, France June-July 2018. Two examples were chosen to illustrate individual variety of regeneration after experimental wounding. W – wound. Scale bar – 1.2 cm.

Figure 2. *Aplysina cavernicola in vivo*

A – intact sponge before operation; B – sponge just after operation; C – sponge after 48 hours after operation.

o – osculum, w – wound.

Figure 3. Intact *Aplysina cavernicola*

A – semi-fin section of upper part of sponge; B – TEM image of ectosome; C – exopinacocyte and spherulous cells (inset: detail of cell junctions between exopinacocytes); D – endopinacocyte; E – choanocyte chamber (inset: choanocyte); F – pocket cell with symbiotic bacteria; G – archaeocyte; H – myocytes (inset: detail of myocytes with myofibrils).

ar – archaeocyte, cb – cell body of exopinacocyte, cc – choanocyte chamber, ch – choanocyte, ect – ectosome, en – endopinacocyte, end – endosome, ex- exopinacocytes, f – flagellum, fp – flat part of exopinacocyte, in – inclusions in spherulous cells, my – myocyte, pc - pocket cell, n – nucleus, sb – symbiotic bacteria, sc – spherulous cell.

Figure 4. Cells of the mesohyl in intact *Aplysina cavernicola*

A – bacteriocyte; B – spongocyte; C – lophocytes; D - spherulous cell at the late stage of evolution expelled into exhalant canal; E – microgranular cell; F – granular cell; G, H – spherulous cells in two stages of their development.

ar – archaeocyte, ba – bacteriocyte, ex- exopinacocytes, exc – exhalant canal, in – inclusions in spherulous cells, lo – lophocyte, mc – microgranular cell, n – nucleus, sb – symbiotic bacteria, sc – spherulous cell, sf – skeleton fiber, sp - spongocyte.

Figure 5. Scheme of wound and their parts in *Aplysina cavernicola.*

ect – ectosome, end – endosome, it - intact tissues, ra – regenerated area, w – wound, wa – wound area, we – wound edge.

Figure 6. 3h of regeneration in *Aplysina cavernicola*

A – wound and a marginal zone; B – zone under the wound; C – internal part of the wound with encapsulated invasive diatoms; D – dedifferentiated choanocyte (flash show the basal flagellum apparatus)

ar – archaeocyte, ba – bacteriocyte, dch – dedifferentiated choanocyte, di – encapsulated diatom, en – endopinacocyte, in – inclusions in spherulous cells, lo – lophocyte, n – nucleus, ph – phagosome, sb – symbiotic bacteria, sc – spherulous cell, scf – spherulous cells fragments, w - wound.

Figure 7. 6h of regeneration in *Aplysina cavernicola*

A – semi thin section of the wound and upper part of endosome; B, C – TEM of the upper part of the wound: it is a choanocyte chamber during their destruction, fragments of spherulous cells, phagocyted spherulous cell; D, E – wound zone with the fragments of cells and phagocytosis of spherulous cells; F – inner part of the wound, degraded choanocyte chamber.

ar – archaeocyte, cc – choanocyte chamber, dcc - destructed choanocyte chamber, dch – dedifferentiated choanocyte, end – endosome, in – inclusions in spherulous cells, n – nucleus, ph – phagosome, sb – symbiotic bacteria, sc – spherulous cell, scf – spherulous cells fragments, w – wound, ws – wound surface.

Figure 8. Boxplot diagram of the number of spherulous cells per mm^2 in intact tissues and during regeneration in *A. cavernicola*. The differences between some of the means are statistically significant (ANOVA p-value = 2.36E-07(<0.01)). Tukey's multiple comparisons showed no significant differences only in 3 pairs: Intact tissues–96 hpo; 6 hpo–12 hpo; 24 hpo–48 hpo. Duncan's new multiple range test (MRT) approve this, grouping these pairs into three clusters (A, B, C). The differences between Duncan's clusters are statistically significant (Supporting Table 4).

Figure 9. 12h of regeneration in *Aplysina cavernicola*

A – semi thin section of the wound and upper part of endosome; B, C – TEM of the upper part of the wound, there are some non-secret cells at the wound surface (arrowheads), dedifferentiated choanocytes and spherulous cells; D – detail of the upper part of the wound;

E – wound zone with dedifferentiated choanocytes; F – marginal zone of the wound with the part of intact exopinacocyte.

ar – archaeocyte, cf – cells fragments, dch – dedifferentiated choanocyte, dsc - dedifferentiated spherulous cell, end – endosome, in – inclusions in spherulous cells, n – nucleus, ph – phagosome, sb – symbiotic bacteria, sc – spherulous cell, scf – spherulous cells fragments, w – wound, ws – wound surface.

Figure 10. 24h of regeneration in *Aplysina cavernicola*

A – semi thin section of the wound and upper part of endosome; B, C – TEM of the upper part of the wound, with flat parts of new exopinacocytes, spherulous and non-secret cells with the phagosomes (arrowhead - basal body of choanocyte flagellum); D – wound zone with dedifferentiated choanocytes; E - upper part of the wound zone with archaeocyte and dedifferentiated choanocyte in the beginning of differentiation into new exopinacocyte, arrow show the basal apparatus of dedifferentiated choanocyte; F - archaeocyte differentiated into exopinacocyte at the upper part of the wound.

ar – archaeocyte, cf – cells fragments, dch – dedifferentiated choanocyte, dsc - dedifferentiated spherulous cell, end – endosome, in – inclusions in spherulous cells, n – nucleus, nu – nucleolus, ph – phagosome, sb – symbiotic bacteria, sc – spherulous cell, scf – spherulous cells fragments, w - wound.

Figure 11. 48h of regeneration in *Aplysina cavernicola*

A – semi thin section of the wound and upper part of endosome; B – TEM of the upper part of the wound, with restored ectosome; C – TEM of the upper part of the wound, showed transdifferentiation of a choanocyte into exopinacocyte; inset – basal apparatus of dedifferentiated choanocyte (arrowhead); D – TEM of the upper part of the wound, showing transdifferentiation of an archaeocyte into exopinacocyte; E, F - TEM of the small apoptotic spherulous cells elimination of apoptotic spherulous cells through forming exopinacoderm.

ac – apoptic cell, asc – apoptic spherulous cell, ar – archaeocyte, cc – choanocyte chamber, ch – choanocyte, cf – cells fragments, dch – dedifferentiated choanocyte, end – endosome, ex-exopinacocytes, fp – flat part of exopinacocyte, in – inclusions in spherulous cells, lo – lophocyte, mc – microgranular cell, my – myocyte, n – nucleus, ph – phagosome, sb – symbiotic bacteria, sc – spherulous cell, scf – spherulous cells fragments, w – wound zone.

Figure 12. 48h of endosome regeneration in *Aplysina cavernicola*

A-C – TEM of the endosome under the wound, showing different stages of restoration of exhalant canals of the aquiferous system; D-F - TEM of the endosome under the wound, showing different stages of restoration of choanocyte chambers.
cc – choanocyte chamber, ch – choanocyte, en – endopinacocyte, exc – exhalant canal, sb – symbiotic bacteria.

Figure 13. 96h of regeneration in *Aplysina cavernicola*
A – semi thin section of the completely restored ectosome and upper part of endosome; B – TEM of the upper part of the restored ectosome; C - the endosome with new choanocyte chamber; D – the endosome with normal cell composition.
ar – archaeocyte, cc – choanocyte chamber, ch – choanocyte, ect – ectosome, end – endosome, exc- exhalant canal, lo – lophocyte, n – nucleus, sb – symbiotic bacteria, sc – spherulous cell.

Figure 14. Cell proliferation in intact tissues of *Aplysina cavernicola*. A – ectosome; B – endosome; C – endosome near the exhalant canal of the aquiferous system; D – DNA-synthesizing choanocytes with small round to oval nuclei; E – mesohyl DNA-synthesizing cells with large round nuclei. Cyan – DAPI, green – α-tubulin, magenta – EdU. cc – choanocyte chamber, end – endosome, ect – ectosome, exc – exhalant canal of the aquiferous system. White arrowheads marks EdU-positive nuclei of DNA-synthesizing cells. Each image is a maximum projection, obtained from 55 µm Z stack.

Figure 15. Cell proliferation during *Aplysina cavernicola* body wall regeneration. A-E – cell proliferation in the wound area at different stages of regeneration: A – 0-6 hpo; B – 0-24 hpo; C – 24-48 hpo; D – 48-72 hpo; E – 120-144 hpo; F – cell proliferation in intact tissues, distant from the wound, during regeneration. Cyan – DAPI, magenta – EdU. Dcc – disintegrating choanocyte chamber, cc – choanocyte chamber. White arrowheads marks EdU-positive nuclei of DNA-synthesizing cells. Each image is a maximum projection, obtained from 15 µm Z stack.

Figure 16. Apoptosis during *Aplysina cavernicola* body wall regeneration. A – 6 hpo; B – 12 hpo; C – 48 hpo. Blue – DAPI, red – TUNEL. White dashed line marks the wound edge, white arrows – TUNEL-positive nuclei of apoptotic cells. Each image is an optical slice through the wound area.

Supporting Figure 1. TEM images of ECM dynamic at the wound surface.

A – intact ; B – 0 hpo ; C - 3 hpo ; D – 6 hpo ; E – 12 hpo ; F – 24 hpo ; G – 48 hpo ; H – 96 hpo.

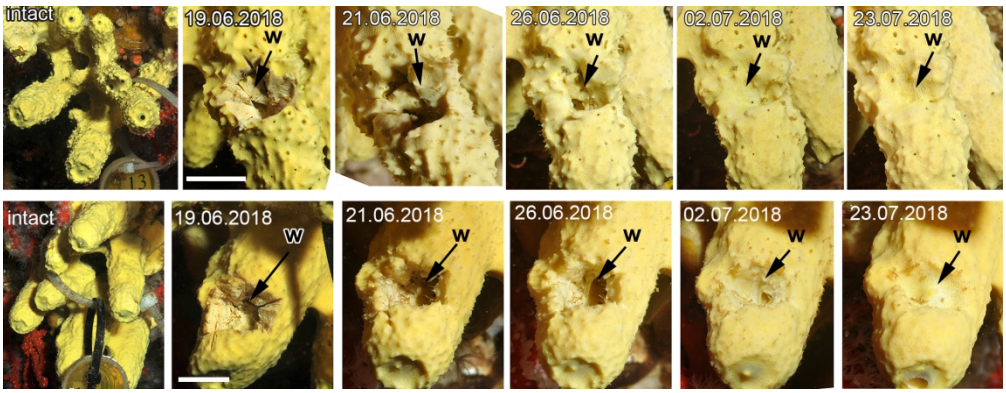

Figure 1. Time series photographs in situ of wounds to Aplysina cavernicola.
Time series photographs of wounds to Aplysina cavernicola, Corrals Cave, Marseille, France June-July 2018. Two examples were chosen to illustrate individual variety of regeneration after experimental wounding. W – wound. Scale bar – 1.2 cm.

179x68mm (300 x 300 DPI)

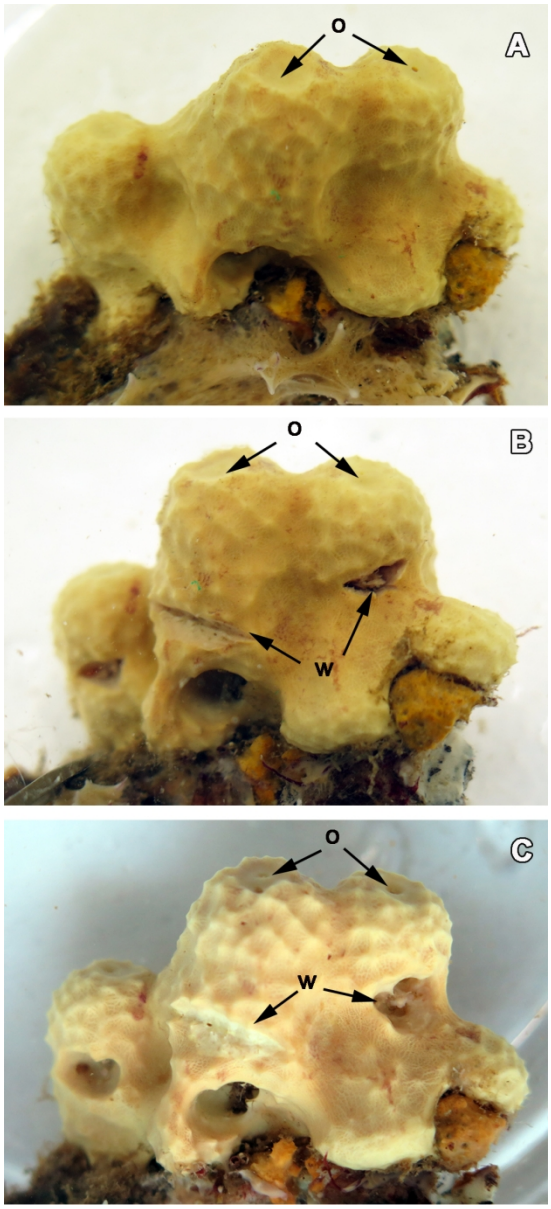

Figure 2. Aplysina cavernicola in vivo
A – intact sponge before operation; B – sponge just after operation; C – sponge after 48 hours after operation.
o – osculum, w – wound.

90x198mm (300 x 300 DPI)

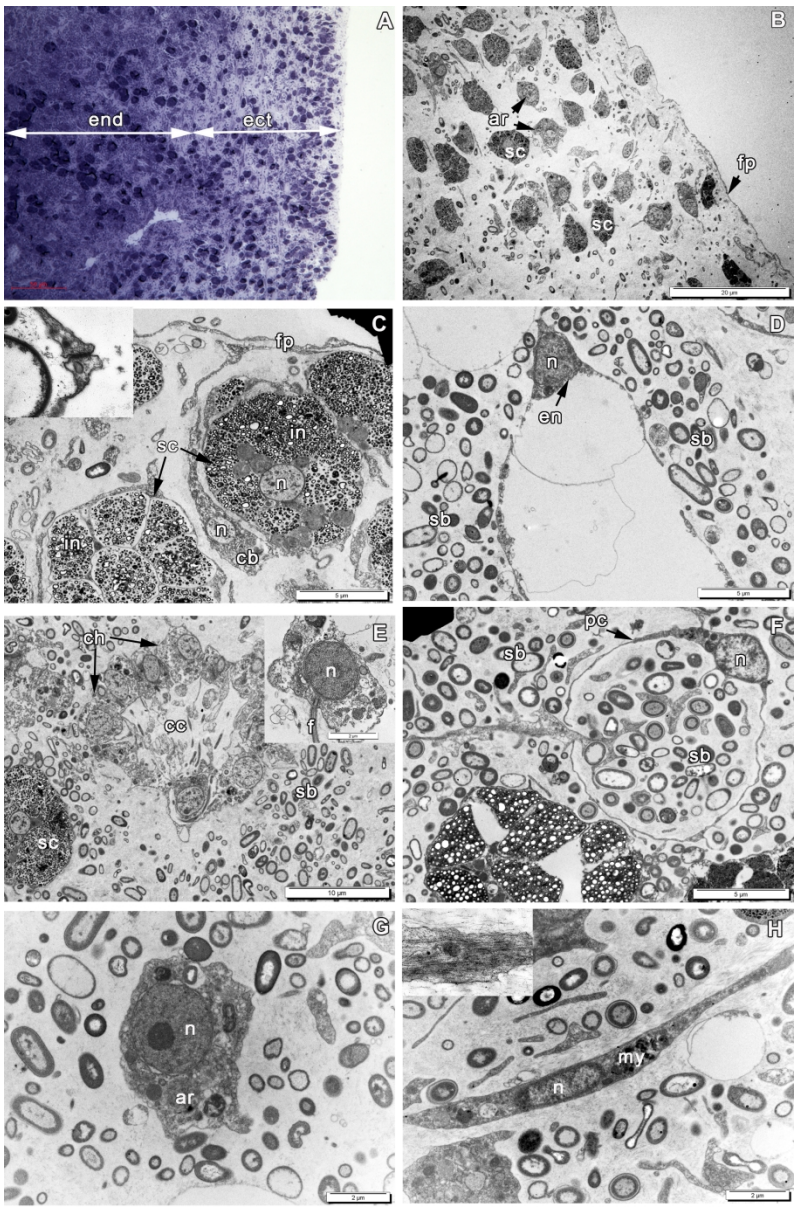

Figure 3. Intact Aplysina cavernicola
A – semi-fin section of upper part of sponge; B – TEM image of ectosome; C – exopinacocyte and spherulous cells (inset: detail of cell junctions between exopinacocytes); D – endopinacocyte; E – choanocyte chamber (inset: choanocyte); F – pocket cell with symbiotic bacteria; G – archaeocyte; H – myocytes (inset: detail of myocytes with myofibrils).
ar – archaeocyte, cb – cell body of exopinacocyte, cc – choanocyte chamber, ch – choanocyte, ect – ectosome, en – endopinacocyte, end – endosome, ex- exopinacocytes, f – flagellum, fp – flat part of exopinacocyte, in – inclusions in spherulous cells, my – myocyte, pc - pocket cell, n – nucleus, sb – symbiotic bacteria, sc – spherulous cell.

180x272mm (300 x 300 DPI)

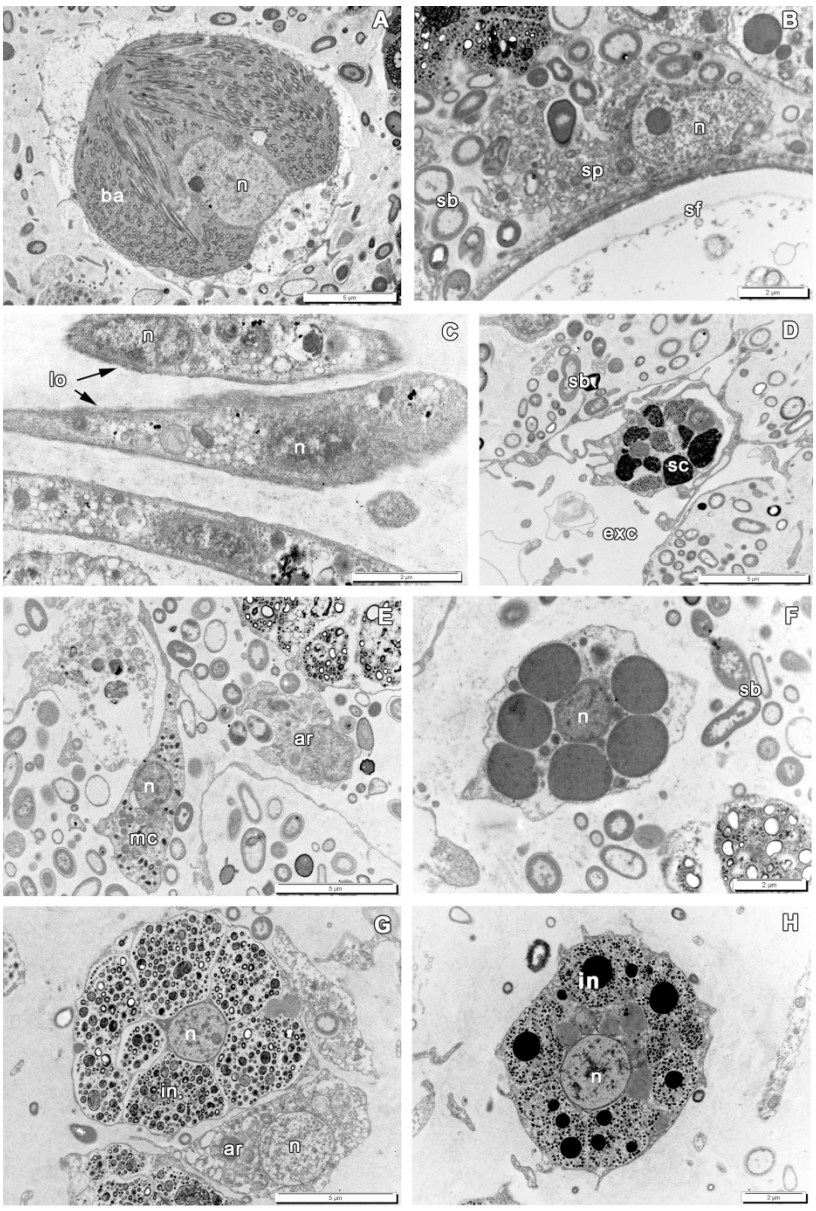

Figure 4. Cells of the mesohyl in intact Aplysina cavernicola
A – bacteriocyte; B – spongocyte; C – lophocytes; D - spherulous cell at the late stage of evolution expelled into exhalant canal; E – microgranular cell; F – granular cell; G, H – spherulous cells in two stages of their development.
ar – archaeocyte, ba – bacteriocyte, ex- exopinacocytes, exc – exhalant canal, in – inclusions in spherulous cells, lo – lophocyte, mc – microgranular cell, n – nucleus, sb – symbiotic bacteria, sc – spherulous cell, sf – skeleton fiber, sp - spongocyte.

180x266mm (300 x 300 DPI)

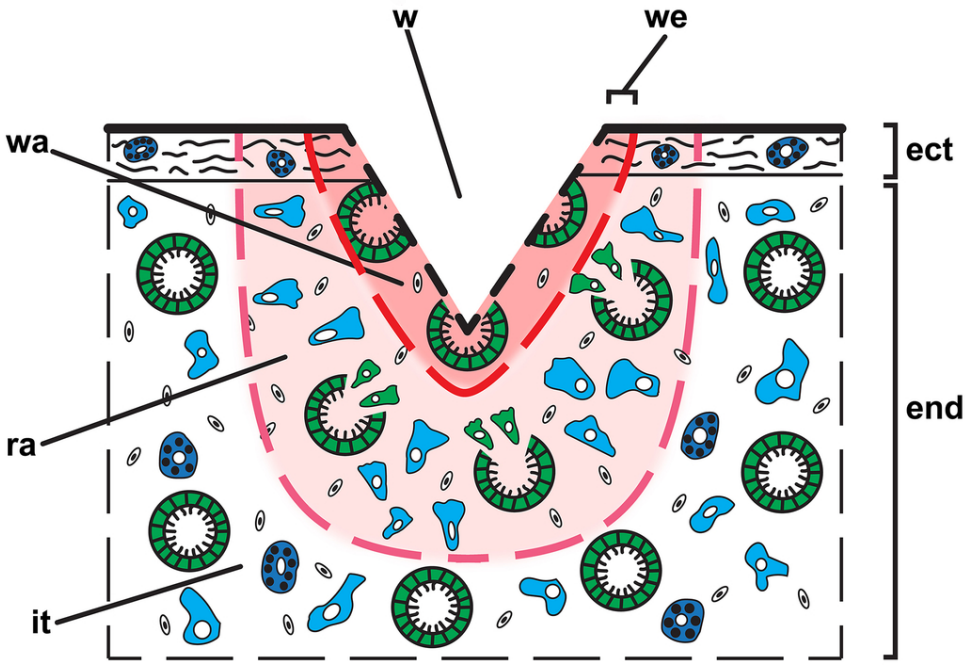

Figure 5. Scheme of wound and their parts in Aplysina cavernicola.
ect – ectosome, end – endosome, it - intact tissues, ra – regenerated area, w – wound, wa – wound area, we – wound edge.

90x68mm (300 x 300 DPI)

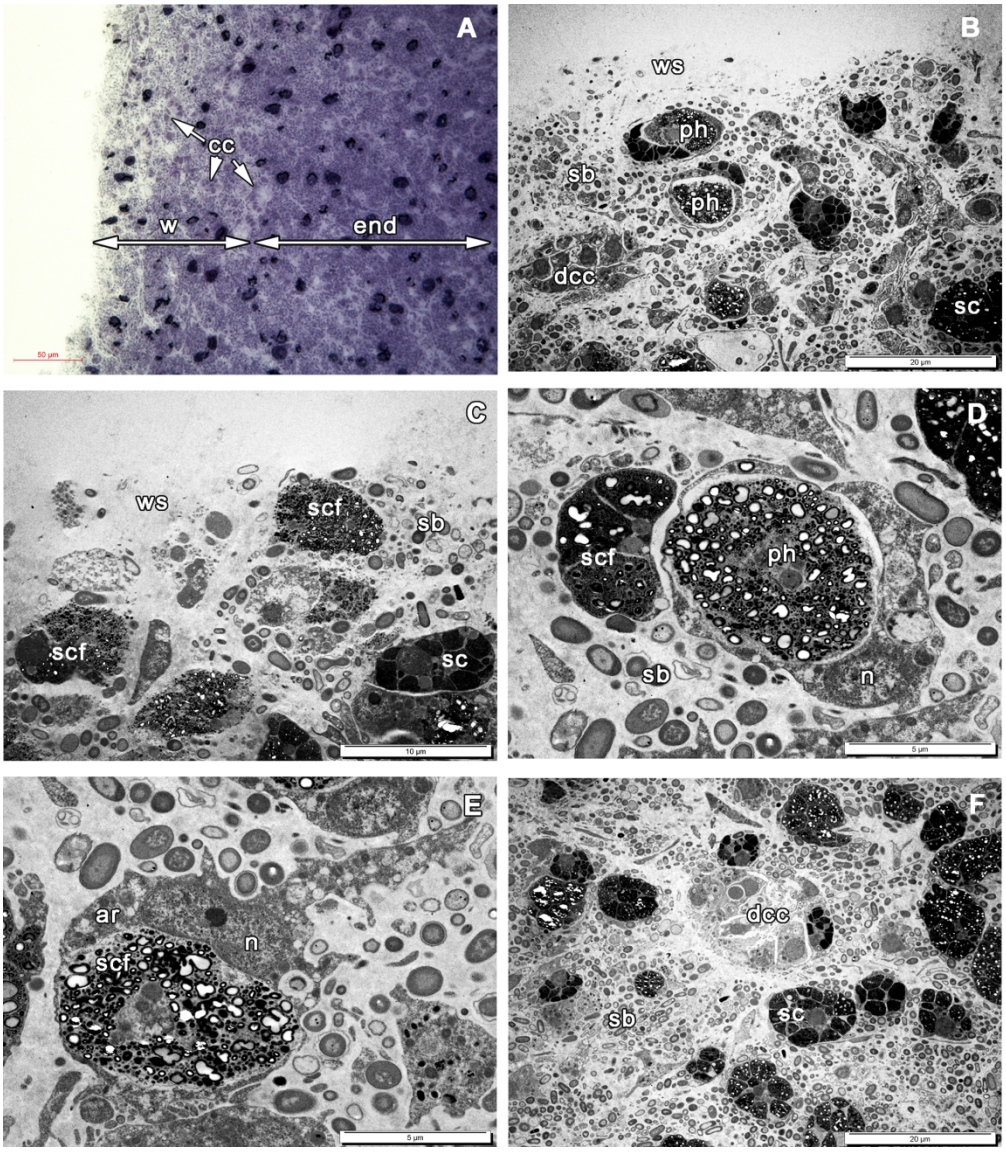

Figure 7. 6h of regeneration in Aplysina cavernicola
A – semi thin section of the wound and upper part of endosome; B, C – TEM of the upper part of the wound: it is a choanocyte chamber during their destruction, fragments of spherulous cells, phagocyted spherulous cell; D, E – wound zone with the fragments of cells and phagocytosis of spherulous cells; F – inner part of the wound, degraded choanocyte chamber.
ar – archaeocyte, cc – choanocyte chamber, dcc - destructed choanocyte chamber, dch – dedifferentiated choanocyte, end – endosome, in – inclusions in spherulous cells, n – nucleus, ph – phagosome, sb – symbiotic bacteria, sc – spherulous cell, scf – spherulous cells fragments, w – wound, ws – wound surface.

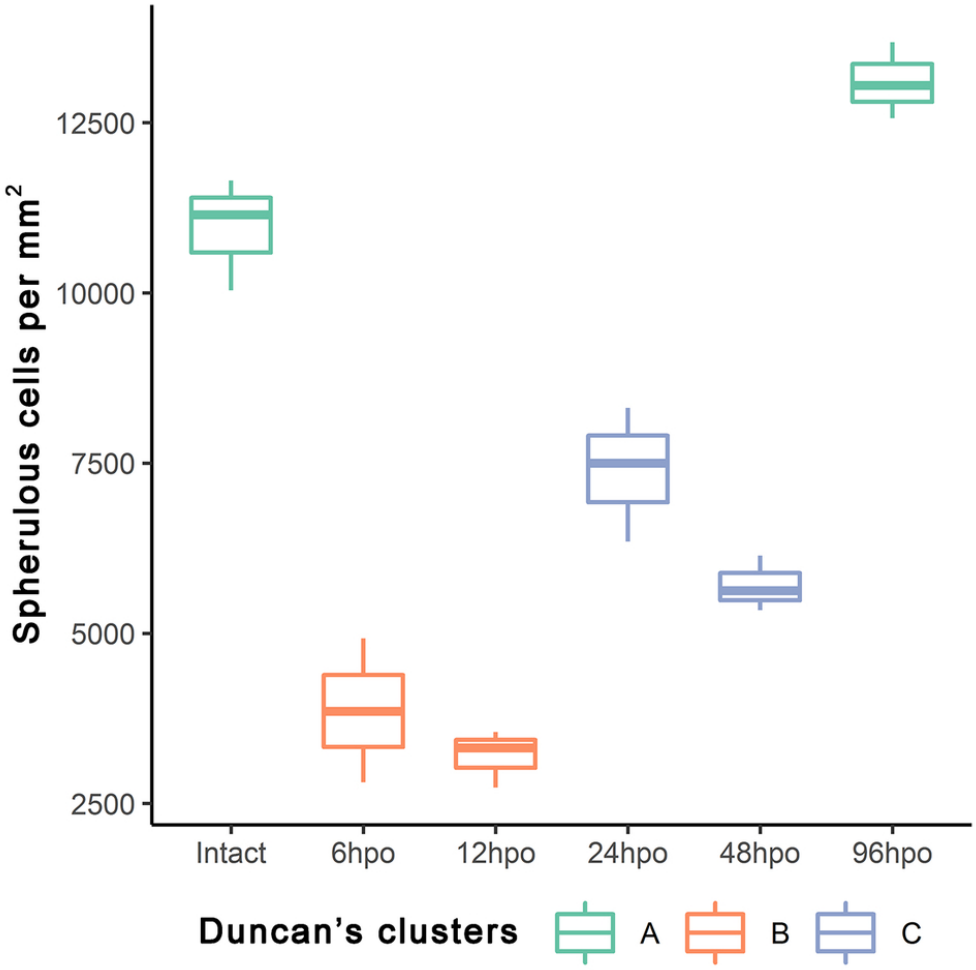

Figure 8. Boxplot diagram of the number of spherulous cells per mm2 in intact tissues and during regeneration in A. cavernicola. The differences between some of the means are statistically significant (ANOVA p-value = 2.36E-07(<0.01)). Tukey's multiple comparisons showed no significant differences only in 3 pairs: Intact tissues–96 hpo; 6 hpo–12 hpo; 24 hpo–48 hpo. Duncan's new multiple range test (MRT) approve this, grouping these pairs into three clusters (A, B, C). The differences between Duncan's clusters are statistically significant (Supporting Table 4).

81x81mm (300 x 300 DPI)

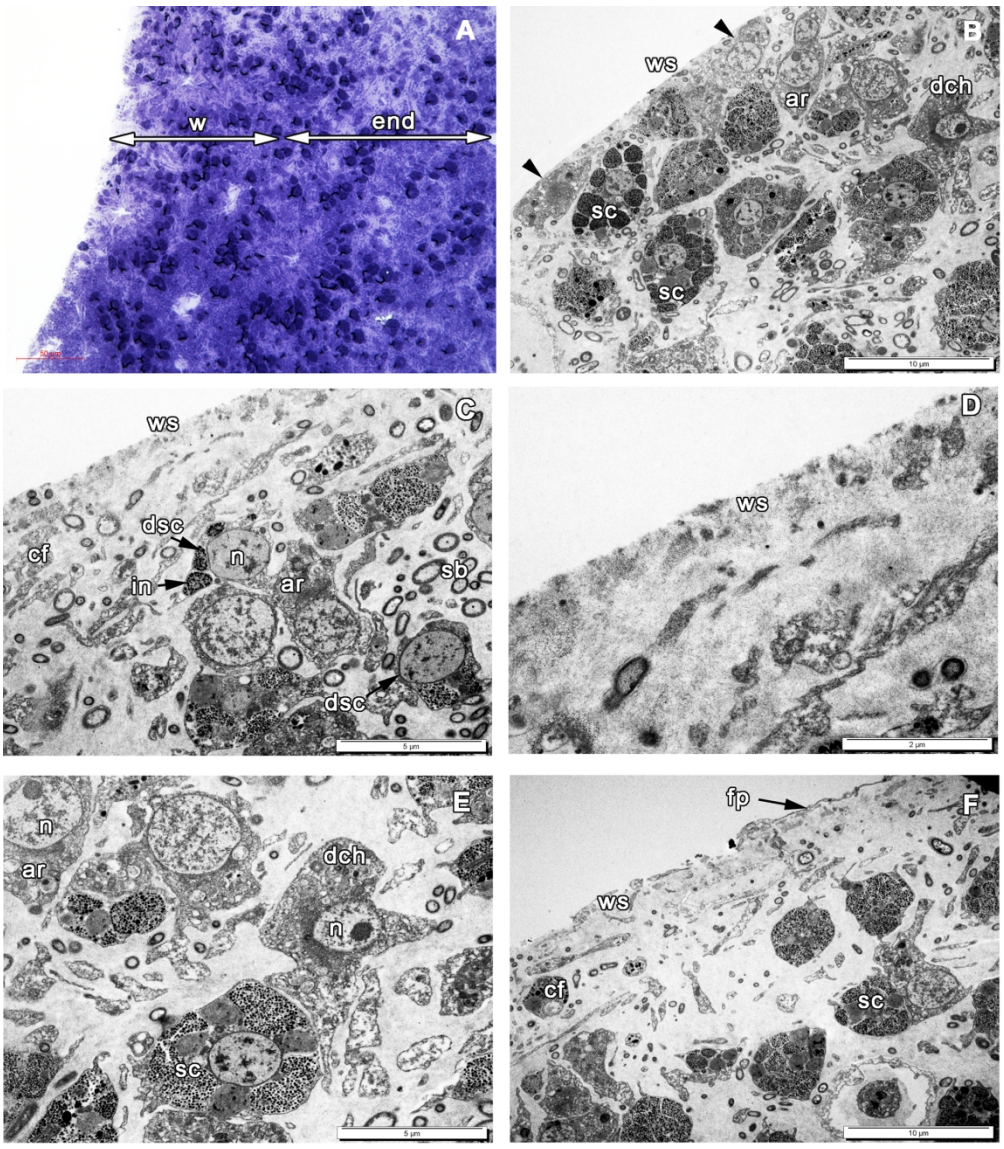

Figure 9. 12h of regeneration in Aplysina cavernicola
A – semi thin section of the wound and upper part of endosome; B, C – TEM of the upper part of the wound, there are some non-secret cells at the wound surface (arrowheads), dedifferentiated choanocytes and spherulous cells; D – detail of the upper part of the wound; E – wound zone with dedifferentiated choanocytes; F – marginal zone of the wound with the part of intact exopinacocyte.
ar – archaeocyte, cf – cells fragments, dch – dedifferentiated choanocyte, dsc - dedifferentiated spherulous cell, end – endosome, in – inclusions in spherulous cells, n – nucleus, ph – phagosome, sb – symbiotic bacteria, sc –spherulous cell, scf – spherulous cells fragments, w – wound, ws – wound surface.

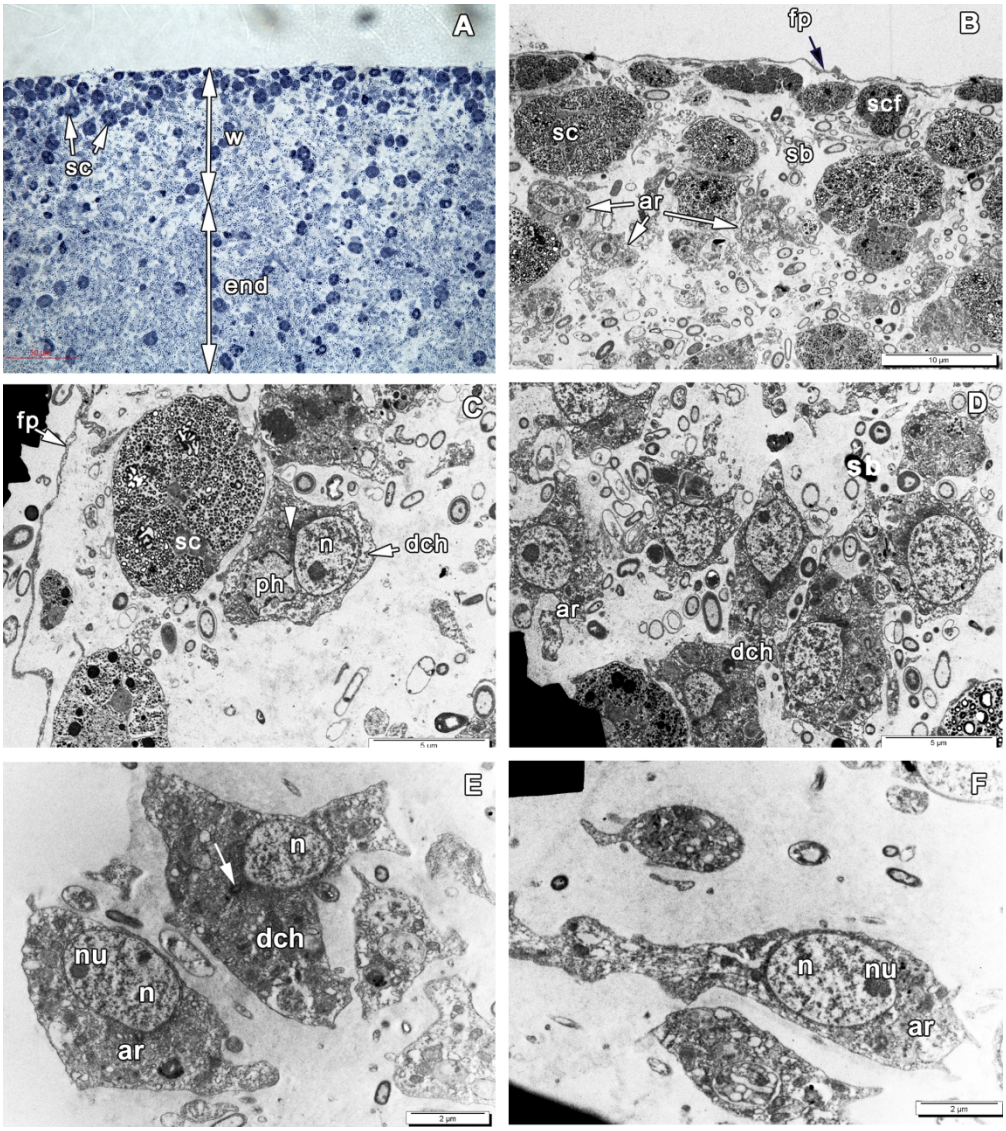

Figure 10. 24h of regeneration in Aplysina cavernicola
A – semi thin section of the wound and upper part of endosome; B, C – TEM of the upper part of the wound, with flat parts of new exopinacocytes, spherulous and non-secret cells with the phagosomes (arrowhead - basal body of choanocyte flagellum); D – wound zone with dedifferentiated choanocytes; E - upper part of the wound zone with archaeocyte and dedifferentiated choanocyte in the beginning of differentiation into new exopinacocyte, arrow show the basal apparatus of dedifferentiated choanocyte; F - archaeocyte differentiated into exopinacocyte at the upper part of the wound.
ar – archaeocyte, cf – cells fragments, dch – dedifferentiated choanocyte, dsc - dedifferentiated spherulous cell, end – endosome, in – inclusions in spherulous cells, n – nucleus, nu – nucleolus, ph – phagosome, sb – symbiotic bacteria, sc – spherulous cell, scf – spherulous cells fragments, w - wound.

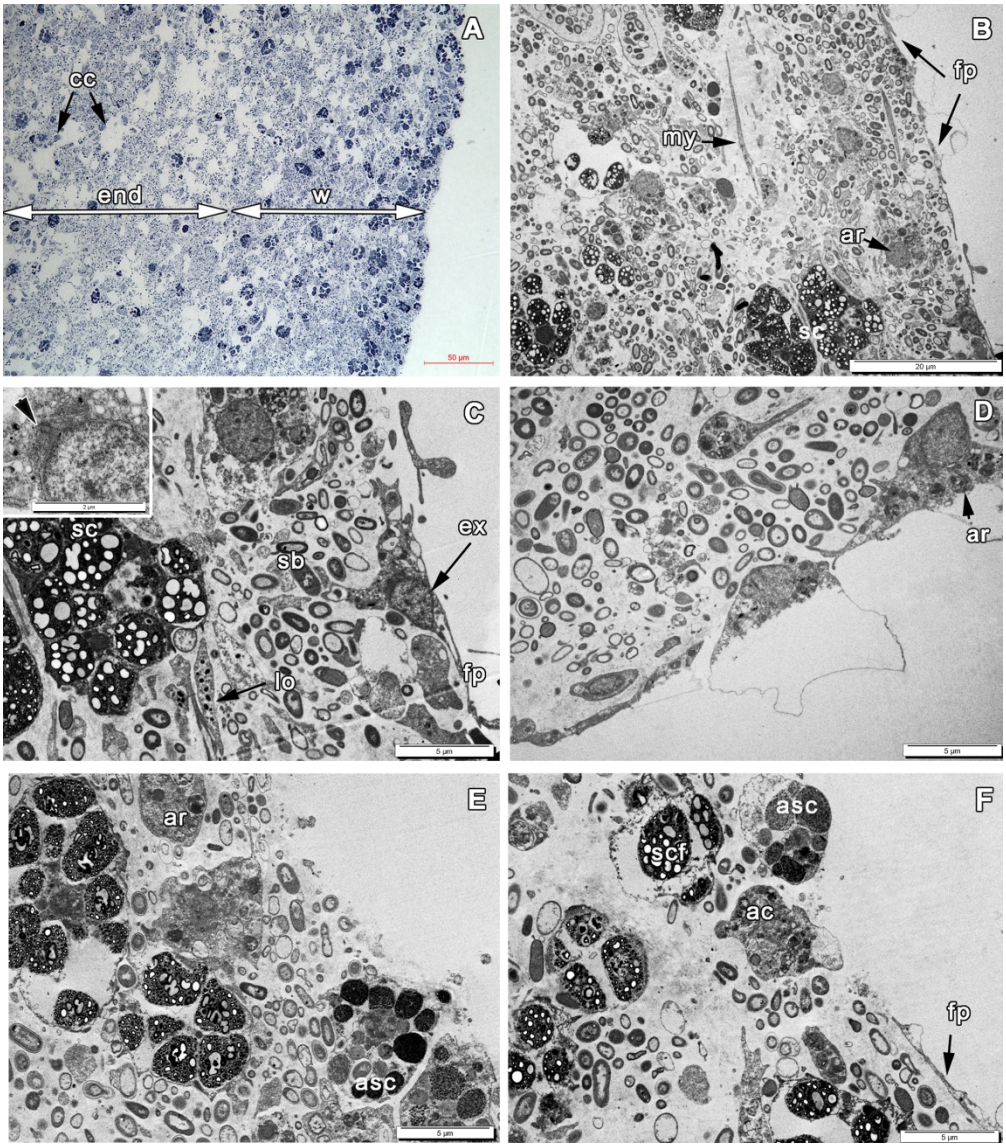

Figure 11. 48h of regeneration in Aplysina cavernicola
A – semi thin section of the wound and upper part of endosome; B – TEM of the upper part of the wound, with restored ectosome; C – TEM of the upper part of the wound, showed transdifferentiation of a choanocyte into exopinacocyte; inset – basal apparatus of dedifferentiated choanocyte (arrowhead); D – TEM of the upper part of the wound, showing transdifferentiation of an archaeocyte into exopinacocyte; E, F - TEM of the small apoptotic spherulous cells elimination of apoptotic spherulous cells through forming exopinacoderm.
ac – apoptic cell, asc – apoptic spherulous cell, ar – archaeocyte, cc – choanocyte chamber, ch – choanocyte, cf – cells fragments, dch – dedifferentiated choanocyte, end – endosome, ex- exopinacocytes, fp – flat part of exopinacocyte, in – inclusions in spherulous cells, lo – lophocyte, mc – microgranular cell, my – myocyte, n – nucleus, ph – phagosome, sb – symbiotic bacteria, sc – spherulous cell, scf – spherulous cells fragments, w – wound zone.

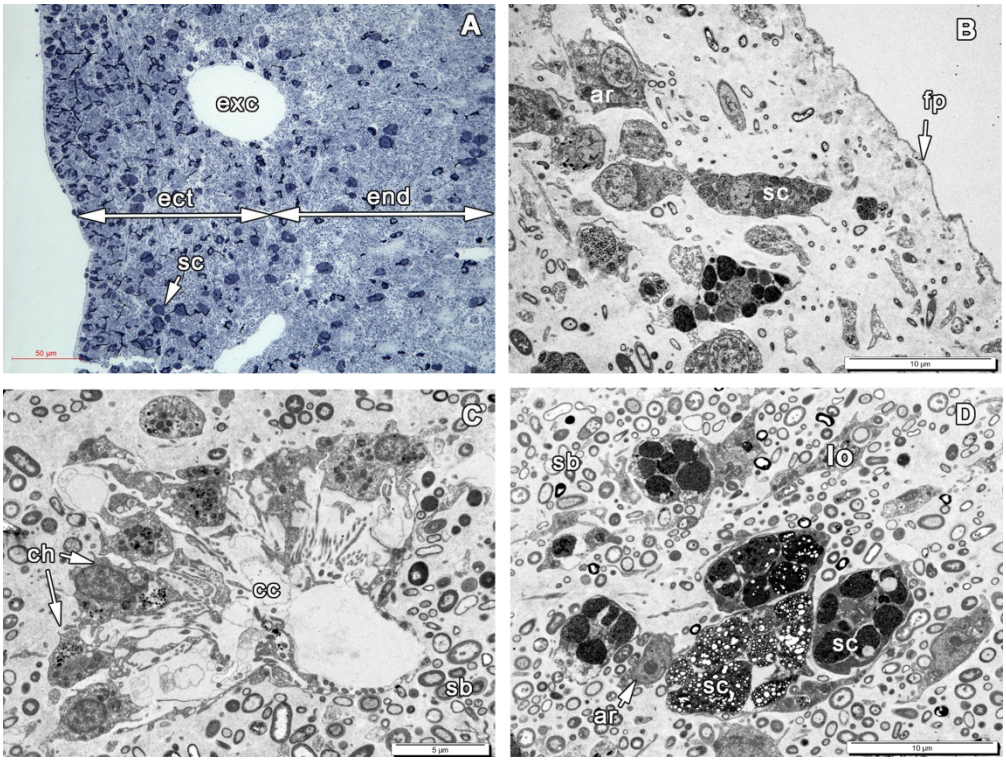

Figure 13. 96h of regeneration in Aplysina cavernicola
A – semi thin section of the completely restored ectosome and upper part of endosome; B – TEM of the upper part of the restored ectosome; C - the endosome with new choanocyte chamber; D – the endosome with normal cell composition.
ar – archaeocyte, cc – choanocyte chamber, ch – choanocyte, ect – ectosome, end – endosome, exc- exhalant canal, lo – lophocyte, n – nucleus, sb – symbiotic bacteria, sc – spherulous cell.

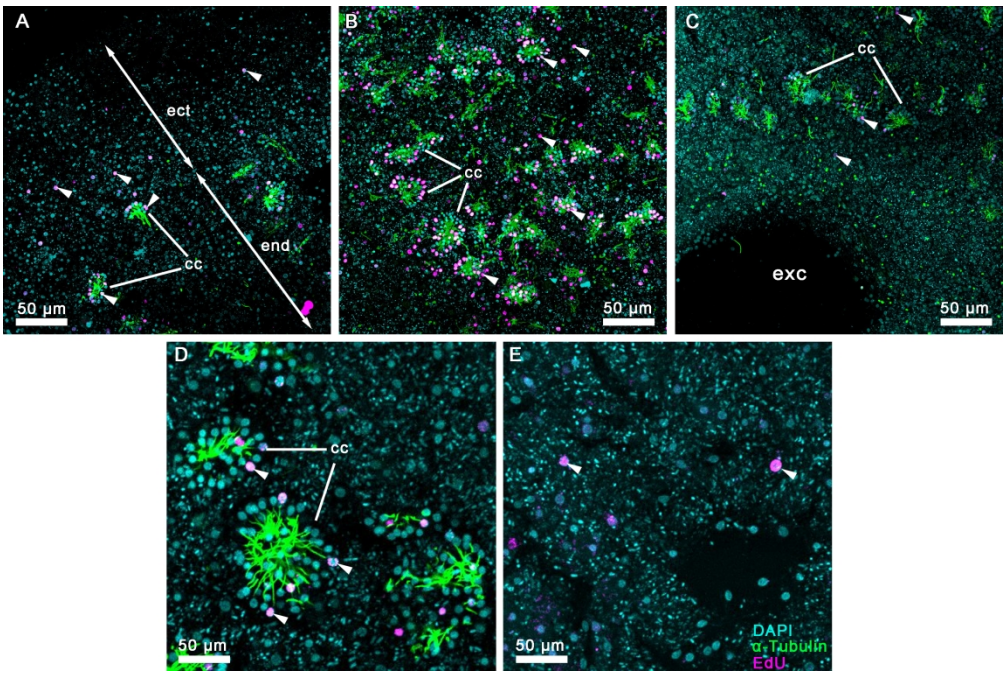

Figure 14. Cell proliferation in intact tissues of Aplysina cavernicola. A – ectosome; B – endosome; C – endosome near the exhalant canal of the aquiferous system; D – DNA-synthesizing choanocytes with small round to oval nuclei; E – mesohyl DNA-synthesizing cells with large round nuclei. Cyan – DAPI, green – α-tubulin, magenta – EdU. cc – choanocyte chamber, end – endosome, ect – ectosome, exc – exhalant canal of the aquiferous system. White arrowheads marks EdU-positive nuclei of DNA-synthesizing cells. Each image is a maximum projection, obtained from 55 µm Z stack

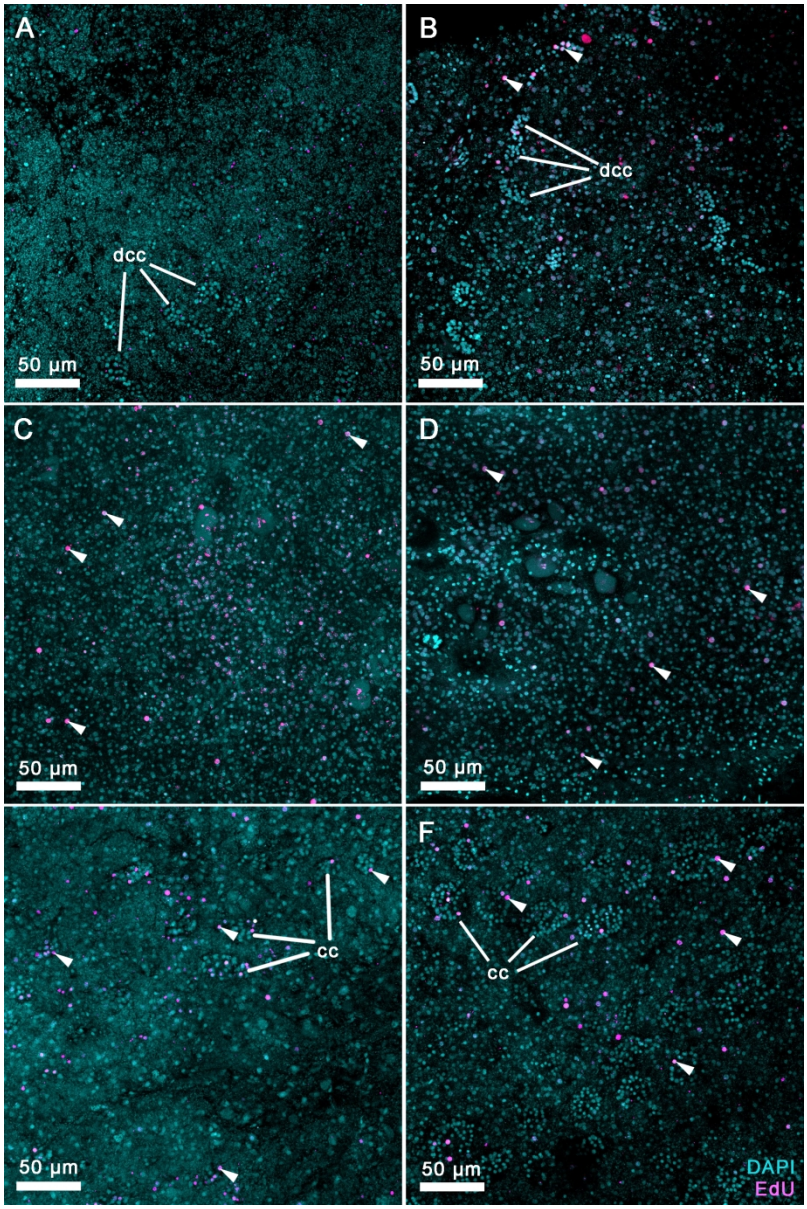

Figure 15. Cell proliferation during Aplysina cavernicola body wall regeneration. A-E – cell proliferation in the wound area at different stages of regeneration: A – 0-6 hpo; B – 0-24 hpo; C – 24-48 hpo; D – 48-72 hpo; E – 120-144 hpo; F – cell proliferation in intact tissues, distant from the wound, during regeneration. Cyan – DAPI, magenta – EdU. Dcc – disintegrating choanocyte chamber, cc – choanocyte chamber. White arrowheads marks EdU-positive nuclei of DNA-synthesizing cells. Each image is a maximum projection, obtained from 15 µm Z stack.

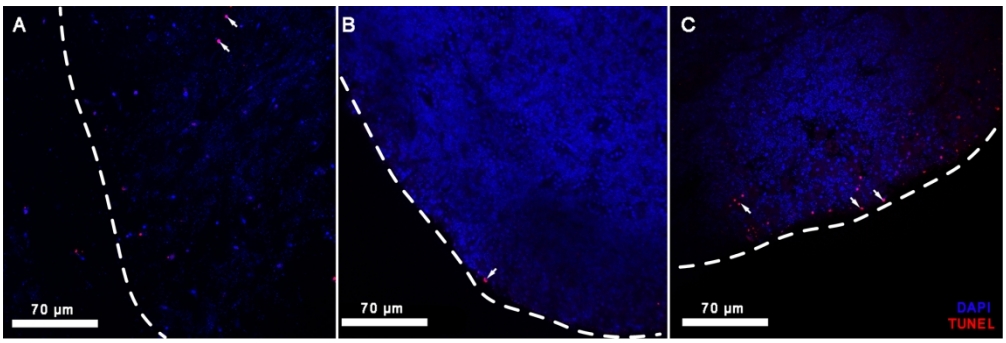

Figure 16. Apoptosis during Aplysina cavernicola body wall regeneration. A – 6 hpo; B – 12 hpo; C – 48 hpo. Blue – DAPI, red – TUNEL. White dashed line marks the wound edge, white arrows – TUNEL-positive nuclei of apoptotic cells. Each image is an optical slice through the wound area.